Robust Topologies for Passive, Fiber Optic Local Communication Networks

Ondria Jaffe Wasem

S.B. Massachusetts Institute of Technology
(1986)
S.M. Massachusetts Institute of Technology
(1986)

Submitted to the Department of
Electrical Engineering and Computer Science
in Partial Fulfillment of
the Requirements for the Degree of
Doctor of Philosophy
at the
Massachusetts Institute of Technology
June 1989

Signature of Author _____

Department of Electrical Engineering and Computer Science
May 18, 1989

Certified by _____

Robert Spayde Kennedy
Professor of Electrical Engineering
Thesis Supervisor

Accepted by _____

Arthur Clarke Smith, Chairman
Departmental Graduate Committee
Department of Electrical Engineering and Computer Science

Robust Topologies for Passive, Fiber Optic Local Communication Networks

Ondria Jaffe Wasem

Submitted to the Department of
Electrical Engineering and Computer Science
on May 19, 1989, in partial fulfillment of
the requirements for the degree of
Doctor of Philosophy

Abstract

Robust, passive, fiber optic local communication networks have multiple paths, so that loss of a link will not preclude communication between any pairs of users. In order for such a network to support a reasonable number (10–10^4) of users, power must be distributed as evenly as possible, with as little loss as possible. Analysis and simulation according to a mathematical model for power distribution allows comparison of various topologies, and demonstrates that a high degree of connectivity aids even distribution of power. Appropriate topological design yields a network that can support thousands of users within a 50 dB loss budget, when low-loss components are used.

Thesis Supervisor: Professor Robert Spayde Kennedy
Title: Professor of Electrical Engineering

Acknowledgements

This work would not have been possible without the generous help and support of those working and living around me. For technical help, I owe thanks to Professor Robert S. Kennedy, for being a sounding board for my ideas, and for giving me direction when I was going in circles; to Professor Pierre A. Humblet, for helping me to make the proofs more direct and intuitive; and to Professor Jeffrey H. Shapiro, for suggesting ways in which to make the document easier for the reader. I also thank the members of the Local Communication Networks Group for asking insightful questions at my presentations of this material. In particular, Walid Hamdy suggested a couple of useful papers, which are cited in the bibliography.

Many thanks to God, my family, and my friends for making my life generally peaceful and happy, thus enabling me to concentrate on my work. I especially appreciate the support of my husband, Peter, who was willing to live like a student through the whole thing.

This material is based upon work supported under a National Science Foundation Graduate Fellowship and a contract from RADC. Any opinions, findings, conclusions, or recommendations are those of the author and do not necessarily reflect the views of NSF or RADC.

Contents

List of Figures

Chapter 1

Introduction

1.1 Motivation

A fiber optic local communication network (FOLCN) is a set of nodes connected to each other and to transceivers by fiber optic links. Figure 1.1 shows a plot of attenuation vs. wavelength for an excellent singlemode silica glass optical fiber. [Per85] The arrows on the horizontal axis bound a low-loss window that is approximately 180 nm, or 1.5×10^4 GHz, wide. In the future, the entire low-loss window of the fiber may be accessible, making available more bandwidth than is needed in forseeable applications. Exploiting this excess bandwidth can make the network simpler and more robust.

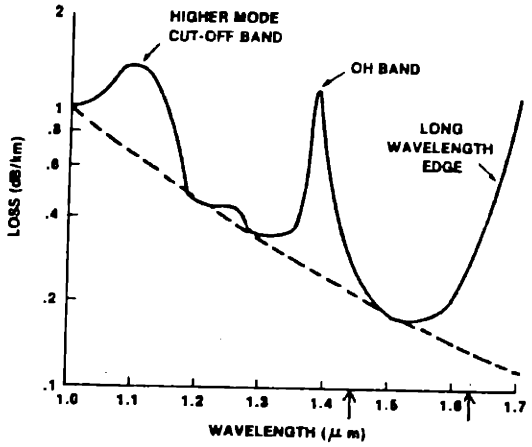

Figure 1.1: Loss vs. Wavelength for an Excellent Singlemode Optical Fiber

In fact, switching may not be necessary in a fiber optic network. Switching provides two functions: selection and localization. [Ken86] Selection can be performed either internally (at nodes) or peripherally (at transceivers), and involves allowing certain signals to reach a receiver, while keeping certain other signals from that receiver. Internal selection entails nodes switching signals toward or away from receivers, as appropriate. Peripheral selection requires a receiver to ignore signals it does not need or should not know about, and to process signals intended for it.

The purpose of localization is to keep a signal from spreading out over all links of a network; thus, localization occurs at nodes. In electrical networks, localization conserves bandwidth. Due to the broad bandwidth in an optical fiber network, conserving bandwidth may not be necessary in some situations, although localizing the signal in order to conserve power may be helpful. Internal selection can accomplish localization to some degree.

With the rapid advance of photonic switching technology, optical switching networks similar to electronic switching networks are possible, but may not be necessary. If, in absence of localization, there is enough bandwidth to support the maximum traffic loads on the links of the network, and the network can distribute enough power between users to support communication, then internal switching becomes unnecessary, since selection can be performed peripherally.

Assuming that there is enough bandwidth and power such that internal switching is unnecessary, I choose a passive network (except for the transceivers), because passive nodes are less expensive, less complex, and more reliable than active nodes. In a fully-connected passive network, one way to ensure that power from a given transmitter gets to a given receiver is to let the power reach every receiver. Thus, all signals are broadcast.

I also desire robustness, defined here as the maximum number of links that can be cut while maintaining full connectivity. In an active network, multiple paths through the network provide robustness, while routing a given message or packet over only one of these paths saves bandwidth. The strategy of employing multiple paths works

in passive networks, too. Of course, the broadcast nature of the passive network in combination with the multiple paths yields multiple receptions of a message at the receiver.

These multiple receptions can be exploited to alleviate the power division problem. The power division problem is simply the problem of dividing the power up among a given number of receivers so that each receives at least the minimum amount of optical power required to detect a signal. This minimum power requirement is determined by the desired signal-to-noise ratio (SNR), which might depend on the received optical power itself, or the square of the received optical power, depending on the particular system employed. If each receiver is to receive an amount of power satisfying that requirement, then obviously the input power can be divided among only so many receivers. [Wag85] If the power is further divided among many paths, the signal strength becomes weaker, and fewer receivers can be supported. Of course, the same thing holds true for electrical networks. What makes it a "problem" in an optical network is that the fraction of the input power required for optical detection in a fiber optic network is much greater than the fraction of power required for detection in an electrical network. [Lie86] Therefore, it is helpful for the receivers to add the power from the multiple receptions of a given signal.

The performance parameter considered in this thesis is the sum of the powers of the multiple receptions. In systems for which the signal-to-noise ratio depends upon the square of the received power, performance would be determined by the sum of the squared powers of the multiple receptions; therefore, my work applies only for systems in which the SNR depends upon the received optical power level itself. Such systems include coherent detection systems, and signal shot noise limited direct detection systems with photon-counting receivers.

Addition of power happens automatically if incoherent light is used, and receptions overlap. If receptions arrive separately, a matched filter receiver might be used to add the power in them. If coherent light is used, resolution of the separate receptions of a signal is sufficient to allow addition of their power. When a signal is designed properly,

separate receptions of it are resolvable if the differential delay between receptions exceeds the reciprocal bandwidth of the signal. [Pri58],[Pro83] The design of a receiver to resolve receptions and add their power in such a passive fiber optic network is analogous to the work done on resolving receptions in multipath radio channels. [Pri58] The wide bandwidth in the fiber aids resolution of receptions, because the lower bound on differential delays becomes negligible as the bandwidth of the signal gets very large. For instance, if the 10^4 GHz consists of 10^3 frequency channels, so that each signal on the network is 10 GHz wide, then receptions arriving more than 0.1 ns apart are resolvable.

While adding power from different receptions of a signal alleviates the power division problem somewhat, distributing power as evenly as possible is also important. To illustrate this, suppose when the input power, P_{in}, is divided into m equal parts, m receivers receive exactly the minimum power, P_{min}. That is, $mP_{min} = P_{in}$. This means that the network supports m receivers, where a "supported" receiver is one that receives at least P_{min}. Now, if one receiver receives $P_{min} + \Delta$, while another receives $P_{min} - \Delta$, where Δ is a very small amount of power, and the total amount of power delivered to all nodes is still P_{in}, then only $m - 1$ receivers are supported. Clearly, the network supports the most receivers when power divides equally among all receivers. [Abe86] So, the power division problem is the problem of dividing the available power efficiently among all receivers. The available power does not necessarily equal the input power, as excess loss can irretrievably drain power from the network.

My goal is to find robust topologies that support enough users for use in passive FOLCNs. "Enough" depends on the application, and can be anywhere from 10 to 10^4.

1.2 Feasibility

As mentioned above, it is reasonable to assume that separate receptions of a signal, such as a pulse representing a symbol, can be resolved. For a 10–10^4 GHz signal, the

differential delays between the receptions need only be 0.1 ns – 0.1 ps for resolution. [Pri58],[Pro83] However, there is still the possibility of intersymbol interference. The same principles used to combat intersymbol interference in multipath radio channels work in fiber optic networks. In fact, Price and Green showed that the RAKE receiver that resolves receptions and adds their power on a multipath radio channel also effectively eliminates intersymbol interference. [Pri58] Alterman recently analyzed the performance of various types of receivers in robust passive FOLCNs, and determined that equalizers perform adequately. [Alt88]

If many users were to send messages on the network simultaneously, there could be multiuser interference, because all signals are broadcast. However, the use of frequency division or code division multiple access could alleviate this problem.

Finally, for full connectivity when using frequency multiplexing, the transmitters and/or receivers must be tunable. There are various ways of tuning lasers, the slower methods yielding tuning ranges of up to 18,000 GHz [WCK87] and the faster methods having smaller ranges. Hamdy has examined combining tuning methods for efficient tuning of transmitters. [Ham88]

1.3 Background

Transceivers in an FOLCN can be anything that produces and/or receives digital, optical information—a telephone (plus A/D converter, optical source, and optical detector), computer terminal (plus optical source and detector), computer (plus optical source and detector), gateway to a subnet, etc. Nodes can be switches, multiplexers, demultiplexers, passive couplers, or anything else on which the fiber links terminate or originate. The term "local" implies that the network spans an area of size somewhere between an office and a small town.

There are three main types of topologies which have been used for FOLCNs. These are the star, the bus, and the ring. In the star, each transceiver connects to the central node by a bi-directional fiber optic link, which can be one or two fibers, as shown

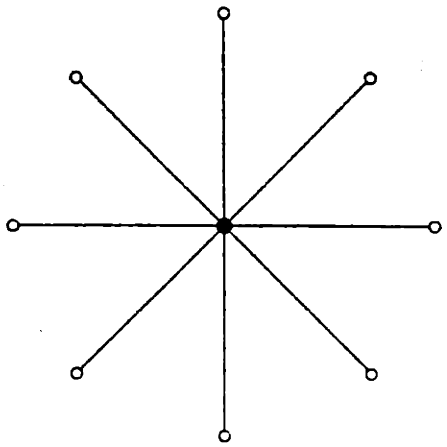

● node

○ transceiver

——— fiber optic link, can be one bi-directional fiber, or two uni-directional fibers

Figure 1.2: Star Topology

in Figure 1.2. In an active star, the node detects and regenerates its input from a source transmitter, directing its output to the destination receiver, while in a passive star, the node is a star coupler that divides the input power among all transceivers. Active stars are attractive because the destination receiver receives most of the power sent to it by the source transmitter, due to the fact that the active central node does not have to broadcast the signal. Furthermore, there is little delay compared to some other active networks, because the signal is detected and regenerated only once on its way to the destination. Unfortunately, the limited bandwidth of the post-detection electronics in the active node prevents utilization of the full optical bandwidth of the fiber. Moreover, failure of the node renders the entire network inoperable; thus, an active star is not robust. [Ros87]

Although a passive star network is not robust either, it has advantages over an active star. Because the central node is passive rather than active, it does not limit the usable bandwidth to that of electronics, and it is less expensive and more reliable than an active node. Using a passive star coupler also eliminates processing delay.

(a) Active Bus (for explanation of symbols, see Fig. 1.2)

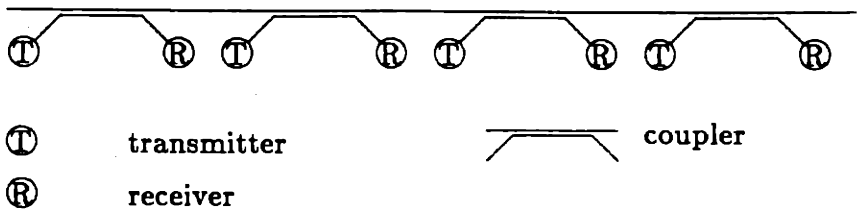

(b) Passive Bus

Figure 1.3: Bus Topology

However, a passive star delivers less power to each connected receiver, because the passive star coupler divides power among all receivers; thus, a passive star supports fewer receivers than an active star. In both types of star, a single cable cut interrupts all communication to or from a transceiver. [Ros87],[Ree86]

Because busses work so well for electronic LCNs, one might consider them for FOLCNs; however, they do not perform as well for fiber. An active bus consists of a series of node-to-node links, which again can consist of two uni-directional fibers or one bi-directional fiber, as in Figure 1.3(a). Each node sends signal to and receives signal from a connected transceiver. A passive bus consists of two uni-directional links or one folded uni-directional link with transceivers connected by passive couplers. Figure 1.3(b) shows a uni-directional passive bus, while a bi-directional bus is simply two of these in parallel (two uni-directional links), or in series (one folded uni-directional link). As is the case for an active star, there is little loss of power on an active bus. However, as mentioned above, electro-optic regeneration limits the amount of usable bandwidth. A passive bus is less expensive than an active bus, due to the lack of electro-optic regenerators. Unfortunately, there is a power distribution problem. As power travels from one end of the bus to the other, some power is cou-

pled to each receiver, and some power is lost at each tap. If the power diminishes too much before the signal reaches its destination, the intended receiver cannot detect it. [Mou87],[Per85],[Tam84],[Wag85],[Wag87] In the active bus, a node failure effectively divides the bus into two non-communicating parts. In either bus, a single cable cut prohibits nodes upstream from the cut from communicating with nodes downstream from the cut. [Ree86],[Ros87] Therefore, the bus topology is not robust.

Of the three topologies mentioned above, a bi-directional ring is the only one which is robust. That is, the bi-directional ring remains fully connected when a link goes down. A ring can be active or passive, like the star and bus. In fact, it is simply a bus with the ends connected together, as shown in Figure 1.4.

The active ring, like the active bus, has little loss of power, requires electro-optic regenerators, and has the bandwidth problem associated with regenerating the signal at every node. [Mou87] If the links of an active ring are bi-directional, full connectivity is retained in the event of a node failure, or up to two link failures. A uni-directional active ring or bus can also recover from node or link failures if it is star-wired, as in Figure 1.5. [Dix87] This means that instead of running between adjacent nodes, fibers run into and out of some central facility. In this way, an inoperable node or link can be bypassed. Unlike the passive bus, the passive ring can be uni-directional and fully-connected simultaneously. However, using two rings, one in each direction, maintains full connectivity in the event of a link failure. [Ree86],[Ros87] The passive ring has the same power distribution problem that the passive bus has. [Mou87] Active stars are not used, because they require more active components than active rings. [Hum89] They also require more fiber than a ring or bus (except in the case of a star-wired ring or bus). [Mou87]

Of course, many networks are hybrids of these topologies. For instance, the optical cascade star network is a star-bus hybrid. [Tam84] My work examines many topologies for robust, passive FOLCNs, and demonstrates that the performance of the passive star upperbounds the performances of robust, passive FOLCNs, and that the bi-directional ring performs much worse than other robust topologies. Chapter 2

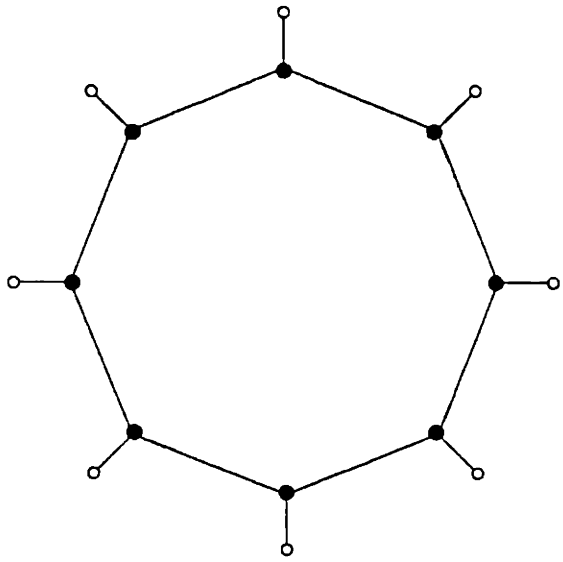

(a) Active Ring

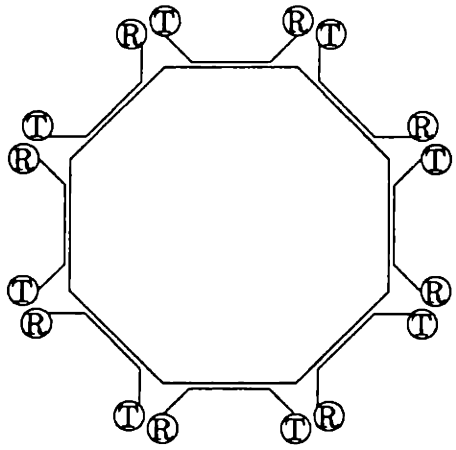

(b) Passive Ring

(see Figs. 1.2 and 1.3 for explanation of symbols)

Figure 1.4: Ring Topology

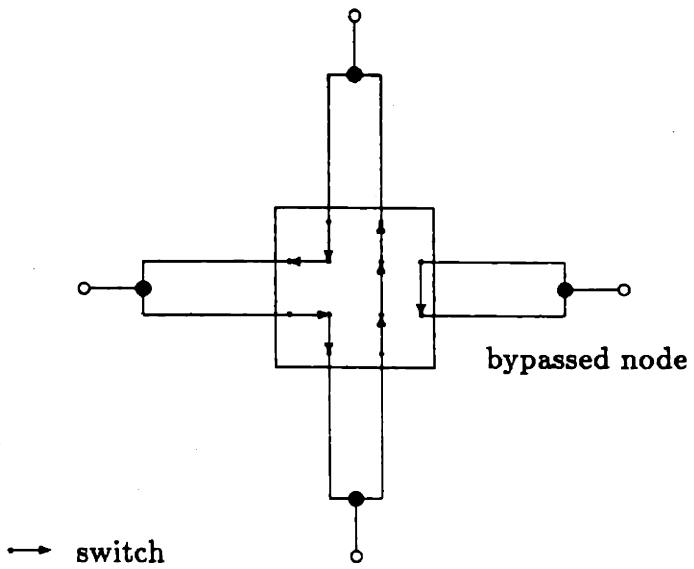

Figure 1.5: Star-Wired Ring

describes the network components, defines performance, and explains the mathematical model used to evaluate performance. The classes of topologies to be studied are described in Chapter 3. I present analytical results in Chapter 4, and numerical results in Chapter 5. In Chapter 6 I draw conclusions and suggest further research topics.

Chapter 2

Mathematical Model of the Network

This chapter describes the components in the network, how they are connected, and what is assumed about them. Then a discussion of the criteria of performance indicates the need to compute the sum of the powers of all of the receptions of a signal. Next, a matrix formulation for computing this quantity is described, and finally some mathematical characteristics of the resulting matrices are discussed.

2.1 Network Description

The networks are composed of subnets of active transceivers, each transceiver corresponding to a user, and passive nodes. A subnet can consist of a single transceiver. A simple example is illustrated in Figure 2.1(a), which shows the logical layout of the network, not the physical layout. The subnets always have a single neighboring node to which they output power, and from which they collect power. Nodes can have an arbitrary number of neighboring nodes and subnets.

The model for a node is a transmissive star coupler, which has total loss in dB equal to the sum of the excess loss within the coupler and the splice loss, and which divides the rest of its input power evenly among its outputs, as illustrated in Figure 2.2.

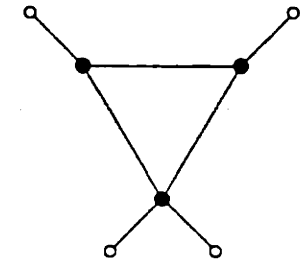

—— bi-directional fiber links

● node

○ subnet

a) A Network of 3 Nodes and 4 Subnets

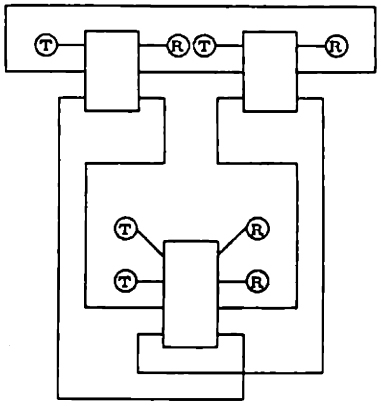

star coupler (inputs on left, outputs on right)

Ⓣ subnet as transmitter (signal source)

Ⓡ subnet as receiver (signal sink)

b) Detailed Connection Scheme of Same Network

Figure 2.1: A Simple Passive Network

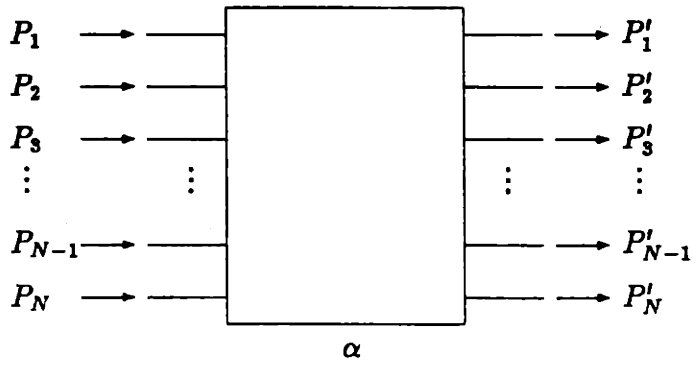

$$P'_n = \left(\frac{1}{N}\sum_{m=1}^{N} P_m\right) 10^{-\alpha/10} \quad n = 1, 2, \ldots, N$$

Figure 2.2: Star Coupler

[Lie86],[Per83],[Per85],[Wag85],[Wag87] In the figure, P_x represents power into input x, P'_x represents power out of output x, and α represents the excess loss of the coupler plus loss of power at the connectors or splices which attach the coupler to the fiber. Figure 2.1(b) shows how star couplers might be connected to implement the network shown in Figure 2.1(a).

Henceforth I refer to the combination of excess loss and connector or splice loss as "insertion loss," and loss due to dividing power as "splitting loss." Fiber loss can also be lumped into the insertion loss. Furthermore, I assume that receivers can add up the power in all receptions of a message. Also, I assume that networks of interest are fully-connected, meaning that all transmitters can send messages to all receivers. Finally, I assume that power from a subnet enters the node before being distributed back into the subnet, and that power entering the subnet from the node does not re-enter the node. That is, from the node's point of view, a subnet behaves as a single transceiver. A subnet is characterized by the minimum power which one of its transmitters can inject into the network, and by the minimum power it must collect in order to distribute the minimum required power to each receiver. Henceforth, when

I use the words "transceiver," "transmitter," or "receiver," I mean a subnet modeled as such, unless I explicitly state otherwise.

2.2 Criteria of Performance

Clearly, if a receiver adds power from more receptions of a signal, then it collects more power. Due to a desire to limit time delay, there will, in practice, be some limit to the number of receptions that are actually detected. The precise implementation of such a scheme depends upon the impulse response of the network, which in turn depends upon the physical locations of transceivers and nodes. Rather than assuming a particular physical layout, I compare topologies in the ideal case, in which receivers can wait forever to collect all of the power that circulates through the network. This case, which entails taking into account power that comes to a receiver over infinitely many paths, provides an upper bound on the power that can be collected.

As stated in Section 1.1, my goal is to find robust topologies that support many users. Ranking topologies according to how many users they support, and then choosing from those supporting the most users, could accomplish this goal. However, since the number of users supported depends upon the power distribution of the network, in most cases, comparison of topologies is based on their power distribution, where the power distribution of a network is the set of power levels delivered between all transmitter-receiver pairs. Specifically, one way in which to compare topologies based on power distribution is to maximize over topologies the minimum power delivered between any transmitter-receiver pair, for a given number of transceivers. As noted before, this performance measure is appropriate for cases in which the output SNR of the receiver is proportional to the sum of the powers in the various receptions of the signal. The reason for maximizing the minimum delivered power is that when the minimum delivered power is sufficiently above the sensitivity threshold of the receivers, more transceivers can be added to the network.

Another way in which to compare topologies based on their power distribution is to

minimize over topologies the probability that the minimum power delivered between any transmitter-receiver pair falls below the sensitivity threshold of the receiver, for a given number of transceivers. To do this, assume that there are m transceivers in the network, and that each of the m^2 transmitter-receiver pairs is equally likely to be the one of interest. In that way, each of the m^2 amounts of power distributed from transmitters to receivers is equally likely. Thus, the distributed power is a random variable taking on each of the m^2 values with probability $1/m^2$. Of course, some of the values may be equal. Now, accomplishing the minimization mentioned above is possible.

Once a group of useful topologies is determined, the best one for a particular application depends upon other criteria. For instance, although there are many paths between nodes in the network, there is only one link from a transceiver to its neighboring node. Shortening this link makes it more reliable. The more nodes in the network, the closer to the transceivers they can be; therefore, for some applications, a topology with as many nodes as possible is best. If large couplers are too expensive, the topology that uses the smallest couplers, or that has the fewest nodes, is attractive. If installing fiber is expensive, choose a topology that uses the least fiber. I discuss such tradeoffs in more detail after useful topologies have been determined.

2.3 An Analogic Mathematical Model

An analogy to Markov chains aids in dealing analytically with the task of adding up power over infinitely many paths. Since the total power that reaches the receivers plus the total power lost equals the total power injected into the network, consider the fraction of power collected by a receiver as the probability that a particular quantum of power is collected by that receiver. Likewise, consider the fraction of power lost as the probability that a particular quantum of power is lost. On a smaller scale, since the power into a node equals the power lost plus the power sent to other nodes and receivers, consider these fractions of power as the probabilities for that node that a

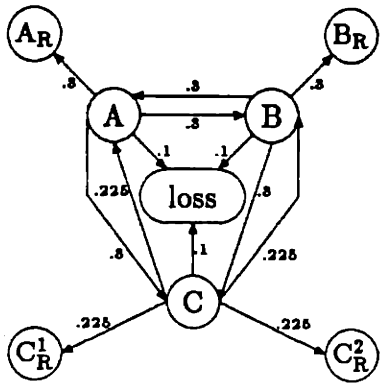

$$M = \begin{array}{c} \\ A \\ B \\ C \\ A_R \\ B_R \\ C_R^1 \\ C_R^2 \\ \text{loss} \end{array} \begin{array}{c} \begin{array}{cccccccc} A & B & C & A_R & B_R & C_R^1 & C_R^2 & \text{loss} \end{array} \\ \left[\begin{array}{cccccccc} 0 & .3 & .3 & .3 & 0 & 0 & 0 & .1 \\ .3 & 0 & .3 & 0 & .3 & 0 & 0 & .1 \\ .225 & .225 & 0 & 0 & 0 & .225 & .225 & .1 \\ 0 & 0 & 0 & 1 & 0 & 0 & 0 & 0 \\ 0 & 0 & 0 & 0 & 1 & 0 & 0 & 0 \\ 0 & 0 & 0 & 0 & 0 & 1 & 0 & 0 \\ 0 & 0 & 0 & 0 & 0 & 0 & 1 & 0 \\ 0 & 0 & 0 & 0 & 0 & 0 & 0 & 1 \end{array}\right] \end{array}$$

Figure 2.3: Analogic Markov Chain

particular quantum of input power is lost or sent to another node or receiver. In fact, if each node and each receiver is considered to be a state, and a loss state is included, then these probabilities become the transition probabilities of a Markov chain. The initial power distribution, which has all power at the node connected to the active transmitter, becomes the initial probability distribution of the Markov chain, in which the state is a node state with probability one. The normalized final power distribution becomes the final probability distribution of the Markov chain.

Figure 2.3 shows the Markov chain for the network in Figure 2.1. States A, B, and C represent nodes, while all other states but the one marked "loss" represent receivers. There are no transmitters in the figure, but assume that, with probability

one, all power that a transmitter transmits goes to the node to which it is attached. The transition probabilities reflect the fact that, in this example, insertion loss is 0.4 dB.

Figure 2.3 also shows a transition matrix, M, for the Markov chain. The i-jth element of M is the probability of the state being j at time $n+1$, given that the state was i at time n. Note that each row of the matrix is a stochastic vector which shows the power distribution after the message has traveled one link, given that it started at the node or receiver corresponding to that row.

A transition matrix for a general network is of the form

$$M = \begin{pmatrix} S & R & L \\ 0 & I & 0 \\ 0 & 0 & I \end{pmatrix}, \tag{2.1}$$

with node states listed first, followed by receiver states, and finally the loss state. Thus the matrix blocks of M, assuming n nodes and m receivers, are:

S: $n \times n$ matrix representing power flow between nodes

R: $n \times m$ matrix representing power flow from nodes to receivers

L: $n \times 1$ matrix representing power lost from nodes

0: $m \times n$ zero-matrix representing the fact that receivers send no power back to nodes

I: $m \times m$ identity-matrix representing the fact that receivers retain power. That is, the only transition from a receiver state is a transition back to itself with probability 1.

0: $m \times 1$ zero-matrix representing the fact that there is no more loss in the network once power arrives at a receiver. (I am not concerned with what the receiver does with the power once it has it.)

0: $1 \times n$ zero-matrix representing the fact that lost power does not return to nodes

0: $1 \times m$ zero-matrix representing the fact that lost power does not return to receivers

I: 1×1 identity-matrix representing the fact that the loss state retains power

Each row of the limiting matrix is also a stochastic vector showing the final power distribution after power has been collected over all possible paths, given that power started at the node or receiver corresponding to that row. The limiting matrix is computed as follows:

$$M^2 = \begin{pmatrix} S^2 & (S+I)R = \sum_{l=0}^{1} S^l R & (S+I)L = \sum_{l=0}^{1} S^l L \\ 0 & I & 0 \\ 0 & 0 & I \end{pmatrix}$$

$$M^3 = \begin{pmatrix} S^3 & (S^2+S+I)R = \sum_{l=0}^{2} S^l R & (S^2+S+I)L = \sum_{l=0}^{2} S^l L \\ 0 & I & 0 \\ 0 & 0 & I \end{pmatrix}$$

$$\vdots$$

$$M^k = \begin{pmatrix} S^k & \sum_{l=0}^{k-1} S^l R & \sum_{l=0}^{k-1} S^l L \\ 0 & I & 0 \\ 0 & 0 & I \end{pmatrix}$$

$$\vdots$$

$$\lim_{k\to\infty} M^k = M_\infty = \begin{pmatrix} 0 & (I-S)^{-1}R & (I-S)^{-1}L \\ 0 & I & 0 \\ 0 & 0 & I \end{pmatrix} \tag{2.2}$$

The next section explains why $\lim_{k\to\infty} S^k = 0$, so that $\sum_{l=0}^{\infty} S^l = (I-S)^{-1}$.

2.4 Matrix Characteristics

The properties of the matrix relate to the properties of the topology. For instance, the size of the matrix relates to the number of nodes and transceivers in the network, and the stochastic nature of its rows reflects the passivity of the network. The various sections of the matrix, described in Section 2.3, reflect the behavior of the couplers and receivers in the network. Also, the density of the matrix relates to the density of

connections in the network. Most importantly, the minimum element of $(I - S)^{-1}R$ represents the minimum fraction of input power received by any receiver from any transmitter.

Since the elements of S, $\{s_{ij}\}$ where s_{ij} is the i-jth element of S, represent transition probabilities of a Markov chain, $0 \leq s_{ij} \leq 1, \forall i, j$, so that S is nonnegative, meaning that all of its elements are nonnegative. This is denoted $S \geq 0$. The following theorem about nonnegative matrices verifies that $\lim_{k\to\infty} S^k = 0$, as indicated in the previous section.

Theorem 1 *A nonnegative matrix always has a nonnegative eigenvalue, r, such that for all eigenvalues λ_i, $|\lambda_i| \leq r$. r is called the dominant eigenvalue. [Gan59]*

PROOF: [Gan59], pp. 80–82

Let σ_i be the i-th row-sum of S. That is,

$$\sigma_i = \sum_{j=1}^{n} s_{ij}. \tag{2.3}$$

Since nodes are lossy,

$$\sigma_i < 1, \forall i. \tag{2.4}$$

Let σ_{min} and σ_{max} be, respectively, the minimum and maximum row-sums of S, and let r_s be the dominant eigenvalue of S. Then, since S is nonnegative,

$$\sigma_{min} \leq r_s \leq \sigma_{max} \qquad \text{[Gan59]} \tag{2.5}$$

Comparing Inequality 2.5 with Equation 2.4 shows that $r_s < 1$; therefore, $\lim_{k\to\infty} S^k = 0$. [Gan59]

Intuition indicates that $\lim_{k\to\infty} S^k = 0$. Recall that nodes lose some power while sending the rest to receivers and other nodes; moreover, power enters a node only from a transmitter or another node. If a transmitter injects finite power into the network, and infinite time passes, then some of that power is lost, and receivers collect the rest, leaving the nodes with no power.

In order for the network to be fully-connected, the graph consisting of the nodes and the links between them must be strongly connected, meaning that there exists a path between every pair of nodes. This strongly connected graph of the nodes and the links connecting them is the directed graph of the matrix S. Since S corresponds to a strongly connected graph, it is irreducible [Fie86],[Min88]; therefore, Inequality 2.5 holds with equality only when $\sigma_{min} = \sigma_{max} = \sigma_i$, $\forall i$. [Gan59] Also, since S is irreducible and nonnegative, with dominant eigenvalue $r_s < 1$, $(I - S)^{-1}$ has positive elements, denoted $(I - S)^{-1} > 0$. [Gan59]

The matrix R is a rectangular matrix corresponding to node to receiver transitions, so that like S, it is nonnegative, with elements less than one. Each column of R contains exactly one positive element. Since $(I - S)^{-1} > 0$ and R contains exactly one positive element in every column, $(I - S)^{-1}R > 0$, thus every receiver gets some power when power is injected into the network, as expected in a fully-connected network.

Another fact that will be useful in the chapter on analytical results is that RR^T is diagonal, where R^T denotes the transpose of the matrix R. Since each column of R has a single positive element, representing power to a receiver from its neighboring node, every row of R has a zero wherever another row has a positive element. The i-jth element of RR^T is simply the dot product of the i-th and j-th rows of R. This dot product must be zero unless $i = j$, therefore RR^T is diagonal.

S has zeroes along its diagonal, because nodes do not have self-loops. Finally, all non-zero elements on any row of the block matrix $[SR]$ are equal, due to the nodes' even splitting of power.

Chapter 3

Topologies

This chapter serves four purposes. First, it examines the appropriate choice of the number of nodes for a topology. Then it introduces several topologies to be used as examples throughout the thesis. Next, some numerical results begin the development of intuition for how the various topologies distribute power. Finally, there is a discussion of classifications of topologies that will aid the analysis in Chapter 4, as well as provide a framework in which to visualize the power distribution and physical structure of some topologies.

3.1 Number of Nodes

There is no restriction on whether there is a single transceiver or multiple transceivers per node, because the choice depends upon the particular topology and insertion loss in question. For example, compare two networks with the same topology, m transceivers, and i_n neighboring nodes per node, where a neighboring node is one to which power is transmitted, not one from which power is collected. Let the insertion loss in dB at each node be α.

Now suppose that in one network, $n = m$, while in the other network, $n < m$, where n is the number of nodes. Assuming that the topology is such that i_n does not change as the number of nodes changes, the topology with more nodes has longer paths

between the worst-case transmitter-receiver pair. These longer paths must have more insertion loss along them. However, if the transceivers are spread somewhat evenly among the nodes in each network, then each node in the toplogy in which $n = m$ has the same or less splitting loss than the nodes in the topology with fewer nodes, because the transceivers are spread more thinly when there are more nodes. Thus, there might be more or less splitting loss on the longer paths of the network with more nodes, depending on how much the splitting loss changed at each node as compared to the change in path lengths. If the splitting loss has increased over each path, then the minimum normalized power delivered will be higher for fewer nodes. If the splitting loss decreased enough to compensate for the increase in insertion loss over the longer paths, then the minimum normalized power delivered will be higher when $n = m$. Therefore, depending on α and the particular topology, performance in terms of delivered power may diminish or improve with fewer nodes than transceivers. In fact, for any topology, insertion loss, and number of transceivers, there is an optimal number of nodes, which will yield the highest minimum power level delivered.

To make this concrete, I now define some topologies to examine, shown in Figure 3.1. Part (a) of the figure shows several transceivers for clarity. In the rest of the figure, assume the transceivers are spread evenly among the nodes. All lines represent bi-directional links composed of two fibers. The figure depicts the logical arrangement of nodes, not the physical arrangement.

Figure 3.1(a) illustrates the star topology. Although it is not robust, it provides an upper bound on the minimum normalized power delivered in robust topologies with the same insertion loss as the star. This occurs because there is loss from only one coupler, and the rest of the power divides evenly, thus maximizing the minimum delivered power. The ring, illustrated in part (b) of Figure 3.1, is included, because it is a commonly used topology. Part (c) of the figure shows the wrap-around triangular mesh. The nodes and unbent links comprise a mesh with triangular cells. The bent links connect nodes at the edges of this mesh, hence the name "wrap-around" triangular mesh. The hexagonal and square meshes are shown in parts (d) and (e).

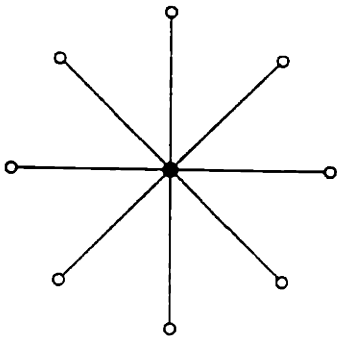

a) Star

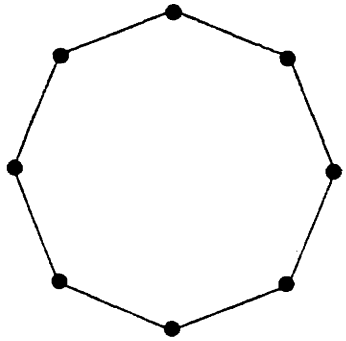

b) Ring

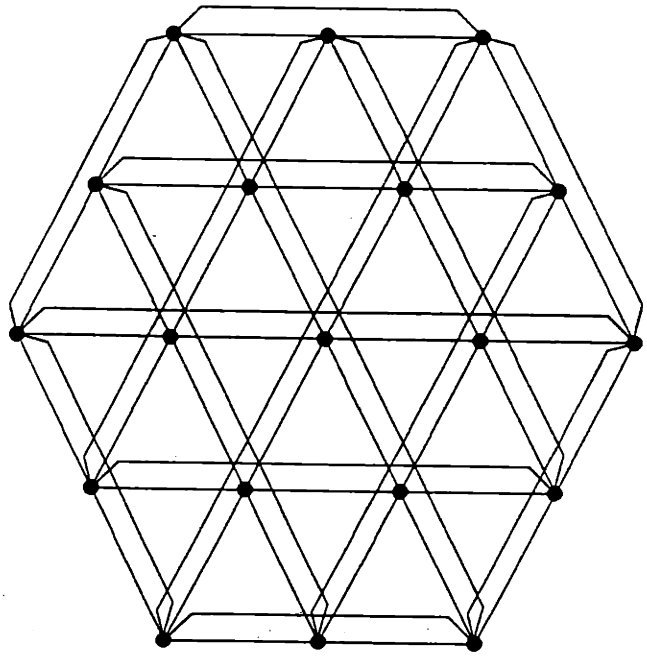

c) Wrap-Around Triangular Mesh

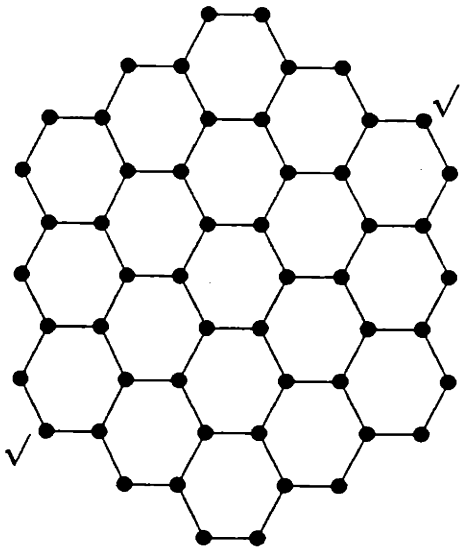

d) Hexagonal Mesh

Figure 3.1: Examples of Topologies

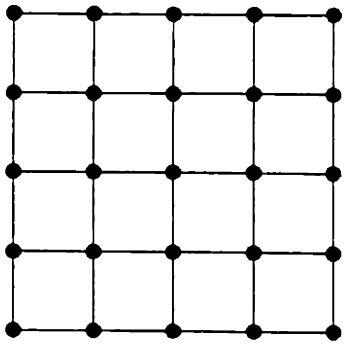

e) Square Mesh

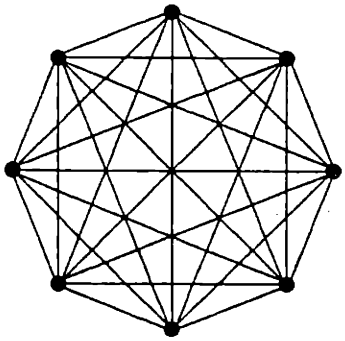

f) Fully-Connected Mesh

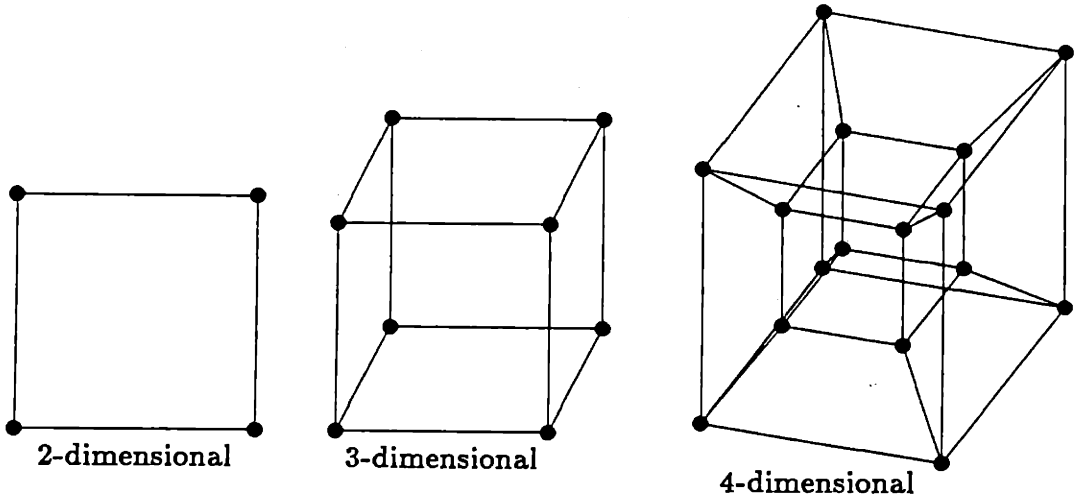

g) Hypercubes

Figure 3.1: Examples of Topologies

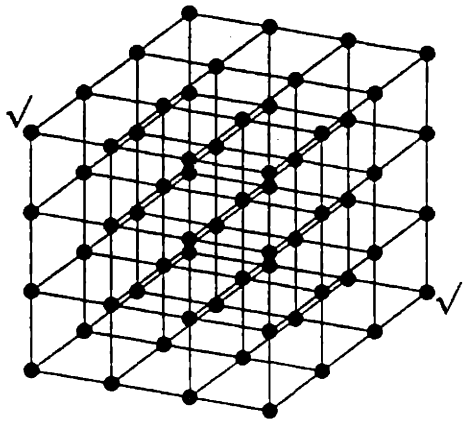

h) Lattice

Figure 3.1: Examples of Topologies

Both of these meshes can also be wrapped. Plots will display results for all of these meshes with and without wrap-around. In the fully-connected mesh of part (f), there are bi-directional links between every pair of nodes. Figure 3.1(g) shows three sizes of hypercubes to illustrate that a d-dimensional hypercube is constructed from two $(d-1)$-dimensional hypercubes joined appropriately. Finally, part (h) depicts the lattice. The wrap-around lattice is simply the lattice with the nodes wrapped left to right, top to bottom, and front to back.

Figures 3.2–3.5 show the normalized minimum power delivered in dB vs. the number of nodes for the topologies illustrated in Figure 3.1, assuming 128 transceivers and 0.3 dB insertion loss. For convenience, data points were computed for numbers of nodes which are powers of 2. To construct a robust topology in which nodes are not doubly-connected requires at least three nodes; therefore, the smallest number of nodes in each curve is 4. Straight lines connect the data points for a single topology. In the discussion of the plots, the term "optimal number of nodes" means the number of nodes corresponding to the data point depicting the highest minimum normalized power delivered. That is, it is the optimal number of nodes, rounded to the nearest power of 2.

I used the MATLAB software package on a DG20000 computer to compute the

results. In the plots, I assume insertion loss is uniform across couplers, even couplers of different sizes. Recall that the normalized minimum power delivered takes into account power collected over infinitely many paths, and thus upperbounds the performances of many practical networks. As long as this quantity exceeds the loss budget, all users are supported in this bounding case.

Before discussing the curves in the plots, a short justification of my choice of insertion loss is in order; therefore, I present current values of losses for very low loss star couplers and splices. Some of these components may not be commercially available now, and they may be expensive, but as this is forward-looking research, I hope that these components or better ones will be affordable when they are needed. At present, singlemode star couplers are difficult to manufacture in sizes larger than 2×2 [Bak87], although there is evidence that some researchers have used 3×3 singlemode couplers in experiments. [Kal86],[Dav87] Therefore, larger singlemode star couplers are typically built by splicing together these smaller couplers, thus the excess loss is strongly dependent on size. 2×2 singlemode couplers can be manufactured with excess loss as low as 0.05 dB [Bak87],[Moo86], while the losses of fusion splices and some mechanical splices for singlemode fiber can be as low as 0.1 dB. [Bak87] Excess loss in multimode couplers is not strongly dependent on size [Per85], and can be as low as 0.1 dB. [Bak87] Molded plastic splices for multimode fibers can have losses as low as 0.05dB. [Yos85] Thus top-grade multimode couplers and splices could produce insertion loss as low as 0.2 dB. Even very large couplers can have splitting ratios balanced to within 3 dB. [Per85]

As noted previously, the performance of the star topology provides an upper bound on the performances of the other topologies. The ring performs the worst, because in the worst-case even the strongest reception of the message has circulated around half the ring. Recall that every pass through a node means more loss, so that fewer nodes ought to provide better performance. The plot in Figure 3.2 demonstrates that within the range 4–128 nodes, the ring performs best with 4 nodes. Of course, for 4 nodes, the ring is indistinguishable from many of the other topologies.

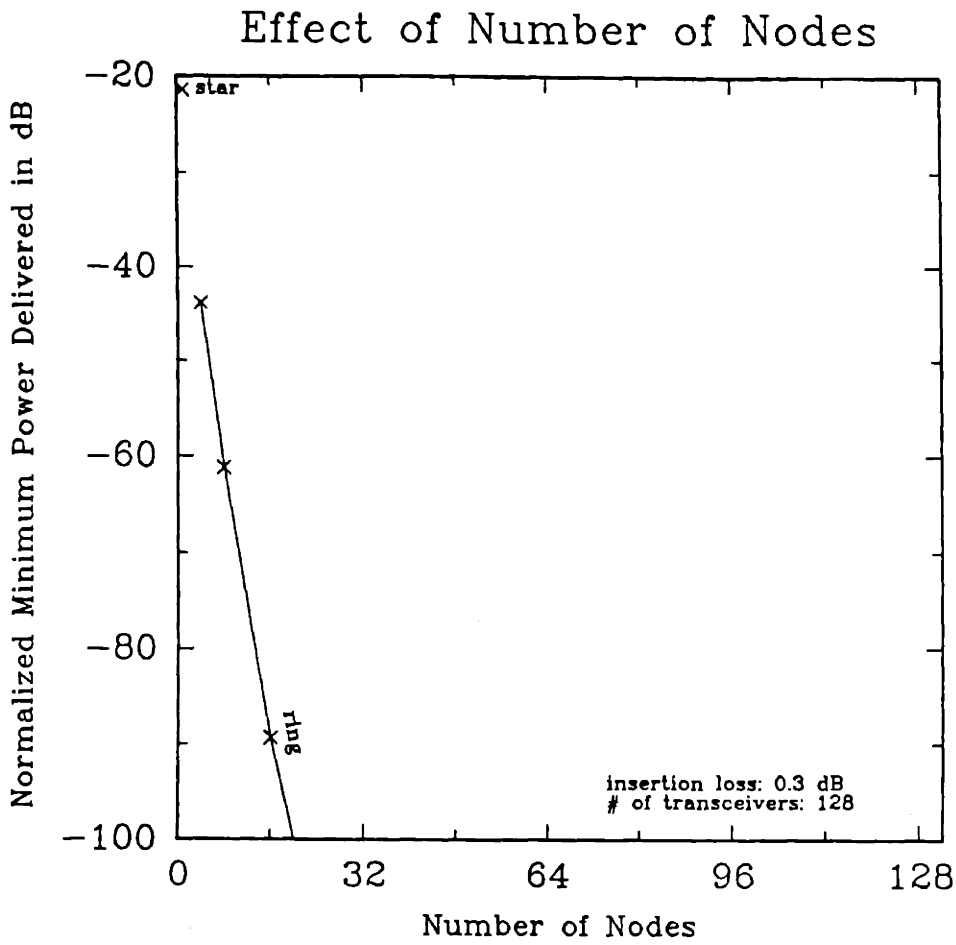

Figure 3.2: Power Delivered vs. Number of Nodes for Ring and Star

For the square, triangular, and hexagonal meshes and the lattice, the minimum power is always delivered between transceivers on "edge" nodes, which are the nodes that appear at the edges of these topologies as drawn in Figure 3.1. Example pairs of edge nodes whose transceivers deliver minimum power to each other have been checked off in the renderings of the hexagonal mesh and the lattice of Figure 3.1(d) and (h). Transceivers on edge nodes perform the worst because they have the fewest neighbor nodes and, therefore, the fewest paths between them; and they have the longest paths between them. Comparison of Figures 3.3 and 3.4 shows that each of these topologies performs worse than the corresponding wrap-around topology, in which edge nodes are connected to each other. The effect of connecting edge nodes is to provide a larger number of shorter paths between transceivers on those nodes, thereby improving the performance of the network overall.

In any of the wrap-around topologies, let m be the number of transceivers, n be the number of nodes, and i_n be the number of neighboring nodes per node. As the number of nodes increases, and the transceivers are spread out more thinly among them, the splitting loss, $10\log[i_n + m/n]$, decreases, so that one might expect the minimum power to increase. However, as the number of nodes increases, the path lengths, in number of links, between worst-case transmitter-receiver pairs increase, causing the loss along each path to increase. For small numbers of nodes, increasing the number of nodes dramatically decreases splitting loss, so that performance improves. As the number of nodes continues to increase, the effect of increasing path lengths becomes stronger than the effect of decreasing splitting loss, and performance diminishes. The expression for splitting loss is approximate when m/n is not an integer, because in such a case, some nodes have more splitting loss than others.

In Figure 3.4, the curve for the wrap-around lattice shows the behavior described in the previous paragraph, as would the curve for the wrap-around triangular mesh if not for the arbitrary definition of it for four nodes. From the plot, the best number of nodes to choose for 128 transceivers and 0.3 dB insertion loss is 64 for the lattice, and 4 for the wrap-around triangular mesh. The curves for the wrap-around square and

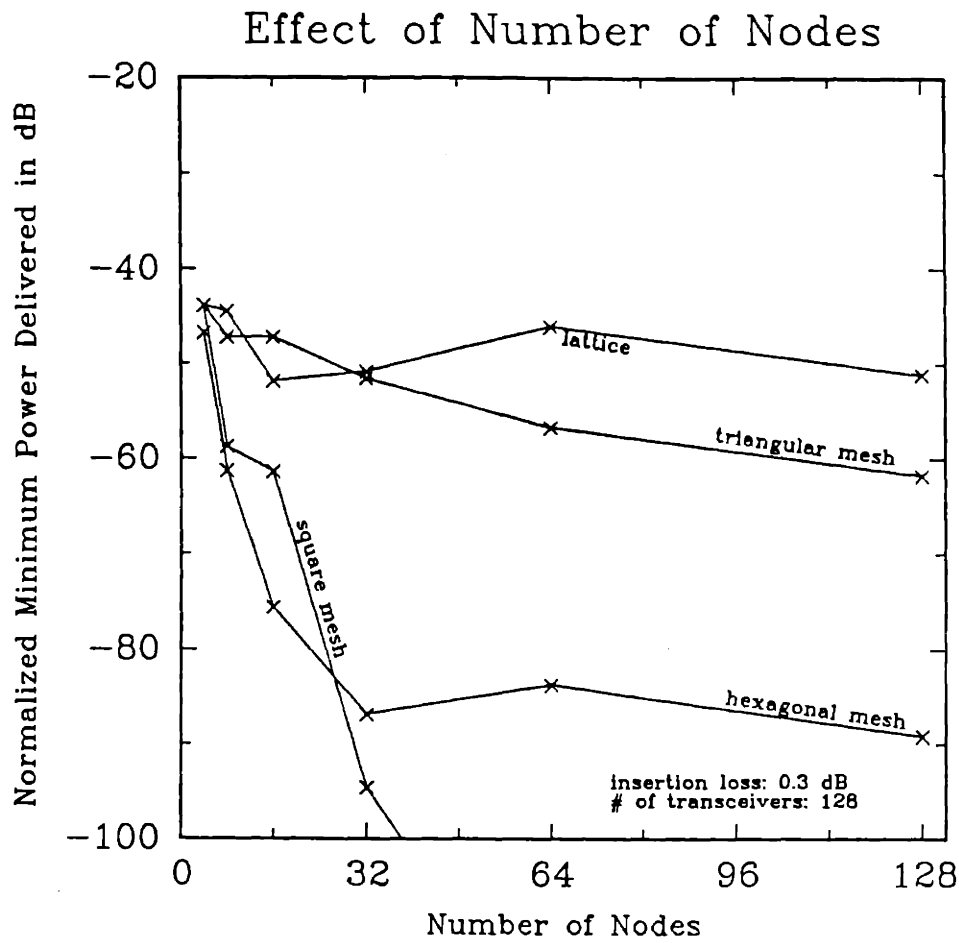

Figure 3.3: Power Delivered vs. Number of Nodes for Three Meshes and Lattice

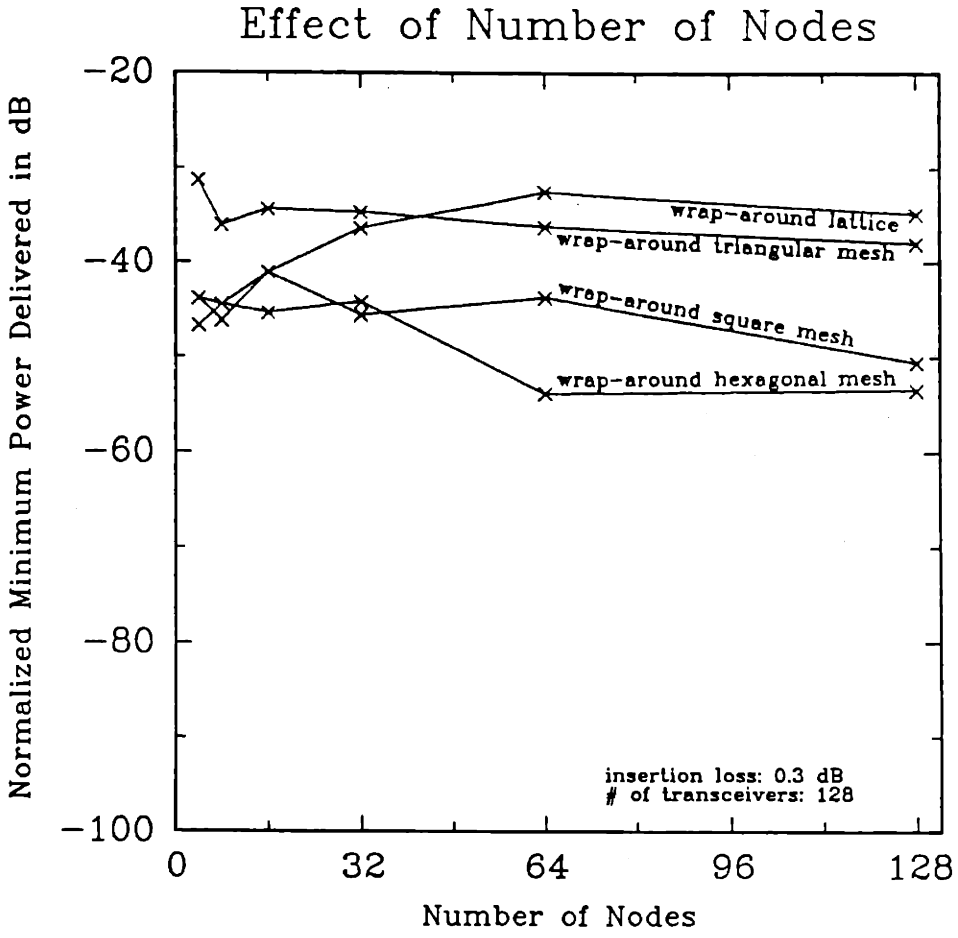

Figure 3.4: Power Delivered vs. Number of Nodes for Three Wrap-Around Meshes and Wrap-Around Lattice

hexagonal meshes are irregular, because the topologies could not be synthesized in exactly the same way for each of the data points plotted. However, looking at every other data point for the wrap-around square mesh reveals the expected behavior. This is because one set of every other point includes only numbers of nodes that are perfect squares, and the other includes only numbers of nodes that are twice perfect squares. Of the data points plotted, the optimal number of nodes for the wrap-around square mesh is 16, while for the wrap-around hexagonal mesh it is 32.

In the fully-connected mesh, the splitting loss at each node is $10\log[n-1+m/n]$. Because of the behavior of the argument of the logarithm, the splitting loss attains a minimum at $n=\sqrt{m}$. Thus for $m=128$, we find that the splitting loss decreases as n increases to 11, and then increases as n continues to increase. The splitting loss is the same for $n=8$ and $n=16$. Naturally, when the splitting loss decreases, the minimum power delivered increases, and vice-versa, as shown in Figure 3.5.

In this topology, every node has a single-link path to every other node, regardless of the number of nodes. Thus, increasing the number of nodes does not tend to increase path lengths. However, another effect of changing the number of nodes is to change the number of paths of a given length between any two transceivers. The reason that the minimum power is higher for $n=16$ than for $n=8$ in the fully-connected mesh is that although insertion loss and splitting loss are the same at every node for both the 8-node and 16-node topologies, there are more paths of any given length and strength in the 16-node fully-connected mesh. Therefore, for 128 users and 0.3 dB insertion loss, the optimal number of nodes for a fully-connected mesh is 16.

For the hypercube, performance unexpectedly diminishes in going from the $n=4$ case to the $n=8$ case. The splitting loss at each node for this topology is $10\log[\log_2 n+m/n]$, so that based on the splitting loss argument, performance should improve. However, path lengths increase as n increases. In jumping from $n=4$ to $n=8$, for 0.3 dB insertion loss, the effect of increasing path lengths dominates, causing performance to diminish, but in increasing the number of nodes beyond $n=8$, the splitting loss effect dominates. The splitting loss will continue to decrease until

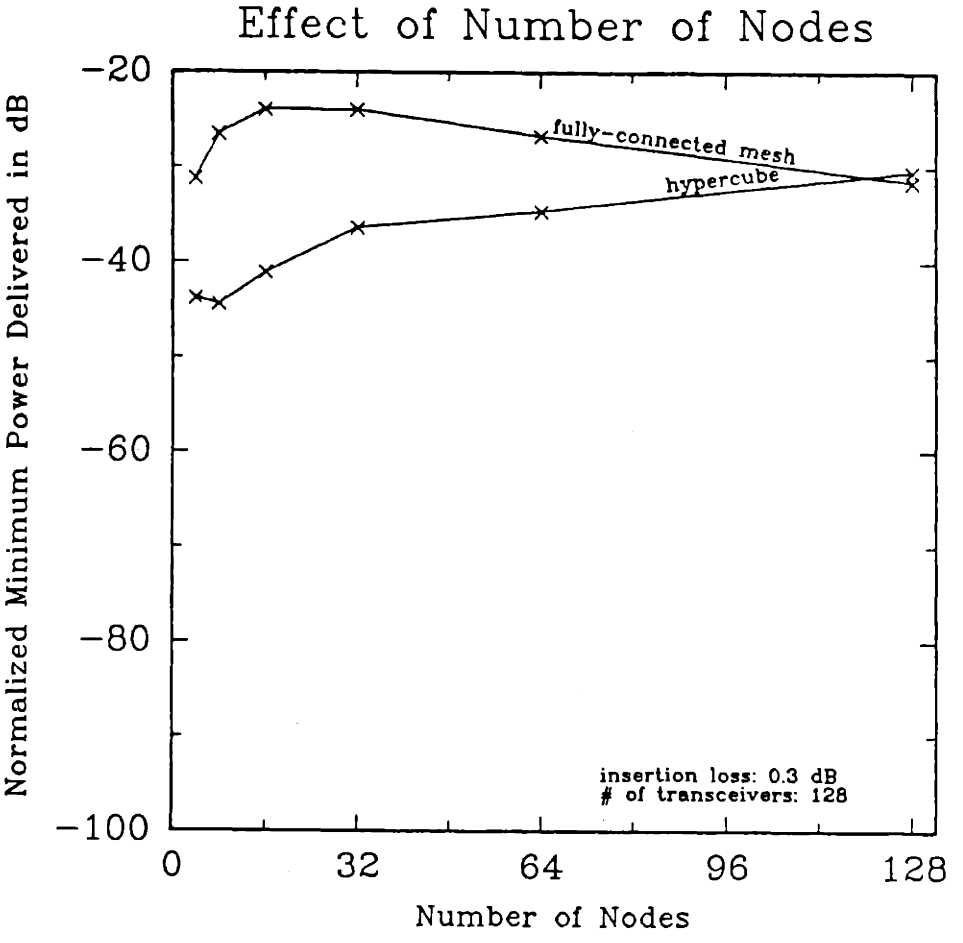

Figure 3.5: Power Delivered vs. Number of Nodes for Fully-Connected Mesh and Hypercube

$n = 88$. For this insertion loss and number of transceivers, the optimal number of nodes for a hypercube (whose number of nodes must be a power of 2) is 128.

3.2 Power Homogeneity

Due to the difficulty of obtaining general results applicable to all topologies, some classification of topologies is necessary. To that end, I first consider power homogeneous topologies, defined to be those for which the power distribution, in terms of the numbers of receivers getting the various levels of delivered power, is the same, no matter which transmitter is active; and, simultaneously, the converse property, that every receiver receives the same set of power levels, holds. The following two paragraphs explain the motivation for focusing on the class of power homogeneous topologies.

The performance of a transceiver is a function of the power distribution in the network. For the case of interest, in which performance is determined by the total power reaching the receiver, the worst that a transceiver can perform and still remain supported is to deliver the minimum detectable power to all receivers, and to collect the minimum detectable power from all transmitters. The minimum detectable power is determined by the modulation scheme and the desired bit error rate. Improving one transceiver's performance diminishes another's performance, unless the improvement was effected by decreasing loss.

I maximize the number of supportable users by maximizing the performance of the transceiver with the worst, or minimum, performance. As long as the worst transceiver performs above some threshold, it may be possible to add more users to the network. Naturally, the minimum is maximized if all transceivers perform identically. This can be achieved independently of how performance depends on power distribution and collection, if all transceivers deliver the same power levels to the same numbers of receivers, and collect the same power levels from the same numbers of transmitters; that is, if the topology is power homogeneous.

To understand the implications of power homogeneity on the matrix which describes the network, let T be the matrix representing transmitter to node power flow. T is a matrix of 1's and 0's, with one 1 on every row, and as many 1's in column i as there are transmitters attached to node i. The property of power homogeneity implies that in the matrix $T(I-S)^{-1}R$, representing power delivered from all transmitters to all receivers over all paths, every row is a permutation of every other row, and every column is a permutation of every other column. The following is an example of a matrix with this property:

$$\begin{pmatrix} a & b & c & d \\ c & d & a & b \\ d & c & b & a \\ b & a & d & c \end{pmatrix}$$

Due to the structure of T, $T(I-S)^{-1}R$ is simply $(I-S)^{-1}R$ expanded so that it becomes a square matrix with the row corresponding to power distribution from node i repeated once for each transmitter on node i. Thus every row of $(I-S)^{-1}R$ is a permutation of every other row.

3.3 Physical Homogeneity

A physically homogeneous topology is one in which the network "looks the same" from the point of view of every transceiver in the network, and that also "looks the same" from every node. Another way of saying this is that nodes are indistinguishable. One property of a topology with indistinguishable nodes is that all nodes must have the same number of neighboring nodes and transceivers, so that power splitting is the same at every node. This property is called "uniform connectivity." To be more specific, imagine a drawing of the network as a collection of black dots (nodes), white dots (transceivers), lines (links), arrows (direction of power flow), and fractions (power splitting). Since every node has the same power splitting, all of the fractions are the same, determined by insertion loss and number of neighboring nodes and transceivers. Therefore, they can be left off of the drawing, since they will not help any further

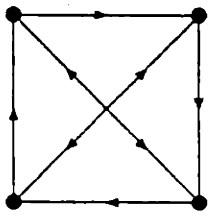

$$S = \begin{pmatrix} 0 & s & s & 0 \\ 0 & 0 & s & s \\ s & 0 & 0 & s \\ s & s & 0 & 0 \end{pmatrix}$$

Figure 3.6: A Directed Graph Representing Nodal Connectivity, and a Corresponding Matrix

in determining whether nodes are indistinguishable. Every node also has the same number of transceivers connected to it by bi-directional links, therefore these do not help to determine whether nodes are indistinguishable, and they can be left off of the drawing. The black dots, lines, and arrows that are left are simply the directed graph of the matrix S, showing connectivity between nodes. There is a directed line from node i to node j if the i-jth element of S is positive. Figure 3.6 shows such a directed graph, along with an example matrix S. The value of the positive elements s depends upon the network's insertion loss and number of transceivers.

A physically homogeneous topology is one such that if the location of any node (black dot) is chosen as the target, and if any node is placed on the target, then the directed graph can be redrawn with nodes, lines and arrows placed in exactly the same positions as before, as long as lines can change length, and arrows can slide along lines, but not through nodes. Another way to describe this is that if any node in the directed graph is numbered "1," there exists a numbering of the other nodes that will yield the same matrix S. Figure 3.7 shows such renumberings of nodes of the toplogy of Figure 3.6, illustrating that the topology is physically homogeneous.

Physical homogeneity has implications for the matrix S. First of all, since every node has the same number of incoming and outgoing links from other nodes, and since power splitting is the same at every node, S has i_n positive elements in every row and column, where i_n is the number of neighboring nodes, and all of the positive elements

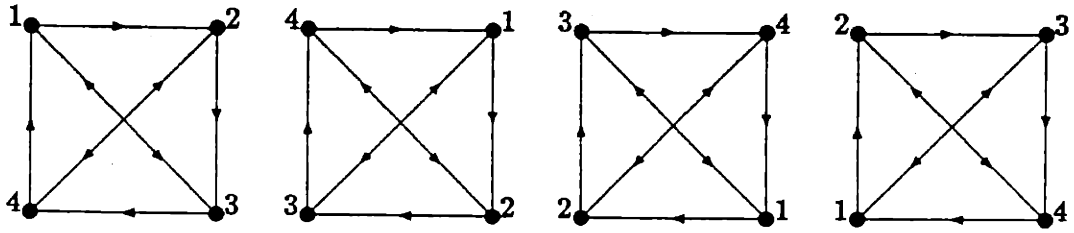

Figure 3.7: Renumberings of Nodes of a Topology, Illustrating that the Topology is Physically Homogeneous

are equal. Also, each node must have the same number of uni-directional and bi-directional links to neighboring nodes, otherwise the nodes would be distinguishable. In the topology of Figure 3.6, each node has one uni-directional link and one bi-directional link to neighboring nodes. Each bi-directional link corresponds to a pair of positive elements reflected across the main diagonal of the matrix, and each uni-directional link corresponds to a positive element which is not reflected across the diagonal. Therefore, if there are i_r positive elements on one row reflected across the main diagonal of the matrix, then there must be i_r elements on every row reflected across the main diagonal. For example, in Figure 3.6, $s_{12} = s$ is not reflected across the diagonal, since $s_{21} = 0$. s_{12} represents a uni-directional link from node 1 to node 2. $s_{13} = s$ is reflected across the diagonal, since $s_{31} = s$ also. Thus, s_{13} and s_{31} represent a bi-directional link between nodes 1 and 3. In Figure 3.6, every row of the matrix has one positive element which is reflected across the main diagonal, and one positive element which is not.

Of the topologies in Figure 3.1, the star, ring, fully-connected mesh, and hypercube are physically homogeneous. The wrap-around meshes and wrap-around lattice are physically homogeneous as long as the nodes are laid out and the links are wrapped properly. For example, the method of wrapping the lattice described in Section 3.1 results in a physically homogeneous topology. Figure 3.8 depicts physically homogeneous wrap-around meshes. In the figure, the dashed lines are the "wrap-around"

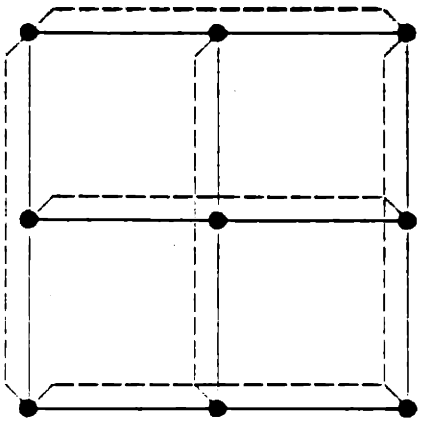

Wrap-Around Square Mesh

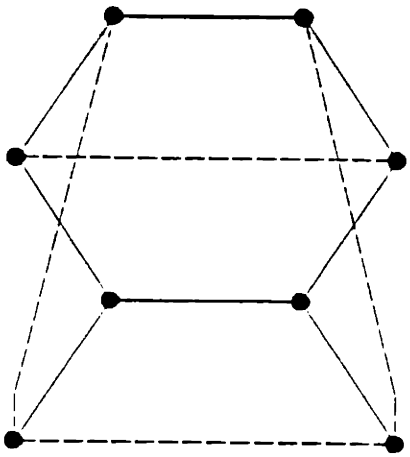

Wrap-Around Hexagonal Mesh

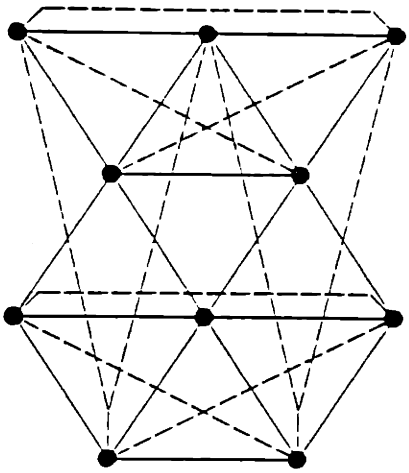

Wrap-Around Triangular Mesh

Figure 3.8: Physically Homogeneous Wrap-Around Meshes

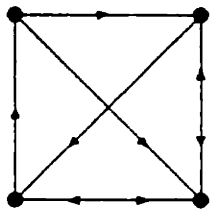

$$S = \begin{pmatrix} 0 & s & s & 0 \\ 0 & 0 & s & s \\ 0 & s & 0 & s \\ s & 0 & s & 0 \end{pmatrix}$$

Figure 3.9: A Uniformly Connected Topology, and a Corresponding Matrix

links.

By symmetry, a physically homogeneous topology is also power homogeneous; therefore, the matrix $T(I-S)^{-1}R$ has rows and columns which are permutations of one another. $T(I-S)^{-1}R$ is simply $(I-S)^{-1}R$ with each row repeated m/n times, where m is the number of transceivers and n the number of nodes in the network. For a physically homogeneous topology, R is simply a scaled version of a matrix with m/n 1's in every row, and one 1 in every column. Thus $(I-S)^{-1}R$ is simply a scaled version of $(I-S)^{-1}$ with every column repeated m/n times. Therefore, for a physically homogeneous topology, $T(I-S)^{-1}R$ is a scaled version of $(I-S)^{-1}$ with each column, and then each row, repeated m/n times. Since the rows and columns of $T(I-S)^{-1}R$ are permutations of one another, so $(I-S)^{-1}$ has each row a permutation of every other row, and each column a permutation of every other column.

Physically homogeneous topologies are always uniformly connected, and always power homogeneous, but in general, a uniformly connected topology is not necessarily power homogeneous or physically homogeneous. Figure 3.9 shows an example of a uniformly connected topology which is neither physically homogeneous nor power homogeneous, and its associated matrix S. Note that the matrix S has all positive elements equal, and that there are the same number of positive elements in every row, but not in every column. The Venn diagram in Figure 3.10 expresses the relationships between the various classes of topologies.

Within these classes of topologies, I can further classify topologies according to

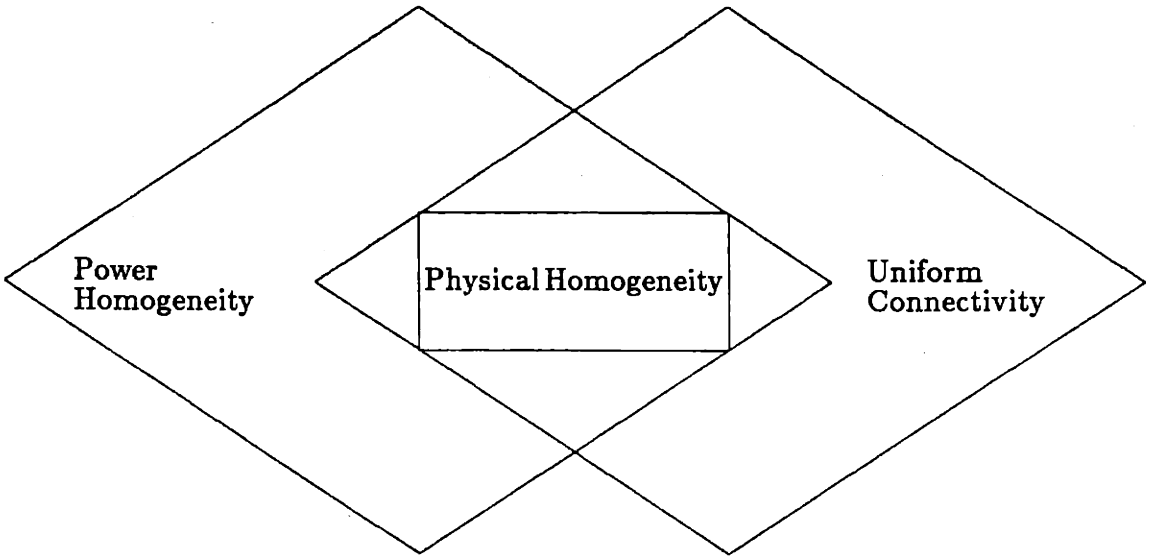

Figure 3.10: Relationships Between Classes of Topologies

characteristics of the matrix S, as in the following chapter on analytical results.

Chapter 4

Analytical Results

The results in this chapter are for uniformly connected topologies, and subclasses of uniformly connected topologies. First, an expression for the mean normalized power delivered between transceivers is derived. Further analysis results from classifying topologies according to matrix properties. There are results for normal matrices, circulant matrices, and generalized circulant matrices. I define the following parameters to be used throughout the analysis:

n number of nodes in network

m number of transceivers in network

α insertion loss of nodes in dB

$g = 10^{-\alpha/10}$ fraction of power into a node which is distributed to other nodes and to receivers

i_n number of neighboring nodes per node

Theorem 2 *Let $\overline{P}$ be the mean of the normalized power delivered between all pairs of transmitters and receivers in a uniformly connected, passive FOLCN.*

$$\overline{P} = \frac{g}{m + n(1-g)i_n}$$

PROOF:

Let s be the fraction of power into a node that goes to another node, or to a receiver.

$$s = \frac{\text{fraction of power distributed from node}}{\text{number of neighboring nodes and transceivers}} = \frac{g}{m/n + i_n} \tag{4.1}$$

assuming m/n is an integer, which it must be for a uniformly connected topology.

The mean power delivered is

$$\begin{aligned}
\overline{P} &= \frac{1}{m} \times (\text{total power delivered to all receivers}) \\
&= \frac{1}{m} \sum_{k=0}^{\infty} (\text{total power delivered over all paths of length } k) \\
&= \frac{1}{m} \sum_{k=0}^{\infty} (\#\text{ paths of length } k) \times (\text{power delivered over path of length } k) \\
\overline{P} &= \frac{1}{m} \sum_{k=0}^{\infty} i_n^k s^k \frac{m}{n} s
\end{aligned} \tag{4.2}$$

i_n^k is the number of paths of k node-to-node links leading from the node connected to the active transmitter. s^k is the fraction of the input power arriving at the last node of a path of k links, while $\frac{m}{n}s$ is the fraction of that power that goes to all of the receivers connected to the last node on the path. Substituting for s from Equation 4.1 completes the proof.

$$\begin{aligned}
\overline{P} = \frac{s}{n} \sum_{k=0}^{\infty} (i_n s)^k = \frac{s}{n(1 - i_n s)} &= \frac{g}{n\left(\frac{m}{n} + i_n\right)\left(1 - \frac{i_n g}{\frac{m}{n} + i_n}\right)} = \frac{g}{n\left[\frac{m}{n} + (1-g)i_n\right]} \\
\overline{P} &= \frac{g}{m + n(1-g)i_n}
\end{aligned} \tag{4.3}$$

As one might expect, the mean power delivered increases as g increases, because the total power and the mean power delivered must increase as the loss in the nodes decreases. The mean power delivered must decrease when power divides among more transceivers. Indeed, according to Equation 4.3, $\overline{P}$ decreases as m increases.

$\overline{P}$ also decreases as n increases. As more nodes are added to a network, two things might happen, depending upon the topology in question. Some path lengths might increase, causing more loss along those paths and a correspondingly lower mean power, or the number of paths of a given length might increase, causing more loss

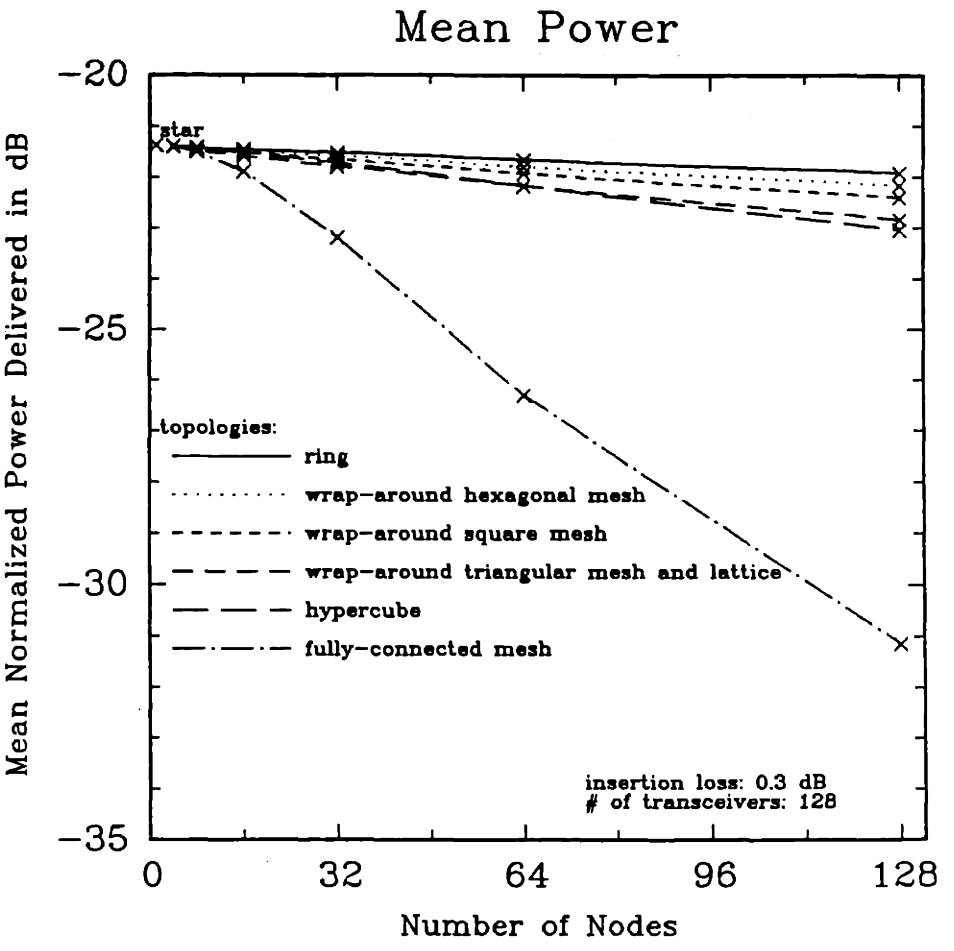

Figure 4.1: Mean Normalized Power Delivered Between All Transmitter-Receiver Pairs for Some Physically Homogeneous Topologies

among the collection of all paths of that length and a correspondingly lower mean power. Increasing the number of neighboring nodes per node also causes the mean power to decrease, due to the increase in the splitting loss at each node, and the increased number of paths of any given length.

Figure 4.1 shows the mean normalized power delivered between all transmitter-receiver pairs plotted against the number of nodes, for some physically homogeneous topologies with 128 transceivers and 0.3 dB insertion loss. These topologies are uniformly connected by virtue of being physically homogeneous. For all topologies, the mean decreases as the number of nodes increases. For a given number of nodes, topologies with fewer neighboring nodes per node have a higher mean power than

topologies with more neighboring nodes per node.

4.1 Results When S is Normal

If the node to node power distribution matrix, S, is normal, then the mean-square of the normalized power delivered between all transmitter-receiver pairs can be found in the form of a summation. The matrix S is normal if $SS^T = S^TS$. An example of a normal matrix is a real, symmetric matrix. [Dav79] Furthermore, any uniformly connected topology with bi-directional links has a matrix S which is real and symmetric.

Theorem 3 *Let $\overline{P^2}$ be the mean-square of the normalized power delivered between all transmitter-receiver pairs in a uniformly connected, passive FOLCN, and let S be the matrix representing node to node power distribution. If S is normal, then*

$$\overline{P^2} = \left(\frac{g}{m + ni_n}\right)^2 \sum_{i=1}^{n} \frac{1}{|1 - \nu_i|^2}$$

where $\{\nu_i | 1 \leq i \leq n\}$ are the eigenvalues of S.

PROOF:

The following lemmas will help in the proof.

Lemma 1 *If $f(\cdot)$ is a polynomial function, and S is a square, $n \times n$ matrix with eigenvalues $\{\nu_i | 1 \leq i \leq n\}$, then the eigenvalues of $A = f(S)$ are $\{\lambda_i = f(\nu_i) | 1 \leq i \leq n\}$.*

PROOF OF LEMMA: Appendix A

Lemma 2 *Let A be an $n \times n$, real, normal matrix, with eigenvalues $\{\lambda_i | 1 \leq i \leq n\}$. If $\{\nu_i | 1 \leq i \leq n\}$ are the eigenvalues of A^TA, then*

$$\nu_i = |\lambda_i|^2, \quad 1 \leq i \leq n$$

PROOF OF LEMMA: [Gan60], pp. 271–272

Let $A = (I - S)^{-1}$. The mean-square of the normalized power delivered is

$$\overline{P^2} = \frac{1}{nm} \sum_{i=1}^{n} \sum_{j=1}^{m} ([AR]_{ij})^2 \tag{4.4}$$

The diagonal elements of $(AR)(AR)^T$ are

$$[(AR)(AR)^T]_{ii} = \sum_{j=1}^{m} ([AR]_{ij})^2, \quad 1 \leq i \leq n \tag{4.5}$$

so that

$$\overline{P^2} = \frac{1}{nm} \sum_{i=1}^{n} [(AR)(AR)^T]_{ii} = \frac{1}{nm} \mathrm{Tr}[(AR)(AR)^T] \tag{4.6}$$

where Tr denotes the trace of a matrix.

Since the trace of a product of matrices does not change when the factors are cyclically permuted [Her75], Equation 4.6 can be rewritten.

$$\overline{P^2} = \frac{1}{nm} \mathrm{Tr}[ARR^T A^T] = \frac{1}{nm} \mathrm{Tr}[RR^T A^T A] \tag{4.7}$$

From Section 2.4, RR^T is diagonal. Since each diagonal element is the dot product of a row of R with itself, and since each row of R contains m/n elements of value s and the remaining elements are 0, the diagonal elements of RR^T have value $s^2 m/n$, with s given by Equation 4.1. Continuing the derivation of $\overline{P^2}$,

$$\overline{P^2} = \frac{1}{nm} \mathrm{Tr}\left[\frac{m}{n} s^2 I A^T A\right] = \frac{s^2}{n^2} \mathrm{Tr}[A^T A] = \left(\frac{g}{m + ni_n}\right)^2 \mathrm{Tr}[A^T A] \tag{4.8}$$

If S is normal, then $A = (I - S)^{-1}$ is normal. By Lemma 1, if $\{\nu_i | 1 \leq i \leq n\}$ are the eigenvalues of S, then $\{\lambda_i = \frac{1}{1-\nu_i} | 1 \leq i \leq n\}$ are the eigenvalues of A. By Lemma 2, the eigenvalues of $A^T A$ are $\{|\lambda_i|^2 = \frac{1}{|1-\nu_i|^2} | 1 \leq i \leq n\}$. Since the trace of a matrix equals the sum of its eigenvalues [Gan60], $\overline{P^2}$ can be expressed as stated in the theorem.

$$\overline{P^2} = \left(\frac{g}{m + ni_n}\right)^2 \sum_{i=1}^{n} \frac{1}{|1 - \nu_i|^2} \tag{4.9}$$

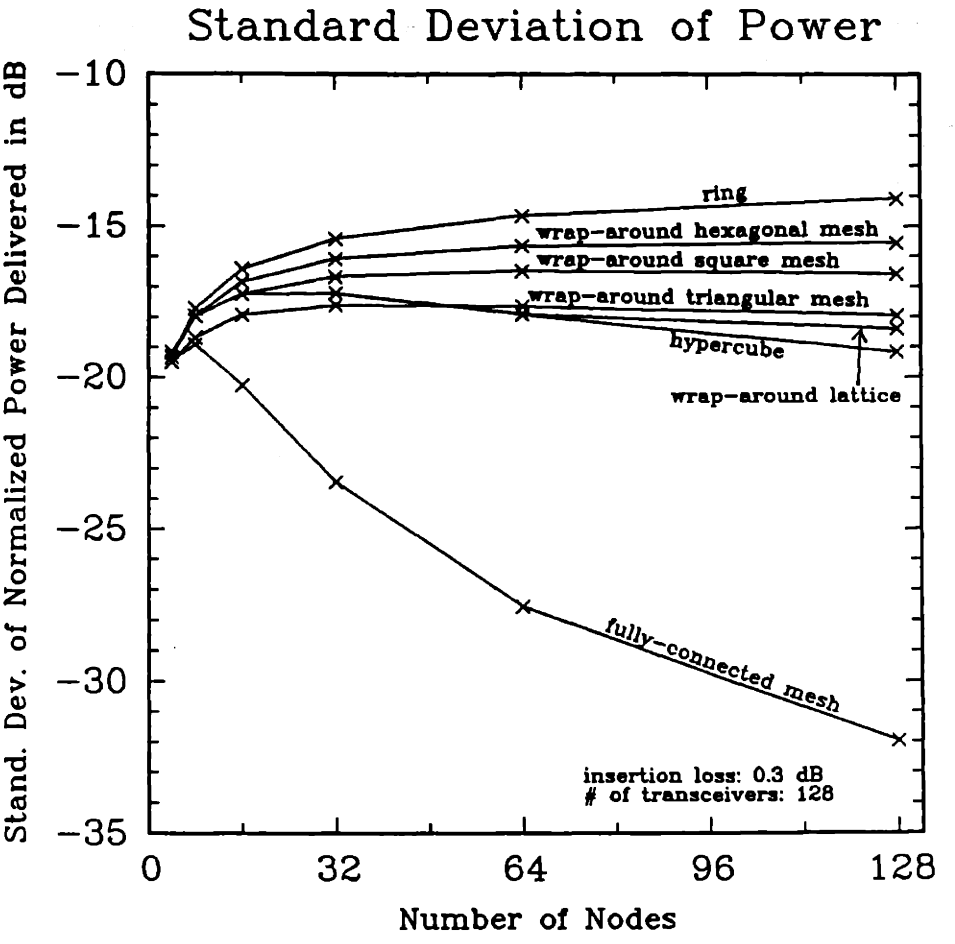

Figure 4.2: Standard Deviation of Normalized Power Delivered Between All Transmitter-Receiver Pairs for Some Physically Homogeneous Topologies

The standard deviation of the normalized power delivered between all transmitter-receiver pairs in a uniformly connected, passive FOLCN with a normal node to node power distribution matrix is

$$\left(\overline{P^2} - \overline{P}^2\right)^{1/2} = \left\{ \left(\frac{g}{m + ni_n}\right)^2 \sum_{i=1}^{n} \frac{1}{|1 - \nu_i|^2} - \left[\frac{g}{m + n(1-g)i_n}\right]^2 \right\}^{1/2} \tag{4.10}$$

Figure 4.2 plots $\left(\overline{P^2} - \overline{P}^2\right)^{1/2}$ vs. the number of nodes for several physically homogeneous topologies with normal node to node power distribution matrices, 128 transceivers, and 0.3 dB insertion loss. These are physically homogeneous topologies with bi-directional links.

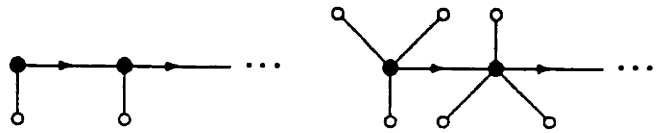

Figure 4.3: Two Busses with Different Splitting Losses

The shapes of the curves in the plots can be understood intuitively. In the ring topology, the more nodes there are, the greater the difference between the power levels received by receivers on the same node as the active transmitter, and receivers halfway around the ring from the active transmitter. Therefore, the more nodes there are, the greater the standard deviation of the power levels delivered by any transmitter.

Another mechanism at work here is the splitting loss at each node. When less power goes to the receivers at a node, the standard deviation tends to decrease. Consider the example of the uni-directional bus topology. Figure 4.3 shows two nodes of two busses, one with splitting loss of 3 dB at each node, and the other with splitting loss of 6 dB per node. On the bus with one transceiver per node, if power starts at the leftmost node, the first receiver gets 1/2 of the input power, the second receiver gets 1/4 of the input power, and the standard deviation of power among receivers on the first two nodes is $\left\{\frac{1}{2}\left[\left(\frac{1}{2}-\frac{3}{8}\right)^2+\left(\frac{1}{4}-\frac{3}{8}\right)^2\right]\right\}^{1/2}=\frac{1}{8}$. On the bus with three transceivers per node, if power starts at the leftmost node, the first three receivers get 1/4 of the input power, the next three receivers get 1/16 of the input power, so that the standard deviation of power among the first two nodes is $\left\{\frac{1}{6}\left[3\left(\frac{1}{4}-\frac{5}{32}\right)^2+3\left(\frac{1}{16}-\frac{5}{32}\right)^2\right]\right\}^{1/2}=\frac{3}{32}<\frac{1}{8}$. Thus, the standard deviation tends to be lower when the splitting loss is higher.

This effect explains some, but not all, of the features in the plot of Figure 4.2. It explains why, for a given number of nodes, the standard deviation is lower for topologies with more neighboring nodes per node, and it explains the shape of the curve for the fully-connected mesh. Notice that the standard deviation is lower for the 16-node fully-connected mesh than for the 8-node fully-connected mesh. For this

topology, all receivers on the same node as the active transmitter get more power than all of the other receivers, and all of the other receivers get the same amount of power, as will be established in Section 4.2.2. Although the splitting loss is the same for both the 8-node and the 16-node fully-connected meshes, the 16-node fully-connected mesh has fewer receivers getting more power than the rest, so that the standard deviation of the power is lower for the 16-node fully-connected mesh.

None of this explains why the standard deviation goes down as the number of nodes increases, for large numbers of nodes, in the other meshes and the lattice; or why, in the hypercube, the standard deviation begins to decrease as the number of nodes increases, for numbers of nodes smaller than 88. I conjecture that this occurs because as the number of nodes increases, the numbers of receivers at the tails of the power distribution, receiving the most power and the least power, decreases.

In some cases, Figures 4.1 and 4.2 are useful for predicting which topologies have a higher minimum power delivered, but in other cases, predictions fail. For instance, the 4-node ring has mean normalized power -21 dB $\approx$ 0.008, with standard deviation -19 dB $\approx$ 0.01. The 64-node wrap-around lattice has mean normalized power -22 dB $\approx$ 0.006, with standard deviation -18 dB $\approx$ 0.02. This information might lead to the conclusion that the minimum power is probably higher in the 4-node ring than in the 64-node wrap-around lattice, for 128 transceivers and 0.3 dB insertion loss. According to Figures 3.2 and 3.4, this conclusion is wrong. The 16-node fully-connected mesh has mean normalized power -22 dB $\approx$ 0.006 with standard deviation -20 dB = 0.01. Therefore, the 16-node fully-connected mesh probably has higher minimum power than the 64-node wrap-around lattice for 128 transceivers and 0.3 dB insertion loss. This prediction is in fact borne out by Figures 3.4 and 3.5.

4.2 Results When S is Circulant

Another type of normal matrix, in addition to a real symmetric matrix, is a circulant matrix. [Dav79] A circulant matrix is one for which every row is equal to the previous

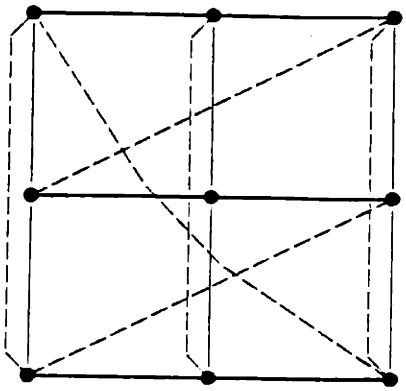

Figure 4.4: Wrap-Around Square Mesh with Circulant Matrix S

row with every element but the last shifted one place to the right, and the last element placed in the first position. In other words, if S is circulant, then $s_{ij} = s_{(j-i) \bmod n+1}$, $1 \leq i,j \leq n$. (S is $n \times n$.) [Dav79] For example, the following 4×4 matrix is circulant:

$$\begin{pmatrix} a & b & c & d \\ d & a & b & c \\ c & d & a & b \\ b & c & d & a \end{pmatrix}$$

In Figure 3.1, the ring and fully-connected mesh must have circulant matrices, while the wrap-around topologies can have circulant matrices if they are wrapped appropriately. Figure 4.4 shows a wrap-around square mesh with a circulant node to node power distribution matrix. When the nodes corresponding to a topology with a circulant matrix S are placed in a circle in order of index, the resulting graph looks the same when it is rotated by one node. For instance, suppose, in Figure 4.4, that the nodes of the wrap-around square mesh were numbered left to right and top to bottom, from 1 to 9. Figure 4.5 shows the same topology with the nodes laid out in a circle, in order from 1 to 9. A topology with a circulant node to node power distribution matrix is always physically homogeneous.

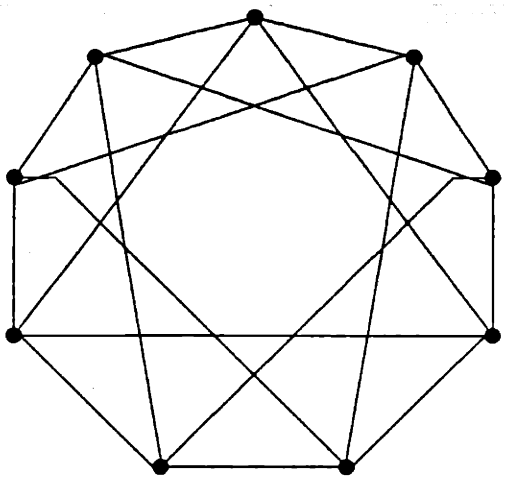

Figure 4.5: Wrap-Around Square Mesh with Circulant Matrix S, Rearranged

4.2.1 Minimum Power Delivered

Because of the structure of the matrix R, described in Section 2.4, the matrix $AR = (I - S)^{-1}R$, representing normalized power delivered between all pairs of transceivers, is simply the matrix A, scaled by s, with each column repeated m/n times. s is given by Equation 4.1. Due to this structure, the minimum normalized power delivered between all pairs of transceivers is simply $p_{min} = s \min_{i,j}[a_{ij}]$, where a_{ij} is the i-jth element of A.

Theorem 4 *If S is circulant, then $A = (I - S)^{-1}$ is circulant.*

PROOF:

The following two lemmas help prove this theorem.

Lemma 3 *A sum of circulant matrices is a circulant matrix.*

Lemma 4 *The inverse of a circulant matrix, if it exists, is a circulant matrix.*

PROOF OF LEMMA: [Dav79], pg. 74

By Lemma 3, S is circulant implies $I - S$ is circulant. By Lemma 4, $I - S$ is circulant implies $(I - S)^{-1}$ is circulant. Therefore, if S is circulant, then A is circulant.

Since A is circulant, all rows are cyclic shifts of the first row, so that the whole matrix is completely characterized by its first row. Therefore, set $a_i = a_{1i}$, so that the minimum normalized power can be expressed as $p_{min} = s \min_i[a_i]$. Now the minimum normalized power can be expressed directly in terms of elements of the matrix S, where $s_i = s_{1i} = 0$ or s.

Theorem 5 *In a passive FOLCN with a circulant node to node power distribution matrix S, the minimum normalized power delivered between all pairs of transceivers is*

$$p_{min} = s \min_i \left[\frac{1}{n} \sum_{j=1}^{n} \frac{\overline{w}^{(i-1)(j-1)}}{1 - \sum_{k=1}^{n} s_k w^{(j-1)(k-1)}} \right]$$

where

$$w = \exp\left[\sqrt{-1}\frac{2\pi}{n}\right]$$

and $\overline{w}$ is the complex conjugate of w.

PROOF:

Lemma 5 *The elements, $\{a_i | 1 \leq i \leq n\}$, and eigenvalues, $\{\lambda_j | 1 \leq j \leq n\}$, of a circulant matrix A, have the following relationships:*

$$a_i = \frac{1}{n} \sum_{j=1}^{n} \lambda_j \overline{w}^{(i-1)(j-1)}, \quad 1 \leq i \leq n$$

$$\lambda_j = \sum_{i=1}^{n} a_i w^{(j-1)(i-1)}, \quad 1 \leq j \leq n$$

where $w = \exp\left[\sqrt{-1}\frac{2\pi}{n}\right]$.

PROOF OF LEMMA: [Dav79], pp. 32, 72–73

Lemma 5 indicates that the sequence $\lambda_1, \lambda_2, \ldots, \lambda_n$ is the discrete Fourier Transform (DFT) of the sequence $a_1, a_2, \ldots, a_n$. Let IDFT stand for "inverse discrete Fourier Transform," and let (I)DFT$\{x_i\}$ be the (I)DFT of the sequence $x_1, x_2, \ldots, x_n$.

If S has eigenvalues $\{\nu_i | 1 \leq i \leq n\}$, and A has eigenvalues $\{\lambda_i | 1 \leq i \leq n\}$, then

$$\begin{aligned} p_{min} &= s \min_i[a_i] = s \min_i[\text{IDFT}\{\lambda_i\}] \quad \text{Lemma 5} \\ &= s \min_i\left[\text{IDFT}\left\{\frac{1}{1-\nu_i}\right\}\right] \quad \text{Lemma 1} \\ &= s \min_i\left[\text{IDFT}\left\{\frac{1}{1-\text{DFT}\{s_i\}}\right\}\right] \quad \text{Lemma 5} \end{aligned} \tag{4.11}$$

Expanding Equation 4.11, using the expressions in Lemma 5 for the DFT and IDFT proves the theorem.

$$p_{min} = s \min_i \left[\frac{1}{n}\sum_{j=1}^{n} \frac{\overline{w}^{(i-1)(j-1)}}{1-\sum_{k=1}^{n} s_k w^{(j-1)(k-1)}}\right] \tag{4.12}$$

The minimum power can be expressed in terms of the insertion loss, number of nodes, number of transceivers, number of neighboring nodes per node, and the precise connection scheme, when the terms s_k in Equation 4.12 are replaced by their appropriate values (either 0 or s), and s is replaced by the expression in Equation 4.1. In this fashion, closed form expressions or expressions involving only one summation can be derived for topologies with circulant node to node power distribution matrices.

For the fully-connected mesh, the minimum power delivered between all transmitter-receiver pairs is

$$p_{min} = \frac{s^2}{[1-(n-1)s](1+s)} \tag{4.13}$$

The minimum power for a ring is

$$p_{min} = \frac{s}{n}\sum_{j=1}^{n} \frac{(-1)^{j-1}}{1-2s\cos[2\pi(j-1)/n]}, \quad n \text{ even} \tag{4.14}$$

$$p_{min} = \frac{s}{n}\sum_{j=1}^{n} \frac{(-1)^{j-1} w^{(j-1)/2}}{1-2s\cos[2\pi(j-1)/n]}, \quad n \text{ odd} \tag{4.15}$$

Appendix B contains derivations of Equations 4.13–4.15. Similar expressions can be derived for other physically homogeneous topologies with circulant node to node power distribution matrices.

When a closed form solution for the minimum power is available, such as that for the fully-connected mesh, it enables more precise optimization of the number of nodes

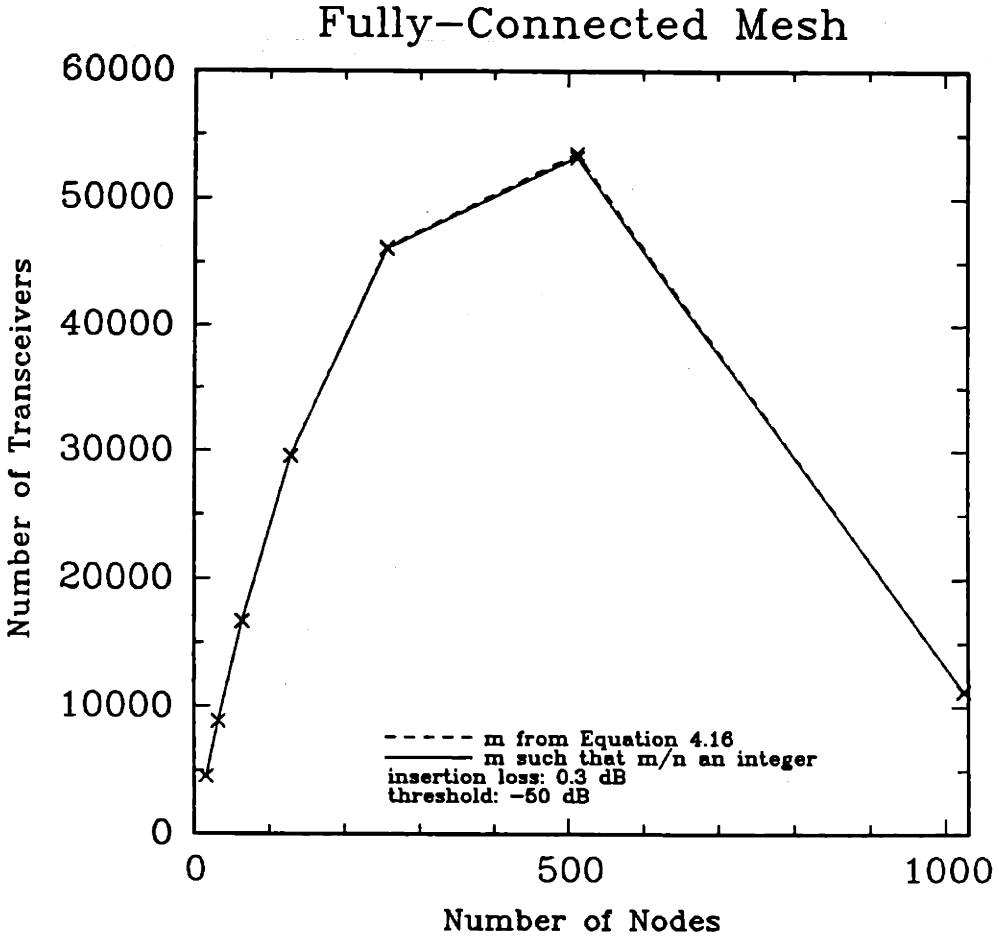

Figure 4.6: Number of Transceivers Supported by a Fully-Connected Mesh

than generating plots such as in Figure 3.5. It also allows a precise expression for the number of supportable transceivers in terms of the number of nodes, the insertion loss, and the desired value for the minimum. For example, for the fully-connected mesh,

$$m = \frac{2gn\left(\frac{1}{p_{min}} + n - 1\right)}{\left(n^2 + \frac{4}{p_{min}}\right)^{\frac{1}{2}} - n + 2} - n(n-1) \tag{4.16}$$

Equation 4.16 is derived in Appendix C by solving Equation 4.13 for s, and setting this equal to the expression for s in Equation 4.1. Of course, the expression is valid only when m/n is an integer, so that the matrix S will indeed be circulant. Figure 4.6 shows the value of m from Equation 4.16 vs. n, and the next lower value of m that would make m/n an integer vs. n, for 0.3 dB insertion loss, and a receiver sensitivity

threshold of -50 dB, or $p_{min} = 10^{-5}$.

4.2.2 Maximizing the Minimum Power Through a Node

Theorem 6 *Of all topologies for passive FOLCNs with n nodes, m transceivers, insertion loss α in dB, and a circulant node to node power distribution matrix S, the fully-connected mesh maximizes the minimum power that passes through any node when power is injected into the network at any other node.*

PROOF:

The element a_i of the matrix A represents the power that passes through node $(i+j) \bmod n$, given that power was injected into the network at node $j+1$, for $0 \leq j \leq n-1$. This is different from the power received by receiver j when power is injected into node i, which is $[AR]_{ij}$. The following lemma will aid the proof of the theorem.

Lemma 6 *Let $\{a_i | 1 \leq i \leq n\}$ be the elements across the first row of $A = (I-S)^{-1}$, where S is the circulant node to node power distribution matrix of a passive FOLCN.*

$$a_1 > a_j, \quad 2 \leq j \leq n \tag{4.17}$$

Furthermore, $a_2 = a_3 = \cdots = a_n$ if and only if $i_n = n-1$.

PROOF OF LEMMA: Appendix D

Let there be a topology, called Topology X, with a circulant node to node power distribution matrix S', having elements $\{s'_i | 1 \leq i \leq n\}$. Let $A' = (I-S')^{-1}$ have elements $\{a'_i | 1 \leq i \leq n\}$. Assume Topology X is not a fully-connected mesh, so that $i_n < n-1$. The following system of equations, derived in Appendix D, expresses the relationships between $\{s'_i | 1 \leq i \leq n\}$ and $\{a'_i | 1 \leq i \leq n\}$.

$$a'_1 = 1 + s'_2 a'_n + s'_3 a'_{n-1} + \cdots + s'_n a'_2 \tag{4.18}$$

$$a'_2 = s'_2 a'_1 + s'_3 a'_n + \cdots + s'_n a'_3 \tag{4.19}$$

$$a'_3 = s'_2 a'_2 + s'_3 a'_1 + \cdots + s'_n a'_4 \tag{4.20}$$

$$\vdots$$

$$a'_n = s'_2 a'_{n-1} + s'_3 a'_{n-2} + \cdots + s'_n a'_1 \tag{4.21}$$

i_n of the elements of $\{s'_i | 2 \leq i \leq n\}$ have value s', given by Equation 4.1, and the other $n-1-i_n$ elements have value 0. According to Lemma 6, $a'_1 > a'_i$ for $2 \leq i \leq n$. Equations 4.19–4.21 indicate that i_n elements of $\{a'_i | 2 \leq i \leq n\}$ have a term $s'a'_1$ on the right hand side of their defining equations, while the other $n-1-i_n$ a'_i's in $\{a'_i | 2 \leq i \leq n\}$ do not have $s'a'_1$ in their equations. Let A_l be the former set of i_n elements, and let A_s be the latter set of $n-1-i_n$ elements. In addition, let a'_l be an upperbound on the elements of A_l, let a'_s be an upperbound on the elements of A_s, and let a' be an upperbound on a'_1. Partitioning $\{a'_i | 1 \leq i \leq n\}$ into a'_1, A_l, and A_s, and using Equations 4.18–4.21, yield the following equations.

$$a' = 1 + i_n s' \max\{a'_l, a'_s\} \tag{4.22}$$

$$a'_l = s'a' + (i_n - 1)s' \max\{a'_l, a'_s\} \tag{4.23}$$

$$a'_s = i_n s' \max\{a'_l, a'_s\} \tag{4.24}$$

Comparison of Equations 4.23 and 4.24, using Lemma 6, indicates that $a'_l > a'_s$. Therefore,

$$a' = 1 + i_n s' a'_l \tag{4.25}$$

$$a'_l = s'a' + (i_n - 1)s'a'_l \tag{4.26}$$

$$a'_s = i_n s' a'_l \tag{4.27}$$

If a'_{min} is the smallest element of A, then

$$a'_{min} \leq a'_s \tag{4.28}$$

Now Equations 4.25–4.28 can be solved for a bound on a'_{min}. Solving Equation 4.26 yields:

$$\begin{aligned} a'_l [1 - (i_n - 1)s'] &= s'a' \\ a'_l &= \frac{s'a'}{1 - (i_n - 1)s'} \end{aligned} \tag{4.29}$$

Substituting into Equation 4.25 yields:

$$\begin{aligned} a' &= 1 + \frac{i_n (s')^2 a'}{1 - (i_n - 1)s'} \\ a' \left[1 - \frac{i_n (s')^2}{1 - (i_n - 1)s'}\right] &= 1 \\ a' &= \frac{1}{1 - \frac{i_n (s')^2}{1 - (i_n - 1)s'}} \end{aligned} \tag{4.30}$$

Substituting Equation 4.30 back into Equation 4.29 yields:

$$a_l' = \frac{s'}{[1-(i_n-1)s']\left[1-\frac{i_n(s')^2}{1-(i_n-1)s'}\right]} = \frac{s'}{1-(i_n-1)s'-i_n(s')^2}$$

$$a_l' = \frac{s'}{(1-i_n s')(1+s')} \tag{4.31}$$

Combining this equation with Equations 4.27 and 4.28 yields the bound on a'_{min}.

$$a'_{min} \leq \frac{i_n(s')^2}{(1-i_n s')(1+s')} \tag{4.32}$$

In the fully-connected mesh, let S be the node to node power distribution matrix with positive elements of value s, and let $A = (I-S)^{-1}$ have minimum element a_{min}. Equation 4.13 gives the expression for the minimum normalized power delivered, $p_{min} = sa_{min}$. Dividing by s yields:

$$a_{min} = \frac{s}{[1-(n-1)s](1+s)} \tag{4.33}$$

If $a'_{min} \leq a_{min}$, then the fully-connected mesh maximizes the power passing through a node when power is injected into the network at any other node. Assume that both topologies have m transceivers, and the same insertion loss.

$$\frac{i_n(s')^2}{(1-i_n s')(1+s')} \stackrel{?}{\leq} \frac{s}{[1-(n-1)s](1+s)}$$

$$\frac{i_n(s')^2}{s}\,\frac{1-(n-1)s}{1-i_n s'}\,\frac{1+s}{1+s'} \stackrel{?}{\leq} 1$$

$$\frac{gi_n\left(\frac{m}{n}+n-1\right)}{\left(\frac{m}{n}+i_n\right)^2}\,\frac{1-\frac{(n-1)g}{\frac{m}{n}+n-1}}{1-\frac{i_n g}{\frac{m}{n}+i_n}}\,\frac{1+\frac{g}{\frac{m}{n}+n-1}}{1+\frac{g}{\frac{m}{n}+i_n}} \stackrel{?}{\leq} 1$$

$$gi_n\frac{\frac{m}{n}+(1-g)(n-1)}{\frac{m}{n}+(1-g)i_n}\,\frac{1+\frac{g}{\frac{m}{n}+n-1}}{\frac{m}{n}+i_n+g} \stackrel{?}{\leq} 1$$

$$K = \frac{gi_n}{\frac{m}{n}+n-1}\,\frac{\frac{m}{n}+(1-g)(n-1)}{\frac{m}{n}+(1-g)i_n}\,\frac{\frac{m}{n}+n-1+g}{\frac{m}{n}+i_n+g} \stackrel{?}{\leq} 1$$

Note that $K = a'_{min}/a_{min}$. Each factor in the expression for K is maximized when m/n is minimized; therefore, K is maximized when m/n is minimized. m/n must be an integer for the networks to have circulant node to node power distribution matrices. Since a network supporting no transceivers is not interesting, I'll maximize K for interesting cases by assuming that $m/n = 1$.

$$K \leq \frac{i_n g}{n}\,\frac{n-(n-1)g}{i_n+1-i_n g}\,\frac{n+g}{i_n+1+g} \stackrel{?}{\leq} 1 \tag{4.34}$$

$$K \leq \frac{i_n}{n}\,\frac{(n-1)g^2+n(n-2)g-n^2}{i_n g^2+(i_n+1)(i_n-1)g-(i_n+1)^2}g \stackrel{?}{\leq} 1 \tag{4.35}$$

The last expression for the bound on K contains a ratio of polynomials in g, with a numerator that grows faster than the denominator as g goes from 0 to 1. Therefore, the bound is maximized when $g = 1$. Substituting $g = 1$ into Inequality 4.34 yields:

$$K \leq \frac{i_n}{n} \frac{n+1}{i_n+2} < 1 \quad \text{for } i_n < n-1 \tag{4.36}$$

Since $K = a'_{min}/a_{min}$, $a'_{min} < a_{min}$.

Therefore, among topologies with n nodes, m transceivers, insertion loss α in dB, and a circulant node to node power distribution matrix, the fully-connected mesh maximizes the minimum power through any node when power is injected into the network at any node.

This result does not directly imply that the fully-connected mesh maximizes the minimum normalized power delivered for this class of topologies. Recall that $p_{min} = sa_{min}$, so that if the fully-connected mesh maximizes the minimum normalized power, then

$$\begin{aligned} s'a'_{min} &< sa_{min} \\ a'_{min} &< \frac{s}{s'} a_{min} < a_{min} \end{aligned} \tag{4.37}$$

In other words, I would have to show that a'_{min} is not only smaller than a_{min}, but smaller by a large enough factor. Define $z(i_n)$ to be this factor:

$$z(i_n) = \frac{s}{s'} = \frac{\frac{g}{m/n+n-1}}{\frac{g}{m/n+i_n}} = \frac{m/n+i_n}{m/n+n-1} \tag{4.38}$$

In absence of a proof that

$$\frac{a'_{min}}{a_{min}} < \frac{m/n+i_n}{m/n+n-1} \tag{4.39}$$

I will discuss the implications of Theorem 6 in light of the factor in Equation 4.38.

First of all, notice that the factor in Equation 4.38 can be made arbitrarily close to 1 by increasing m/n. Therefore, in the limit where transceivers are heavily concentrated at the nodes, the fully-connected mesh does maximize the minimum normalized power delivered between all pairs of transceivers. Thus, if one were building a network which would be expanded in the future by adding transceivers at nodes, without changing the number of nodes, building a fully-connected mesh would ensure that in

the long run, when the number of transceivers might be well above n^2, the network has the best performance as far as power distribution.

a_{min} represents the minimum power arriving at a node, not the power leaving it. This power is the sum of the power that arrives over the various paths of different lengths. s^k of the input power arrives over a single path of length k, so that power arriving over a path of length k in the fully-connected mesh is $[z(i_n)]^k$ times the power arriving over a path of length k in a topology with i_n neighboring nodes. On the other hand, a topology with i_n neighboring nodes can have at most i_n^{k-1} paths of length k between any two nodes. The fully-connected mesh has on the order of $(n-1)^{k-1}$ paths of length k between any two nodes. Thus, in the fully-connected mesh, the presence of many paths compensates for the smaller amount of power arriving over each path.

Examine the ring, for example. Each node has two neighboring nodes, the fewest neighbors a robust topology can have. Within the range $2 \leq i_n \leq n-1$, $z(i_n)$ is minimized for $i_n = 2$, so that the bound on a'_{min} for the ring,

$$a'_{min} < z(2)a_{min} \tag{4.40}$$

is tighter than for any other robust topology with a circulant, symmetric matrix S. Is this bound satisfied?

The shortest path between worst-case nodes in the ring has length $n/2$, and there are two paths of length $n/2$ between the worst case nodes, assuming for the moment that n is even. The power arriving over these paths is:

$$2(s')^{n/2} \tag{4.41}$$

The power arriving over the single one-link path in the fully-connected mesh is s. The question is:

$$\begin{aligned} \frac{s}{2(s')^{n/2}} &> \frac{n-1}{2} \,? \\ \frac{\frac{g}{m/n+n-1}}{2\left(\frac{g}{m/n+2}\right)^{n/2}} &> \frac{n-1}{2} \,? \end{aligned} \tag{4.42}$$

Choosing $g = 1$ and $m = 0$ minimizes the left-hand side of Inequality 4.42.

$$\frac{2^{n/2}}{2(n-1)} > \frac{n-1}{2} \; ? \tag{4.43}$$

This inequality holds for $n \geq 16$, as shown below:

$$\begin{aligned} \frac{n}{2} - 1 - \log_2(n-1) &> \log_2(n-1) - 1 \; ? \\ n &> 4\log_2(n-1), \quad n \geq 16 \end{aligned} \tag{4.44}$$

On the other hand, the assumption that

$$\frac{a_{min}}{a'_{min}} > \frac{n-1}{2} \tag{4.45}$$

for arbitrary n is reasonable, since the above calculation did not take into account the $n-2$ paths of length 2, the $(n-2)^2 + n - 1$ paths of length 3, and all of the other paths of length less than or equal to $n/2$, in the fully-connected mesh.

I am convinced by what is written in this section, and by the numerical results in the following chapter, that similar exercises with other topologies will also lead to the conclusion that among topologies with n nodes, m transceivers, insertion loss α in dB, and a circulant node to node power distribution matrix, the fully-connected mesh maximizes the minimum power delivered between all pairs of transceivers, in addition to maximizing the minimum power passing through any node when power is injected into the network at any other node. However, this conviction is as yet only a conjecture.

4.2.3 Chernoff Bound on Probability of Received Power Falling Below Threshold

In a network with a physically homogeneous topology, the power distribution is the same, no matter which transmitter is active. All receivers attached to a single node receive the same power level, so that each transmitter delivers n possible power levels to receivers on the various nodes. Call these power levels $\{p_i | 1 \leq i \leq n\}$. Assuming that all of the p_i's are distinct, if a transmitter-receiver pair is chosen at random,

with all pairs equally likely to be chosen, each of the n power levels is equally likely to be the one delivered between the transmitter and receiver. That is, each p_i occurs with probability $1/n$. If the p_i's are not distinct, then each distinct power level occurs with a probability that is an integer multiple of $1/n$. Any other power level occurs with probability 0. Therefore, if the probability of a given power level occurring when a transmitter-receiver pair is chosen at random, with all pairs being equally likely, is less than $1/n$, then that probability must be 0. Moreover, if the probability of the delivered power being below the receiver sensitivity is less than $1/n$, then that probability is 0, and the network supports all transceivers.

Let B_r be the receiver sensitivity, or lower bound on the energy required for the receiver to detect a signal, expressed as a fraction of the input energy. Then $B_a = \frac{m/n+i_n}{g} B_r$ is the lower bound on the elements of the matrix A for all transceivers to be supported.

Theorem 7 *Let a passive FOLCN have a circulant node to node power distribution matrix, S. Furthermore, let $F_a(B_a)$ be the probability that some element of the matrix $A = (I - S)^{-1}$ is less than or equal to B_a.*

$$F_a(B_a) \leq \frac{1}{n} \sum_{i=1}^{n} \exp \left\{ t \left[\frac{1}{n} \sum_{j=1}^{n} \frac{\overline{w}^{(i-1)(j-1)}}{1 - \sum_{k=1}^{n} s_k w^{(j-1)(k-1)}} - B_a \right] \right\}, \quad t < 0$$

where $\{s_k | 1 \leq k \leq n\}$ are the elements across the first row of S, and $w = \exp\left[\sqrt{-1}\frac{2\pi}{n}\right]$.

PROOF:

Let $\psi_a(t)$ be the moment generating function for the random variable a, which takes on any of the values $\{a_i | 1 \leq i \leq n\}$ with probability $1/n$, where $\{a_i | 1 \leq i \leq n\}$ are the elements across the first row of the matrix A.

$$\psi_a(t) = \mathrm{E}\left[e^{ta}\right] = \frac{1}{n} \sum_{i=1}^{n} e^{ta_i} \quad \text{[Par60]} \tag{4.46}$$

The Chernoff bound on the probability that the value of a is less than or equal to B_a is

$$F_a(B_a) \leq e^{-tB_a} \psi_a(t), \quad t < 0 \quad \text{[Gal68]} \tag{4.47}$$

Combining Equations 4.46 and 4.47, and using Lemma 5 to expand the result, proves the theorem.

$$
\begin{aligned}
F_a(B_a) &\leq e^{-tB_a}\frac{1}{n}\sum_{i=1}^{n} e^{ta_i} = \frac{1}{n}\sum_{i=1}^{n} e^{t(a_i - B_a)}, \quad t < 0 \\
F_a(B_a) &\leq \frac{1}{n}\sum_{i=1}^{n} \exp\left[t\left(\frac{1}{n}\sum_{j=1}^{n}\lambda_j \overline{w}^{(i-1)(j-1)} - B_a\right)\right], \quad t < 0 \\
F_a(B_a) &\leq \frac{1}{n}\sum_{i=1}^{n} \exp\left[t\left(\frac{1}{n}\sum_{j=1}^{n}\frac{\overline{w}^{(i-1)(j-1)}}{1-\nu_j} - B_a\right)\right], \quad t < 0 \\
F_a(B_a) &\leq \frac{1}{n}\sum_{i=1}^{n} \exp\left[t\left(\frac{1}{n}\sum_{j=1}^{n}\frac{\overline{w}^{(i-1)(j-1)}}{1-\sum_{k=1}^{n} s_k w^{(j-1)(k-1)}} - B_a\right)\right], \quad t < 0
\end{aligned}
\tag{4.48}
$$

Consider the bound in the form:

$$
\frac{1}{n}\sum_{i=1}^{n} e^{t(a_i - B_a)}, \quad t < 0 \tag{4.49}
$$

This summation exhibits very interesting behavior as $|t|$ gets large.

$$
\lim_{t \to -\infty} \frac{1}{n}\sum_{i=1}^{n} e^{t(a_i - B_a)} = \begin{cases} 0 & \text{all transceivers supported} \\ \infty & \text{not all transceivers supported} \end{cases} \tag{4.50}
$$

Thus for any topology, there is some value of t, called $\hat{t}$, such that if $t < \hat{t}$, the bound is guaranteed to be less than $1/n$ if all transceivers are supported.

$$
\hat{t} = \frac{-\ln n}{\min_i a_i - B_a} \tag{4.51}
$$

Equation 4.51 is derived in Appendix E. Of course, for any negative value of t, the bound will be greater than $1/n$ if any transceiver is not supported, because the summation in Equation 4.49 has positive addends, and the one(s) with a positive exponent will be greater than 1.

One would not actually compute the value of $\hat{t}$ in order to bound the probability that $a < B_a$, because computing it requires knowledge of $\min_i a_i$. However, there are other ways to tell whether all transceivers are supported. For one thing, no matter the value of t, the bound is always greater than $1/n$ if the network does not support all

transceivers. Thus, whenever the bound is less than $1/n$, all transceivers are definitely supported. Furthermore, when $|t|$ is large enough, increasing it further will cause the bound to grow if the network does not support all users, and shrink if it does.

Figure 4.7 plots the Chernoff bound on the probability that the normalized power delivered to a receiver is less than -50 dB, vs. the number of transceivers in the network, for the fully-connected mesh, the wrap-around triangular mesh, and the ring. All networks have 16 nodes and 0.3 dB insertion loss. The Chernoff parameter is -10,000. The graph illustrates that the bound is less than $1/n = 1/16 = 0.06$ when all transceivers are supported, and rises rapidly when they are not. It also demonstrates that with 0.3 dB insertion loss, 16 nodes, and a -50 dB loss budget, the fully-connected mesh supports over 4000 transceivers, the wrap-around triangular mesh supports about 500 transceivers, and the ring supports only 16 transceivers.

Figure 4.8 plots the Chernoff bound on the probability that the normalized power delivered to a receiver is less than -50 dB, vs. the number of transceivers in the network, for the 16-node fully-connected mesh, and three different Chernoff parameters. The insertion loss is 0.3 dB. The plot illustrates that as the magnitude of the Chernoff parameter increases, the bound gets tighter when all transceivers are supported, and looser when they are not.

4.3 Results When S is Block Circulant With Circulant Blocks

A block circulant matrix is one in which, when the matrix is written in block form, each row is the previous row with all blocks but the last shifted to the right by one place, and the last block moved into the first position in the row. The following matrix

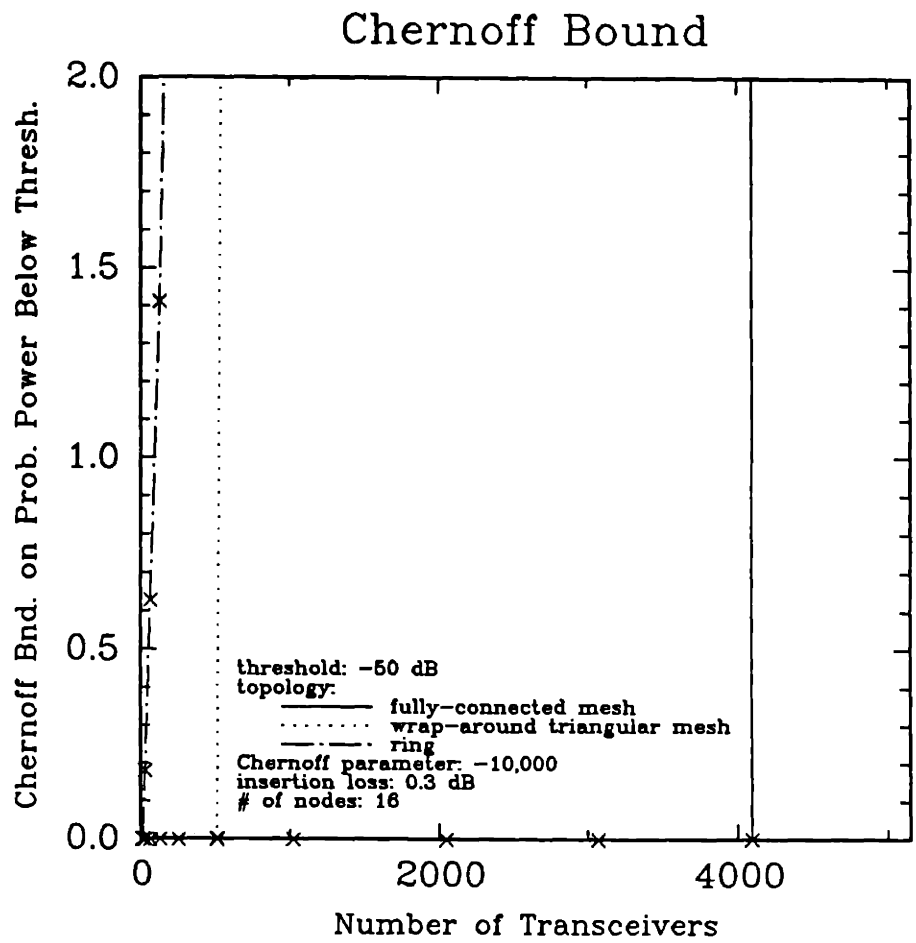

Figure 4.7: Chernoff Bound on Probability Delivered Power Below Threshold for Three Topologies

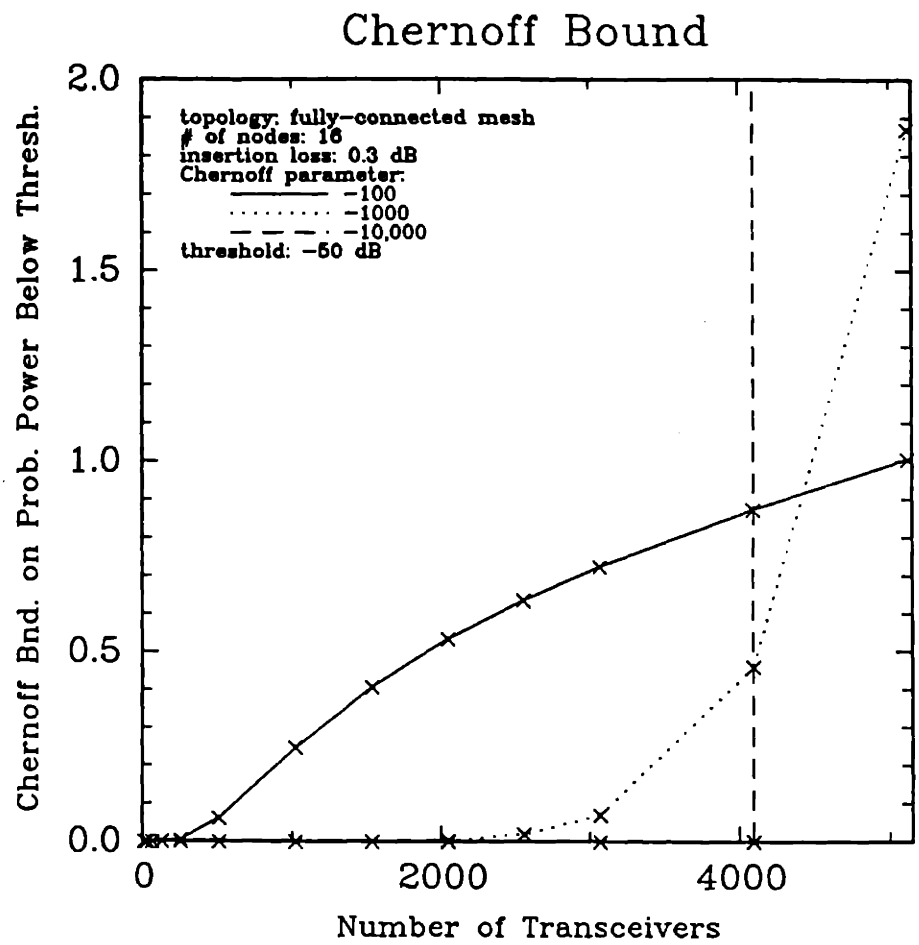

Figure 4.8: Chernoff Bound on Probability Delivered Power Below Threshold for Three Chernoff Parameters

is a block circulant matrix in which each of the matrices, A, B, C, and D is $p \times p$:

$$\begin{pmatrix} A & B & C & D \\ D & A & B & C \\ C & D & A & B \\ B & C & D & A \end{pmatrix} = E \tag{4.52}$$

If A, B, C, and D are circulant matrices, then E is block circulant with circulant blocks. [Dav79]

A regular circulant matrix is a level 1 circulant. A level 2 circulant is a block circulant with circulant blocks. In other words, a level 2 circulant is a block circulant in which each block is a level 1 circulant. Similarly, a level k circulant is a block circulant in which each block is a level $k-1$ circulant. [Dav79]

As it turns out, a passive FOLCN with a d-dimensional hypercube topology, having the same number of transceivers on every node, has a node to node power distribution matrix S which is a level d circulant matrix. Moreover, the wrap-around square mesh with the wrapping shown in Figure 3.8 has a level 2 circulant node to node power distribution matrix, while the wrap-around lattice with the wrapping described in Section 3.1 has a level 3 circulant node to node power distribution matrix. In the following examples, s, defined in Equation 4.1, changes value appropriately with the number of nodes.

Let S_2 be the node to node power distribution matrix of a 2-dimensional hypercube. The 2-dimensional hypercube was depicted in Figure 3.1.

$$S_2 = \left(\begin{array}{cc|cc} 0 & s & s & 0 \\ s & 0 & 0 & s \\ \hline s & 0 & 0 & s \\ 0 & s & s & 0 \end{array}\right) \tag{4.53}$$

The lines emphasize that S_2 has the structure of a level 2 circulant. A 3-dimensional hypercube is two 2-dimensional hypercubes with corresponding nodes connected together, as was shown in Figure 3.1. Let S_3 be the node to node power distribution

matrix of a 3-dimensional hypercube topology. The matrix equivalent of describing a 3-dimensional hypercube in terms of 2-dimensional hypercubes is:

$$S_3 = \begin{pmatrix} S_2 & sI_4 \\ sI_4 & S_2 \end{pmatrix} \tag{4.54}$$

The blocks S_2 represent the two 2-dimensional hypercubes composed of distinct sets of nodes. I_4 is the 4×4 identity matrix, so that sI_4 represents connection of corresponding nodes. Since I_4 can be considered a level 2 circulant with level 1 blocks I_2 and 0_2 (the zero matrix), S_3 is a level 3 circulant matrix. In general, if S_d is the node to node power distribution matrix of a d-dimensional hypercube topology, then it is the following level d circulant matrix:

$$S_d = \begin{pmatrix} S_{d-1} & sI_{2^{d-1}} \\ sI_{2^{d-1}} & S_{d-1} \end{pmatrix} \tag{4.55}$$

Let S_{l_1} be the node to node power distribution matrix of an l_1-node ring.

$$S_{l_1} = \begin{pmatrix} 0 & s & 0 & \cdots & 0 & s \\ s & 0 & s & \cdots & 0 & 0 \\ 0 & s & 0 & \cdots & 0 & 0 \\ \vdots & \vdots & \vdots & & \vdots & \vdots \\ 0 & 0 & 0 & \cdots & 0 & s \\ s & 0 & 0 & \cdots & s & 0 \end{pmatrix} \tag{4.56}$$

Stacking l_2 of these rings on top of each other, and connecting corresponding nodes of appropriate pairs of rings yields an $l_1 \times l_2$ wrap-around square mesh, with l_1 nodes on each row, and l_2 nodes in each column. The node to node power distribution matrix corresponding to this is S_{l_1,l_2}, a level 2 circulant matrix.

$$S_{l_1,l_2} = \begin{pmatrix} S_{l_1} & sI_{l_1} & 0 & \cdots & 0 & sI_{l_1} \\ sI_{l_1} & S_{l_1} & sI_{l_1} & \cdots & 0 & 0 \\ 0 & sI_{l_1} & S_{l_1} & \cdots & 0 & 0 \\ \vdots & \vdots & \vdots & & \vdots & \vdots \\ 0 & 0 & 0 & \cdots & S_{l_1} & sI_{l_1} \\ sI_{l_1} & 0 & 0 & \cdots & sI_{l_1} & S_{l_1} \end{pmatrix} \tag{4.57}$$

Stacking these wrap-around square meshes l_3 deep and connecting corresponding nodes of appropriate pairs yields an $l_1 \times l_2 \times l_3$ wrap-around lattice with the following level 3 circulant node to node power distribution matrix.

$$S_{l_1,l_2,l_3} = \begin{pmatrix} S_{l_1,l_2} & sI_{l_1l_2} & 0 & \cdots & 0 & sI_{l_1l_2} \\ sI_{l_1l_2} & S_{l_1,l_2} & sI_{l_1l_2} & \cdots & 0 & 0 \\ 0 & sI_{l_1l_2} & S_{l_1,l_2} & \cdots & 0 & 0 \\ \vdots & \vdots & \vdots & & \vdots & \vdots \\ 0 & 0 & 0 & \cdots & S_{l_1,l_2} & sI_{l_1l_2} \\ sI_{l_1l_2} & 0 & 0 & \cdots & sI_{l_1l_2} & S_{l_1,l_2} \end{pmatrix} \tag{4.58}$$

Thus, the wrap-around square mesh and wrap-around lattice can be considered 2-dimensional and 3-dimensional "hyperrings," from which one can construct "hyperrings" of even higher dimension.

There are formulas to express the elements and eigenvalues of level d circulants in terms of each other, but beyond level 1 it is simpler to write them in matrix form. The formulas in Lemma 5 came out of the following theorem.

Theorem 8 *Let C be an $n \times n$, level 1 circulant matrix, and let Λ be the diagonal matrix of its eigenvalues.*

$$C = F_n^* \Lambda F_n \quad \textit{and} \quad \Lambda = F_n C F_n^*$$

where $*$ denotes the conjugate transpose of a matrix,

$$[F_n^*]_{ij} = \frac{1}{\sqrt{n}} w_n^{(i-1)(j-1)}$$

$$F_n^* = \frac{1}{\sqrt{n}} \begin{pmatrix} 1 & 1 & 1 & \cdots & 1 \\ 1 & w_n & w_n^2 & \cdots & w_n^{n-1} \\ 1 & w_n^2 & w_n^4 & \cdots & w_n^{2(n-1)} \\ \vdots & \vdots & \vdots & & \vdots \\ 1 & w_n^{n-1} & w_n^{2(n-1)} & \cdots & w_n^{(n-1)(n-1)} \end{pmatrix}$$

and $w_n = \exp\left[\sqrt{-1}\frac{2\pi}{n}\right]$. [Dav79]

PROOF: [Dav79], pp. 72–73

A level 2 circulant of type (p, q) has p blocks in each row and column, and each block is of order q. The matrix E in Equation 4.52 is a level 2 circulant of type $(4, p)$. The node to node power distribution matrix of a 2-dimensional hypercube, S_2 from Equation 4.53, is a level 2 circulant of type $(2, 2)$. S_{l_1,l_2} of Equation 4.57 is a level 2 circulant of type (l_2, l_1).

Theorem 9 *Let C be a level 2 circulant of type (p, q), and let Λ be the diagonal matrix of its eigenvalues.*

$$C = (F_p \otimes F_q)^* \Lambda (F_p \otimes F_q)$$

where

$$\begin{aligned} \left[F_p^*\right]_{ij} &= \frac{1}{\sqrt{p}} w_p^{(i-1)(j-1)} \\ \left[F_q^*\right]_{ij} &= \frac{1}{\sqrt{q}} w_q^{(i-1)(j-1)} \\ w_p &= \exp\left[\sqrt{-1}\frac{2\pi}{p}\right] \\ w_q &= \exp\left[\sqrt{-1}\frac{2\pi}{q}\right] \end{aligned}$$

and $\otimes$ denotes the direct (Kronecker) product of matrices. [Dav79]

PROOF: [Dav79], pp. 184–185

A level 3 circulant of type (p, q, r) is a $p \times p$ block matrix, with blocks that are $q \times q$ block matrices, in which each block is $r \times r$. S_3 in Equation 4.54 is a level 3 circulant of type $(2, 2, 2)$, while S_{l_1,l_2,l_3} of Equation 4.58 is a level 3 circulant of type (l_3, l_2, l_1).

Theorem 10 *A level 3 circulant matrix of type (p, q, r) is diagonalizable by $F_p \otimes F_q \otimes F_r$. [Dav79]*

PROOF: [Dav79], pp. 189–190

From this discussion, it is clear that a d-dimensional hypercube topology has a node to node power distribution matrix S_d, which is a level d circulant matrix of type $(2,2,\ldots,2)$, where the parentheses contain a sequence of d 2's. Due to the particular structure of the hypercube, S_d can also be considered a level 2 circulant of type $(2^{d-1},2)$, where all blocks are $\begin{pmatrix} 0 & s \\ s & 0 \end{pmatrix}$, $\begin{pmatrix} s & 0 \\ 0 & s \end{pmatrix}$, or $\begin{pmatrix} 0 & 0 \\ 0 & 0 \end{pmatrix}$.

Theorem 11 *In a passive FOLCN with a node to node power distribution matrix S which is level 2 circulant of type (p,q), where $pq = n$, the minimum normalized power delivered between all pairs of transceivers is*

$$p_{min} = s \min_{l,i} \left[a_{(l-1)q+i} \right]$$

$$p_{min} = s \min_{l,i} \left[\frac{1}{pq} \sum_{k=1}^{p} \sum_{j=1}^{q} \frac{\overline{w}_p^{(l-1)(k-1)} \overline{w}_q^{(i-1)(j-1)}}{1 - \sum_{u=1}^{p} \sum_{v=1}^{q} s_{(u-1)q+v} w_p^{(k-1)(u-1)} w_q^{(j-1)(v-1)}} \right]$$

where s is given in Equation 4.1, $w_p = \exp\left[\sqrt{-1}\frac{2\pi}{p}\right]$, and $w_q = \exp\left[\sqrt{-1}\frac{2\pi}{q}\right]$.

PROOF:

The proof draws upon the following lemma:

Lemma 7 *The elements, $\{a_{(l-1)q+i} | 1 \le l \le p,\ 1 \le i \le q\}$, and eigenvalues, $\{\lambda_{(l-1)q+i} | 1 \le l \le p,\ 1 \le i \le q\}$, of A, a level 2 circulant matrix of type (p,q), have the following relationships:*

$$a_{(l-1)q+i} = \frac{1}{pq} \sum_{k=1}^{p} \sum_{j=1}^{q} \lambda_{(k-1)q+j} \overline{w}_p^{(l-1)(k-1)} \overline{w}_q^{(i-1)(j-1)} \quad 1 \le l \le p,\ \ 1 \le i \le q$$

$$\lambda_{(l-1)q+i} = \sum_{k=1}^{p} \sum_{j=1}^{q} a_{(k-1)q+j} w_p^{(l-1)(k-1)} w_q^{(i-1)(j-1)} \quad 1 \le l \le p,\ \ 1 \le i \le q$$

PROOF OF LEMMA: Appendix F

To prove the theorem, simply expand the first equation from Theorem 11 by applying Lemma 7 repeatedly, using $A = (I - S)^{-1}$ and Lemma 1. Let $\{\nu_{(l-1)q+i} | 1 \le l \le p,\ 1 \le i \le q\}$

be the eigenvalues of S, and let $\{\lambda_{(l-1)q+i} | 1 \le l \le p,\ 1 \le i \le q\}$ be the eigenvalues of A. If S is a level 2 circulant of type (p, q), then so is A. [Dav79]

$$
\begin{aligned}
p_{min} &= s \min_{l,i} \left[a_{(l-1)q+i} \right] = s \min_{l,i} \left[\frac{1}{pq} \sum_{k=1}^{p} \sum_{j=1}^{q} \lambda_{(k-1)q+j} \overline{w}_p^{(l-1)(k-1)} \overline{w}_q^{(i-1)(j-1)} \right] \\
p_{min} &= s \min_{l,i} \left[\frac{1}{pq} \sum_{k=1}^{p} \sum_{j=1}^{q} \frac{\overline{w}_p^{(l-1)(k-1)} \overline{w}_q^{(i-1)(j-1)}}{1 - \nu_{(k-1)q+j}} \right] \\
p_{min} &= s \min_{l,i} \left[\frac{1}{pq} \sum_{k=1}^{p} \sum_{j=1}^{q} \frac{\overline{w}_p^{(l-1)(k-1)} \overline{w}_q^{(i-1)(j-1)}}{1 - \sum_{u=1}^{p} \sum_{v=1}^{q} s_{(u-1)q+v} w_p^{(k-1)(u-1)} w_q^{(j-1)(v-1)}} \right]
\end{aligned}
\tag{4.59}
$$

Thus the theorem is proven.

This expression can be simplified for particular topologies, such as the hypercube. In fact, for the d-dimensional hypercube, for which $n = 2^d$,

$$
p_{min} = \frac{1}{2^d} \sum_{k=1}^{2^{d-1}} \sum_{j=1}^{2} \frac{\overline{w}_{2^{d-1}}^{(2^{d-1}-1)(k-1)} (-1)^{j-1}}{1 - s(-1)^{j-1} - s \sum_{x=0}^{d-2} w_{2^{d-1}}^{(k-1)2^x}} \tag{4.60}
$$

Equation 4.60 is derived in Appendix G.

The next chapter includes numerical results for classes of topologies analyzed in this chapter, as well as for other topologies with less structure, illustrated in Figure 3.1.

Chapter 5

Numerical Results

Results in this chapter show the variation of the minimum normalized power delivered as various parameters of the network change values. The delay between arrivals of receptions and the dynamic range of received power levels are also examined for several topologies. Finally, a numerical example illustrates how one might choose a topology for a particular, idealized application. These numerical results were computed using UNIX shell programming and the MATLAB software package on a DG20000 computer, using the matrices described in Section 2.3. Where possible the matrix structures and closed form results described in Section 3.3 and Chapter 4 are used to make computations more efficient. For convenience, on all but one plot, I only used numbers of nodes and transceivers that are powers of 2, so that there would always be the same number of transceivers on every node. Therefore, results are accurate to the nearest power of 2.

5.1 Connectivity in Topologies in Which S is Circulant

Section 4.2.2 suggests that the fully-connected mesh maximizes the minimum power delivered for a given insertion loss and number of nodes and transceivers, in physically homogeneous topologies with circulant node to node power distribution matrices.

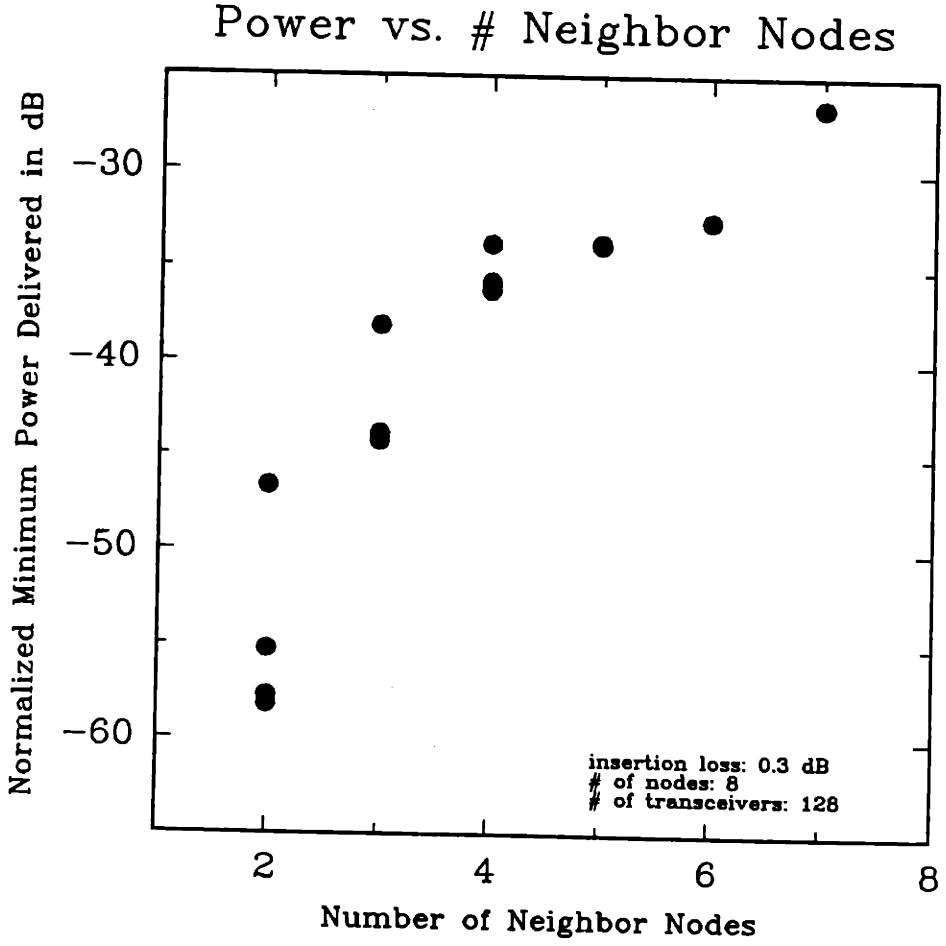

Figure 5.1: Power Delivered vs. Number of Neighboring Nodes per Node for Topologies With 8 Nodes and 128 Transceivers, in Which S is Circulant

The plots in Figures 5.1 and 5.2 illustrate this point. Figure 5.1 shows the normalized minimum power delivered in dB vs. the number of neighboring nodes per node for some physically homogeneous topologies with circulant node to node power distribution matrices, 8 nodes, 128 transceivers, and 0.3 dB insertion loss. Figure 5.2 shows the same thing for networks with 9 nodes and 135 transceivers. The topologies used were those with node 1 connected to node 2. Notice that the minimum power increases as the connectivity increases.

Figure 5.3 shows the minimum normalized power delivered in dB vs. the number of nodes, for some topologies, illustrated in Figure 3.1, that have circulant node to node power distribution matrices, 0.3 dB insertion loss, and 128 transceivers. The

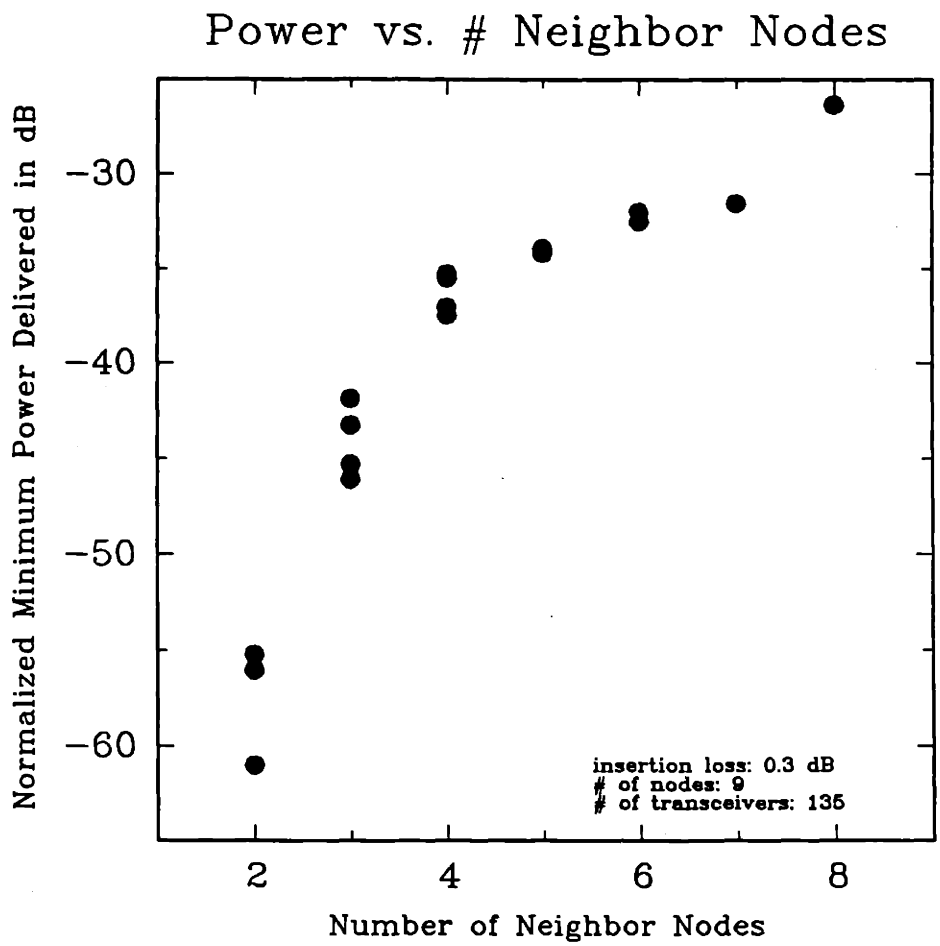

Figure 5.2: Power Delivered vs. Number of Neighboring Nodes per Node for Topologies With 9 Nodes and 135 Transceivers, in Which S is Circulant

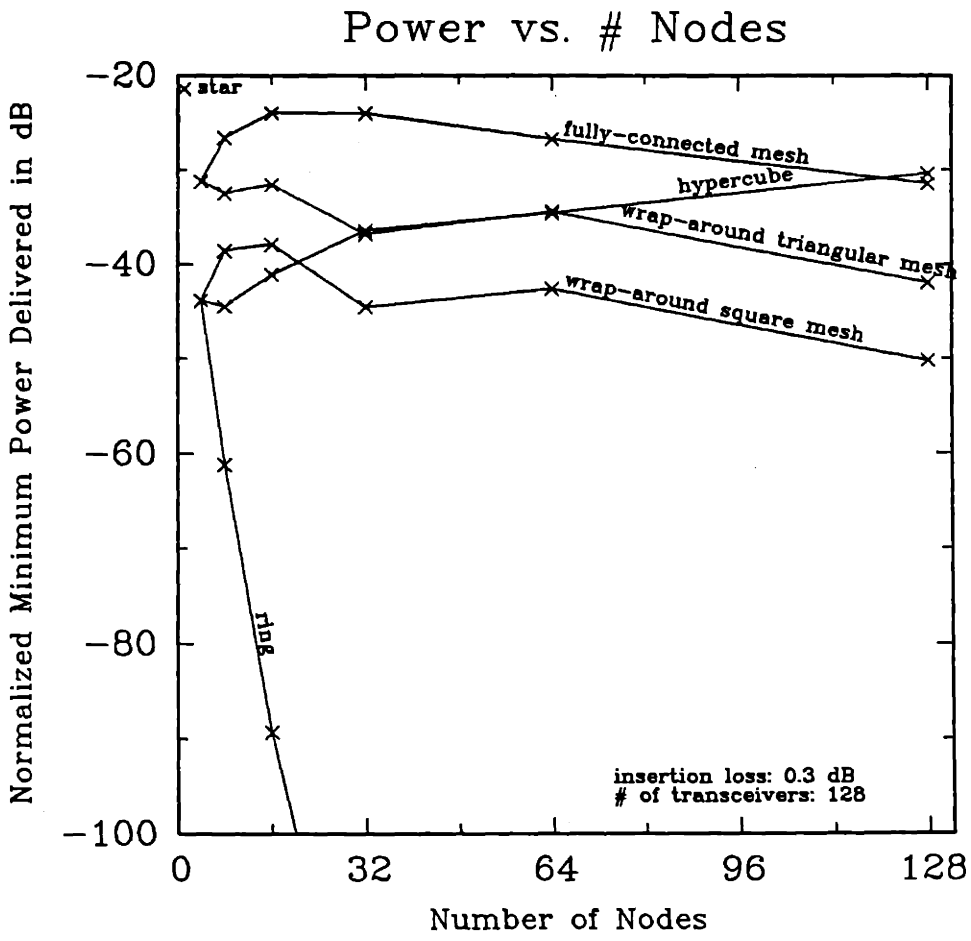

Figure 5.3: Power Delivered vs. Number of Nodes for Topologies in Which S is Circulant, or Level $\log_2 n$ Circulant

hypercube is also included, although its node to node power distribution matrix is a level $\log_2 n$ circulant matrix, where n is the number of nodes. Note that among the topologies with circulant node to node power distribution matrices, for a given number of nodes, topologies with more connectivity have higher normalized minimum power delivered. For $n < 64$, the hypercube performs worse than the wrap-around triangular mesh, which has more neighboring nodes per node than the hypercube for $n < 64$. For $n > 64$, the hypercube performs better than the wrap-around triangular mesh. Although the 128-node hypercube outperforms the 128-node fully-connected mesh, the minimum normalized power delivered is even higher for the 16-node fully-connected mesh.

5.2 Number of Subnets

Recall that in Section 2.1, I stated that "transceiver" means a subnet modeled as a transceiver. For the remainder of this chapter, I specifically refer to subnets and transceivers separately. Figures 5.4–5.9 show how the minimum power delivered varies with the number of subnets, for networks with 4, 16, 128, and 256 nodes and 0.3 dB insertion loss. Figures 5.6 and 5.8 contain copies of the plots from Figures 5.5 and 5.7, respectively, with the horizontal axes expanded, so that the curves can be seen more clearly. The dotted lines in these figures depict various loss budgets used in the discussion to follow.

The results confirm intuition, since the more subnets there are, the less power each receives. This is because the more subnets there are, the more ways power must divide to support them, as evidenced by the greater splitting loss at each node. Note that since the number of nodes is not optimized for each data point, the results could be better than those depicted in the plot.

Assume that there is only one transceiver per subnet, and a 50 dB loss budget is desired. Each plot has a horizontal dotted line drawn at -50 dB. According to Figures 5.4–5.9, within a 50 dB loss budget, the 128-node fully-connected mesh supports over

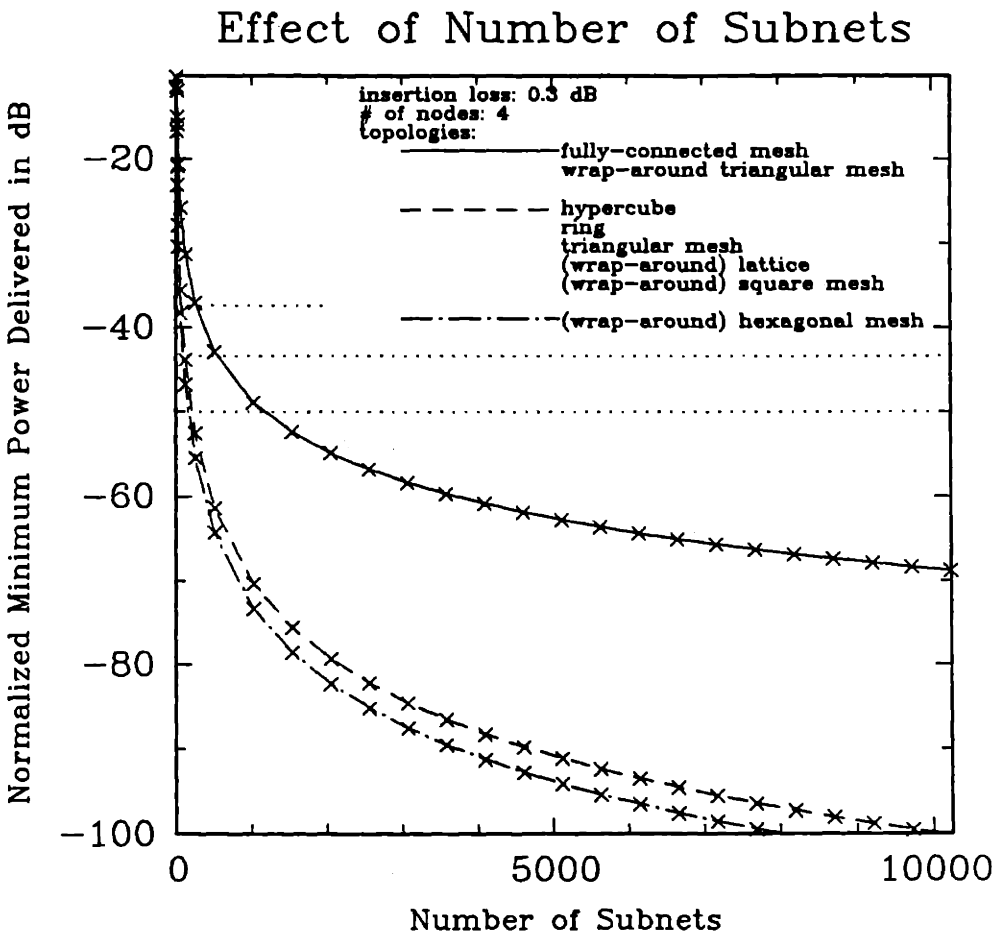

Figure 5.4: Power Delivered vs. Number of Subnets, 4 Nodes

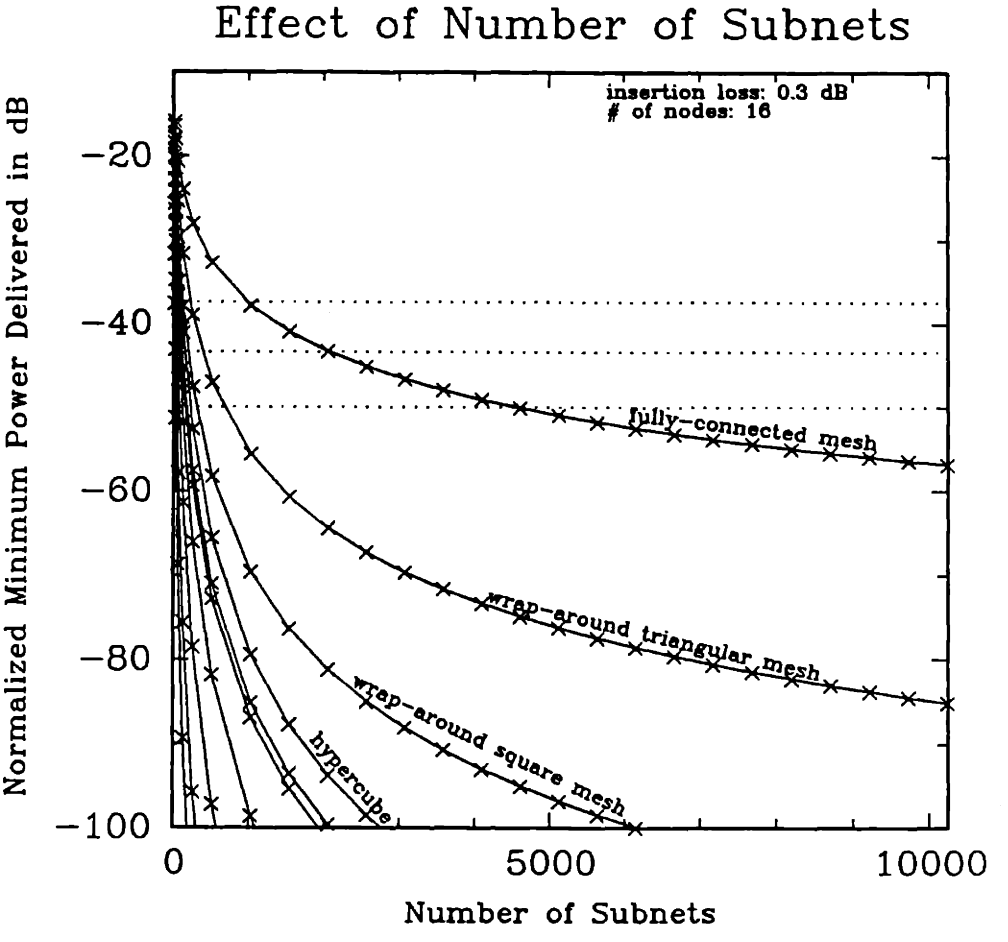

Figure 5.5: Power Delivered vs. Number of Subnets, 16 Nodes

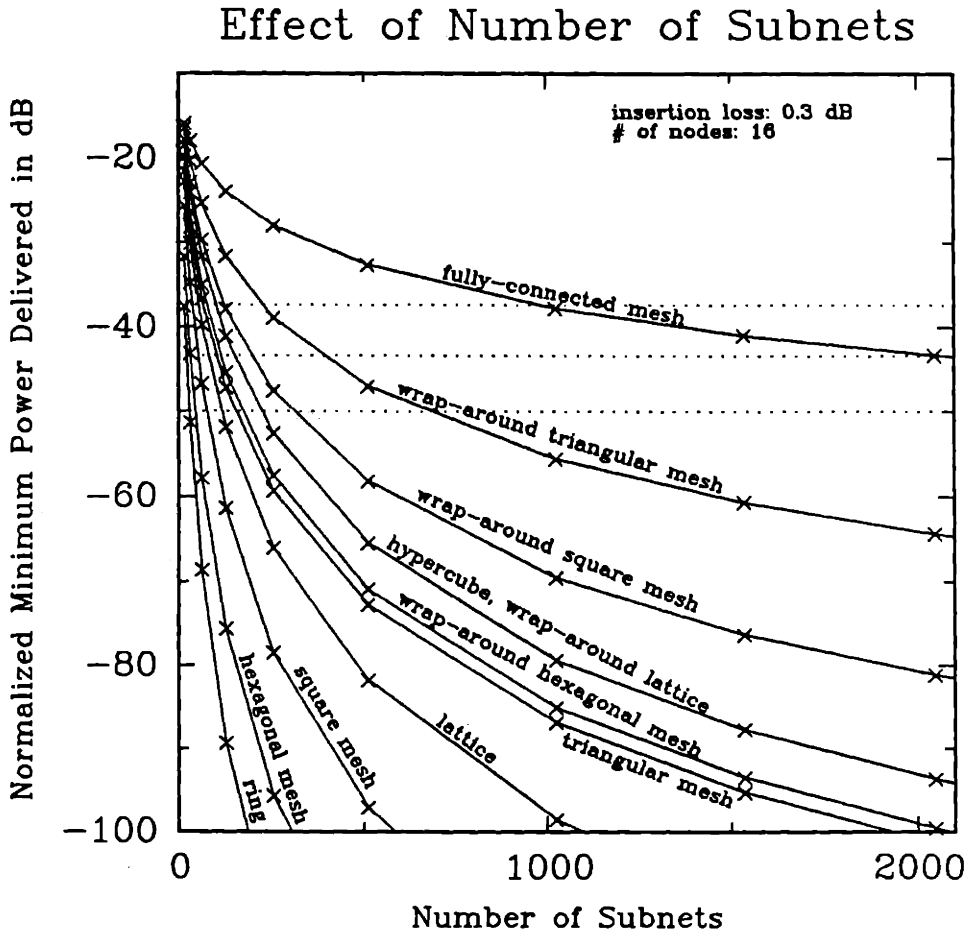

Figure 5.6: Power Delivered vs. Number of Subnets, 16 Nodes, Expanded

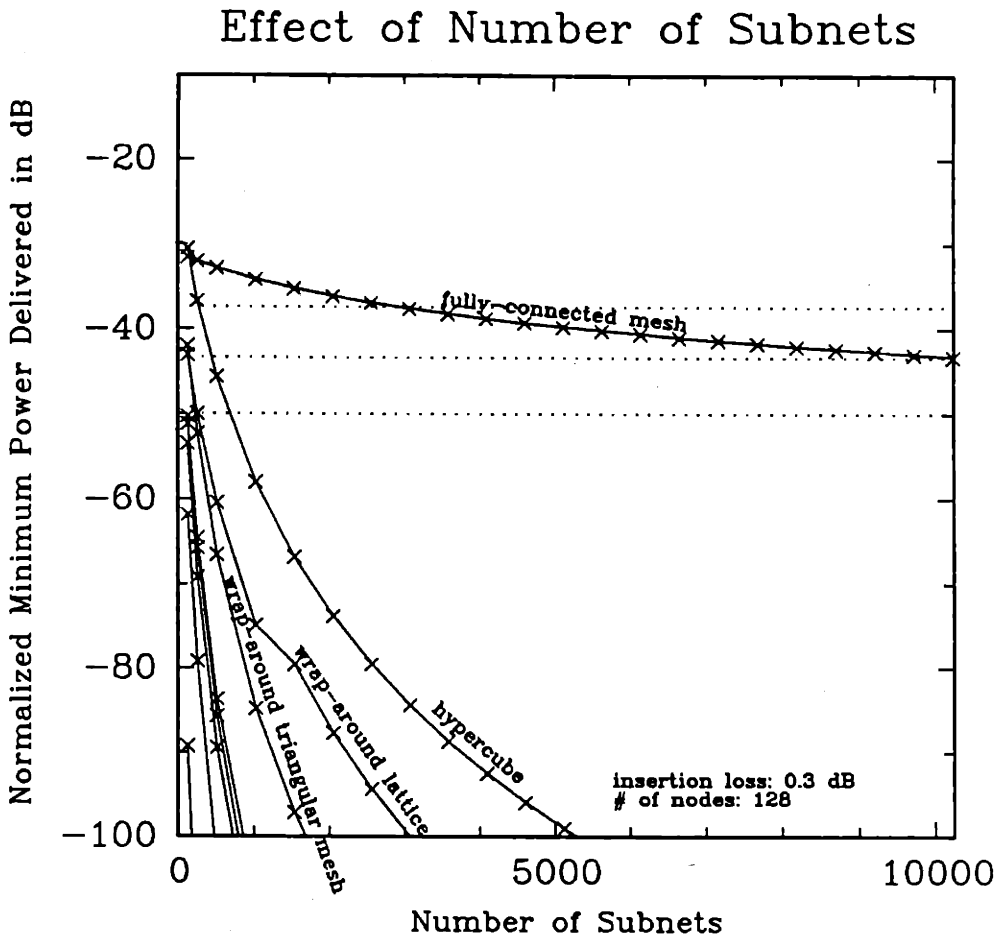

Figure 5.7: Power Delivered vs. Number of Subnets, 128 Nodes

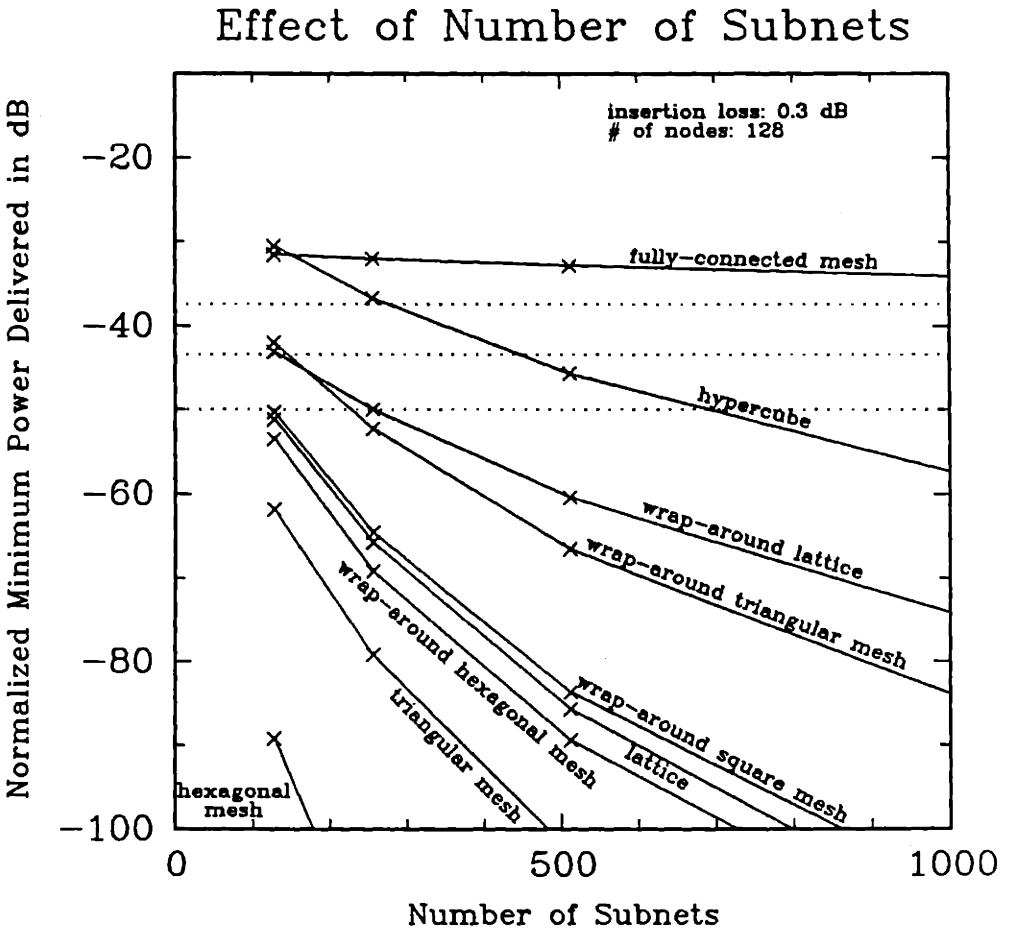

Figure 5.8: Power Delivered vs. Number of Subnets, 128 Nodes, Expanded

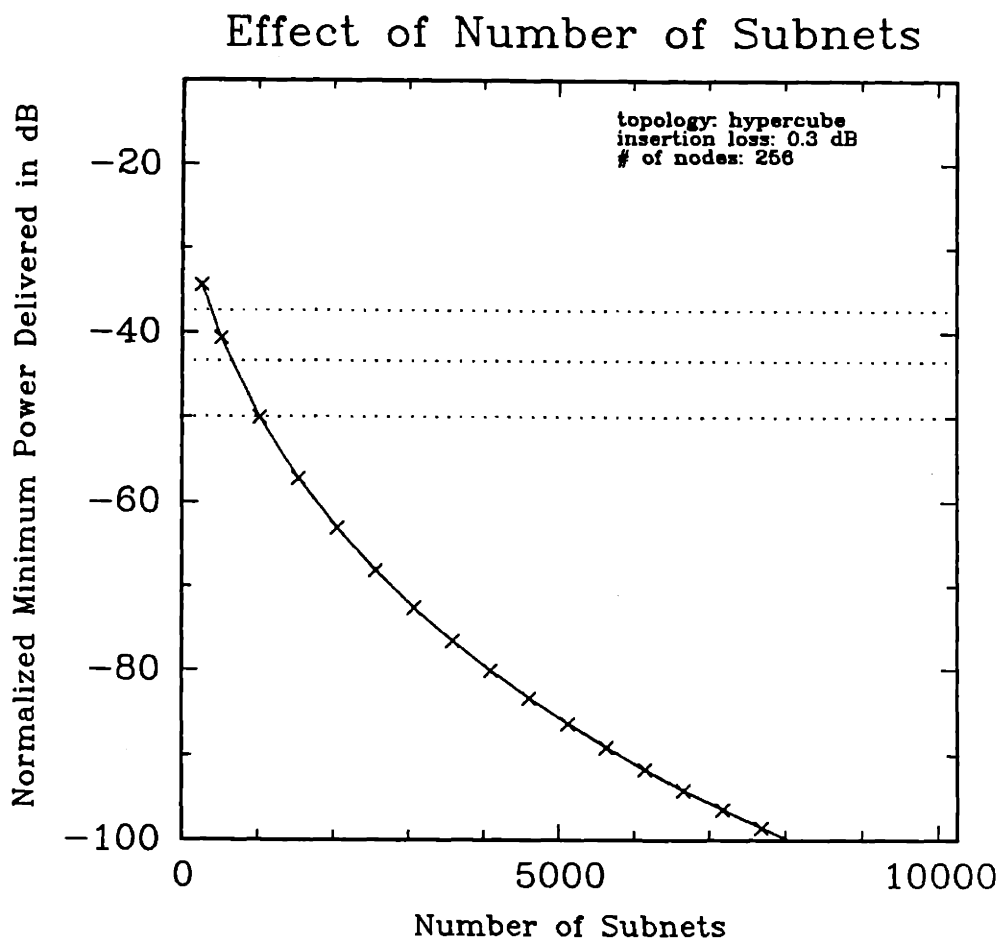

Figure 5.9: Power Delivered vs. Number of Subnets for the Hypercube, 256 Nodes

10,000 transceivers. This is consistent with Figure 4.6, which shows that the 128-node fully-connected mesh with 0.3 dB insertion loss can actually support nearly 30,000 transceivers within a 50 dB loss budget. The 4-node wrap-around triangular mesh and the 256-node hypercube support over 1000 transceivers. Other topologies support fewer transceivers.

Figure 5.7 shows that although the 128-node hypercube has a higher minimum normalized power delivered than the 128-node fully-connected mesh for 128 subnets, the power level diminishes more rapidly in the hypercube, as the number of subnets grows. This is because the path lengths are longer in the hypercube. The increased splitting loss due to the larger number of subnets diminishes the power delivered over long paths more than it diminishes the power delivered over short paths. In fact, Figures 5.4, 5.5, and 5.7 show that when there are more nodes in the topologies, there is a greater difference between the rate at which power delivered decreases with the number of subnets in the fully-connected mesh, and the corresponding rate in the other topologies. This is because the fully-connected mesh is the only topology for which the path lengths do not grow with the number of nodes.

Consider the example subnet in Figure 5.10, in which the transmitters and receivers represented are individual transmitters and receivers within the subnet. If the subnet nodes have 0.3 dB insertion loss, then the loss between a transmitter within the subnet and the network node is $0.3 + 10 \log N$, where N is the number of outputs on the subnet coupler. The same loss occurs between the network node and a receiver within the subnet. Thus, maintaining a 50 dB loss budget between transceivers requires a loss budget of $50 - 0.6 - 20 \log N$ between subnets.

The plots in Figures 5.4–5.9 contain horizontal dotted lines at -43.4 dB and -37.4 dB, representing the subnet to subnet loss budget required to maintain a 50 dB transceiver to transceiver loss budget, for the cases with 2 transceivers per subnet, and 4 transceivers per subnet, respectively. Figure 5.7 shows that with 2 transceivers per subnet, yielding a 43.4 dB loss budget, the 128-node fully-connected mesh can still support over 10,000 subnets. Therefore, it supports over 20,000 transceivers,

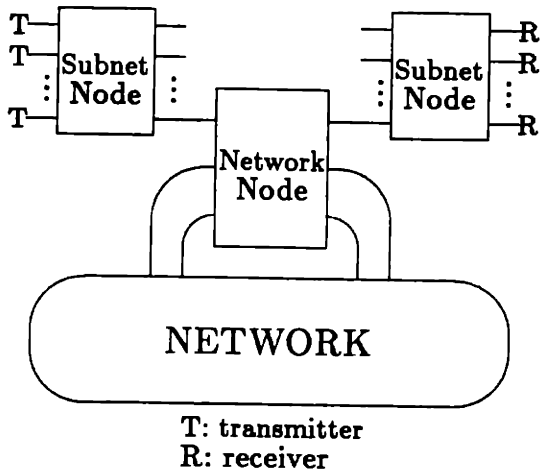

Figure 5.10: Example Subnet

again consistent with Figure 4.6. According to Figure 5.9, each time the number of transceivers per subnet doubles, the number of supportable subnets is halved, so that for the 256-node hypercube with 0.3 dB insertion loss, clustering transceivers into subnets does not increase the number of supportable transceivers. The number of transceivers supported by the 4-node wrap-around triangular mesh also does not increase, when transceivers are clustered into subnets.

Table 5.1 indicates how many transceivers each topology can support, and with what number of nodes, for three different sizes of subnets. The number of supported subnets is simply the number of supported transceivers divided by the number of transceivers per subnet.

These results indicate that clustering transceivers into subnets improves performance, when the loss and splitting within the subnet are outweighed by the decrease in loss that comes from reducing the total number of subnets in the network. The amount of improvement depends upon the characteristics of the subnets and topologies in question.

Table 5.1: Numbers of Transceivers Supported by Various Topologies

Topology	# Nodes	# Supported Transceivers		
		1 Transceiver per Subnet	2 Transceivers per Subnet	4 Transceivers per Subnet
Fully-Connected Mesh	128	10240	20480	10240
Hexagonal Mesh	4	128	128	128
Hypercube	256	1024	1024	1024
Lattice	4	128	128	256
Ring	4	128	128	256
Square Mesh	4	128	128	256
Triangular Mesh	4 or 16	128	128	256
Wrap-Around Hexagonal Mesh	16	128	128	256
Wrap-Around Lattice	16	128	256	256
Wrap-Around Lattice	128	256	256	—
Wrap-Around Square Mesh	16	256	256	256
Wrap-Around Triangular Mesh	4	1024	1024	1024

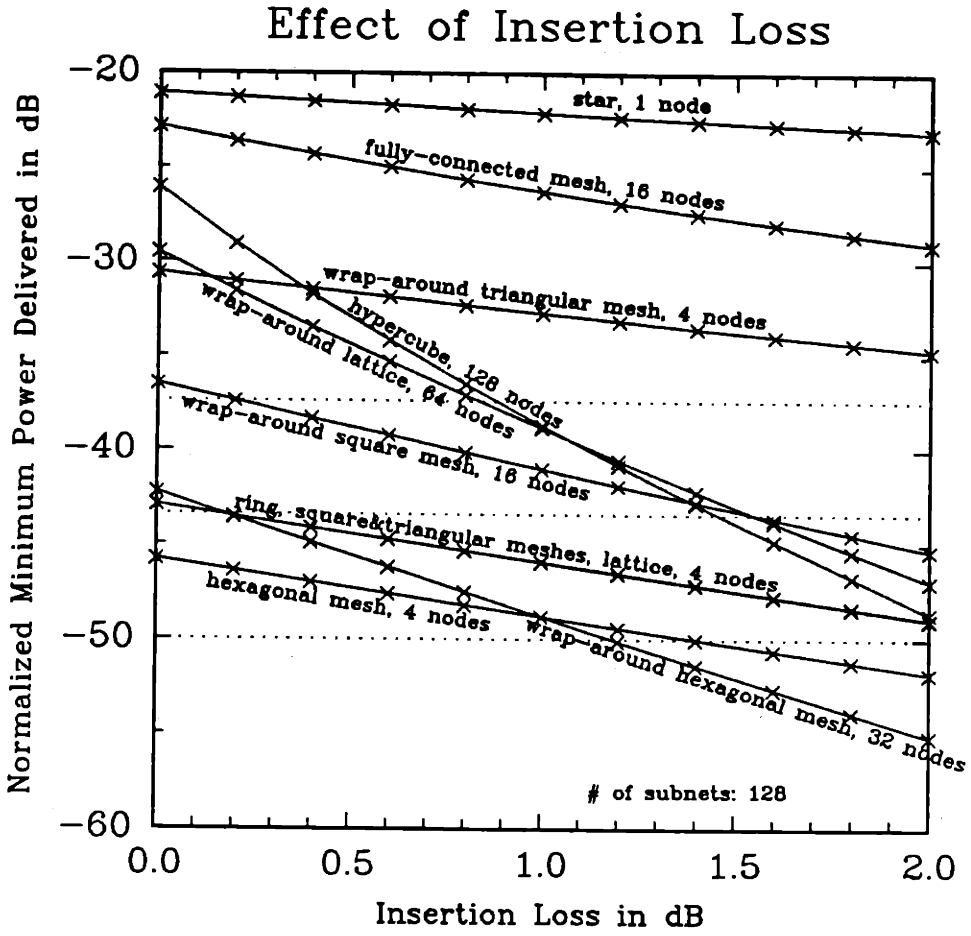

Figure 5.11: Power Distributed vs. Insertion Loss

5.3 Insertion Loss

Figure 5.11 plots the normalized minimum power delivered in dB vs. the insertion loss for the topologies illustrated in Figure 3.1, with 128 subnets and the optimal number of nodes for supporting 128 subnets from Figures 3.2–3.5. An increase in insertion loss produces more degradation of performance in topologies with longer paths, such as the 128-node hypercube, the 64-node wrap-around lattice, and the 32-node wrap-around hexagonal mesh, than in topologies with shorter paths, such as the star, fully-connected mesh, and 4-node wrap-around triangular mesh. Table 5.2 indicates how many transceivers each topology can support with lossless couplers, 1 dB insertion loss, and 2 dB insertion loss, when the transceiver to transceiver loss

Table 5.2: Numbers of Transceivers Supported by Various Topologies with 128 Subnets, for Three Values of Insertion Loss

Topology	# Nodes	# Transceivers Supported		
		0 dB Loss	1 dB Loss	2 dB Loss
Fully-Connected Mesh	16	512	512	512
Hexagonal Mesh	4	128	128	—
Hypercube	128	512	256	128
Lattice	4	256	128	128
Ring	4	256	128	128
Square Mesh	4	256	128	128
Triangular Mesh	4	256	128	128
Wrap-Around Hexagonal Mesh	32	256	128	—
Wrap-Around Lattice	64	512	256	128
Wrap-Around Square Mesh	16	512	256	128
Wrap-Around Triangular Mesh	4	512	512	512

budget is 50 dB, according to the data in Figure 5.11. All topologies have 128 subnets. Recall that the dotted lines in the plot of Figure 5.11, from the top down, represent the subnet to subnet loss budgets required to maintain a 50 dB transceiver to transceiver loss budget, for 4-transceiver, 2-transceiver, and 1-transceiver subnets.

The next two sections describe and illustrate aspects of the power distribution, other than the minimum power delivered, which must be taken into account when choosing a topology for a specific application.

5.4 Delayed Arrival of Receptions

The performance measure I have used is the normalized minimum energy delivered over all paths and all time. In a practical situation, receivers would collect energy

from only a finite number of receptions, acquiring some percentage of the total energy. The order in which receptions arrive depends upon the lengths of the fiber links, which is determined by the placement of the nodes and subnets. The lengths of the links might also be designed by placement of fiber spools along the links. Rather than assume a particular physical layout, I assume all links are of unit length, so that stronger receptions arrive over shorter paths, and weaker receptions arrive over longer paths. This idealization implies that receptions arriving over equal length paths arrive simultaneously. Within practical tolerances of measurement, the links would actually differ in length a bit, and the receptions arriving over paths of the same length would be staggered somewhat.

Suppose ninety percent of the minimum energy delivered over all paths allows a subnet to distribute to each receiver at least enough energy to support it. Collecting this amount of energy requires adding energy from some number of receptions, arriving over some time span. If the desired bit rate is chosen independently of this time span, then there might be intersymbol interference, requiring some equalization in the receiver, as mentioned in Section 1.2. A longer time span between the first and last required receptions, and a greater number of required receptions, result in a more complicated receiver. I assume that the remaining receptions, whose energy is not collected, can be treated as noise.

Figures 5.12–5.14 plot the minimum normalized energy received, expressed as a percentage of the minimum normalized energy received over all paths, vs. the maximum path length included in the calculation. The figures show the results for the fully-connected mesh, wrap-around triangular mesh, and hypercube, for 128 subnets, 0.3 dB insertion loss, and various numbers of nodes. Each curve stops at the first data point above ninety percent.

The results for the fully-connected mesh are in Figure 5.12. Recall from Figure 5.3, that for 128 subnets and 0.3 dB insertion loss, 16 is the optimal number of nodes for a fully-connected mesh, and that the minimum normalized power delivered for 16 nodes is about -24 dB. If -27 dB is adeqate, then the subnets must get at least half

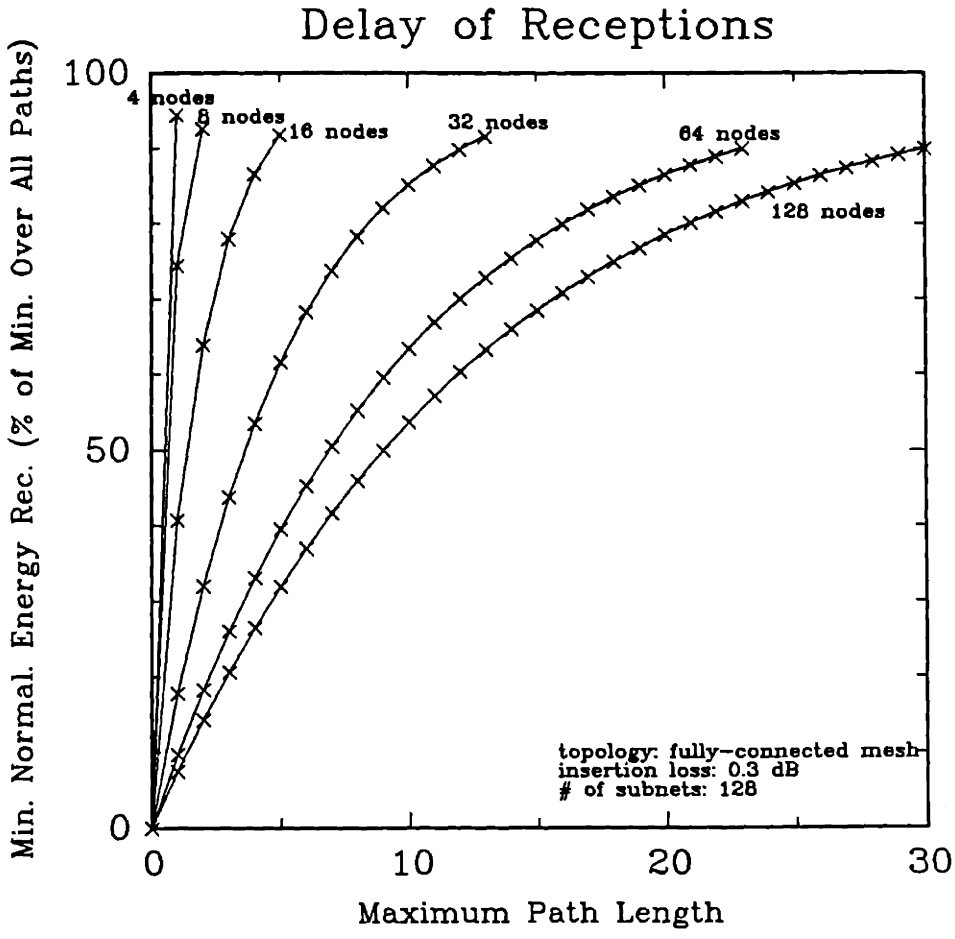

Figure 5.12: Delay of Receptions in the Fully-Connected Mesh

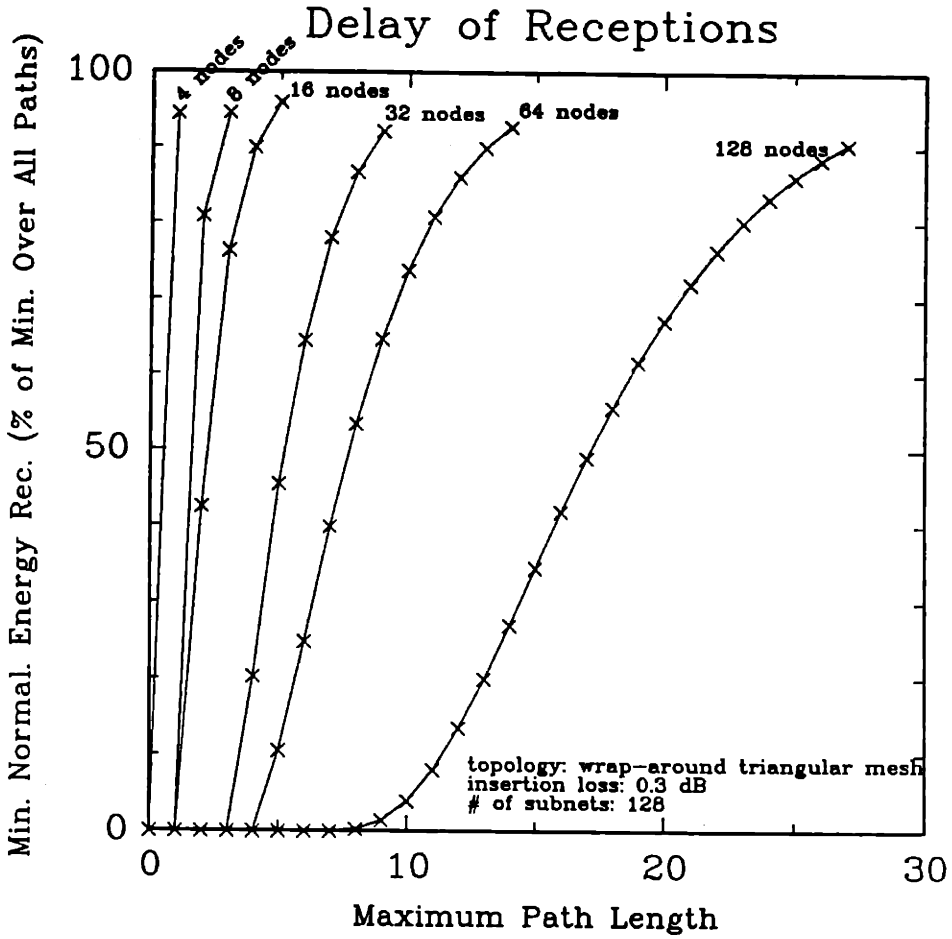

Figure 5.13: Delay of Receptions in the Wrap-Around Triangular Mesh

of the possible energy. According to Figure 5.12, this requires reception of energy arriving over paths of lengths one and two. If all path lengths were precisely the same, this would require two receptions, but there will probably have to be more than two receptions, due to varying link lengths. Then again, one can settle for the 8-node fully-connected mesh, and collect over fifty percent of the total energy in one reception. However, assuming that the loss within a subnet grows with its size, the 16-node fully-connected mesh can ultimately support larger subnets.

The optimal number of nodes for a wrap-around triangular mesh to support 128 subnets with 0.3 dB insertion loss is 4, from Figure 5.3. The minimum normalized power delivered for this case is about -31 dB. Again, suppose that another 3 dB loss is allowable, so that subnets need acquire only fifty percent of the total energy.

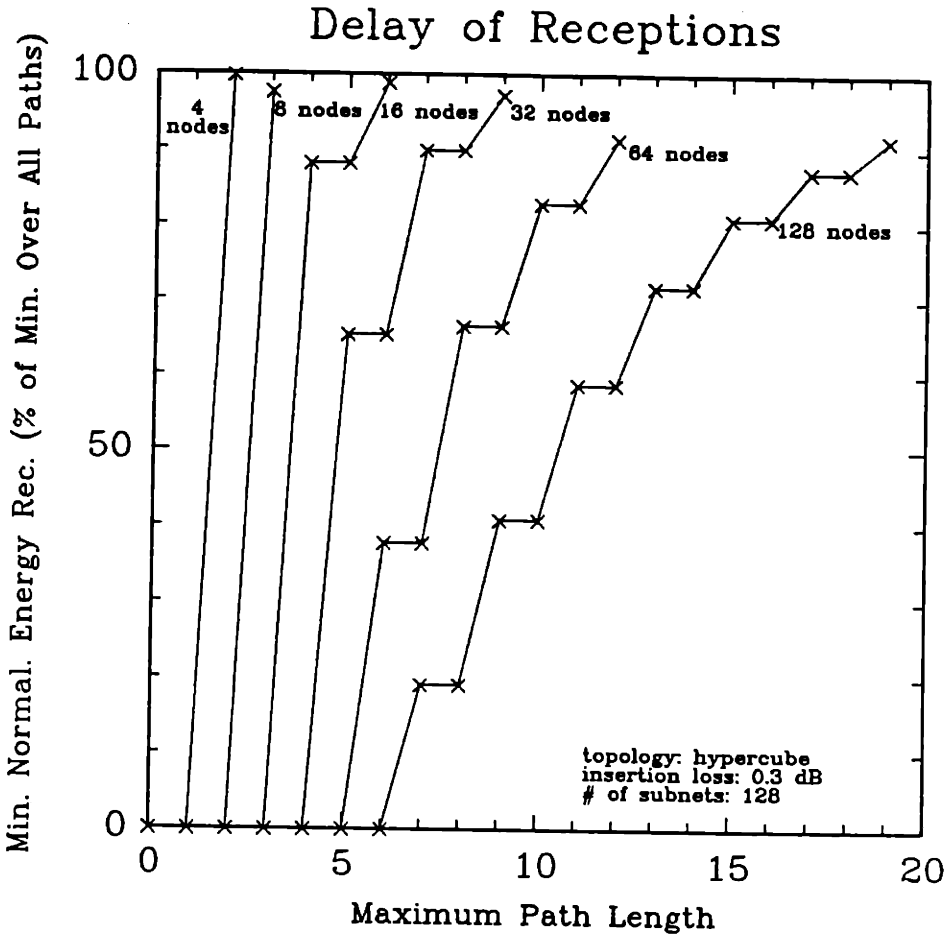

Figure 5.14: Delay of Receptions in the Hypercube

Figure 5.13 indicates that they actually get almost ninety-five percent of the possible energy in the first reception. Note that the 4-node wrap-around triangular mesh is equivalent to the 4-node fully-connected mesh.

The best size for a hypercube supporting 128 subnets with 0.3 dB insertion loss is 128 nodes, as shown in Figure 5.3. The minimum normalized power delivered is about -30 dB. Figure 5.14 illustrates that receivers must add energy from receptions over all paths of lengths 7, 9, and 11, in order to collect at least fifty percent of the total minimum normalized energy. The longer time span between the first and last receptions in this topology could make the receiver more complicated than that for the 16-node fully-connected mesh. Cutting back to 64 nodes would help, but then the power margin dimishes, so that the 64-node hypercube cannot support subnets

as large as the 128-node hypercube can.

Plots showing delay of receptions for other topologies appear in Appendix H.

5.5 Dynamic Range

Up until now, I have been concerned with the minimum power delivered between subnet pairs. The maximum power is also important, because together, the minimum and maximum power delivered determine the upperbound of the required dynamic range for a receiver. The reason this is an upperbound is that a receiver that gets the overall minimum power from some transmitter does not necessarily receive the overall maximum power from some other transmitter, unless the topology is power homogeneous.

Figure 5.15 shows the dynamic range required of receivers, vs. the number of nodes, for various physically homogeneous topologies with 128 subnets and 0.3 dB insertion loss. Since physically homogeneous topologies are power homogeneous, the quantities in the plots are actual dynamic ranges, rather than upperbounds to the dynamic range. The size of the subnets does not affect the dynamic range, since loss through the subnet is the same for every reception of a message. The dynamic range is

$$10 \log \frac{\text{maximum normalized power received over all paths}}{\text{minimum normalized power received over all paths}}$$

Note that the dynamic range connot be larger than the loss budget, since the maximum power must be less than 0 dB, and the loss budget in dB is maximum power minus minimum power. Thus, any topologies with dynamic range greater than 50 dB are not supporting 128 subnets within a 50 dB loss budget.

Among the topologies examined, the fully-connected mesh minimizes the dynamic range. Earlier plots in this chapter show that among the topologies discussed, and except for the point at 128 nodes, the fully-connected mesh maximizes the minimum power delivered for 128 subnets and 0.3 dB insertion loss. Chapter 4 showed that among physically homogeneous topologies, the fully-connected mesh minimizes the

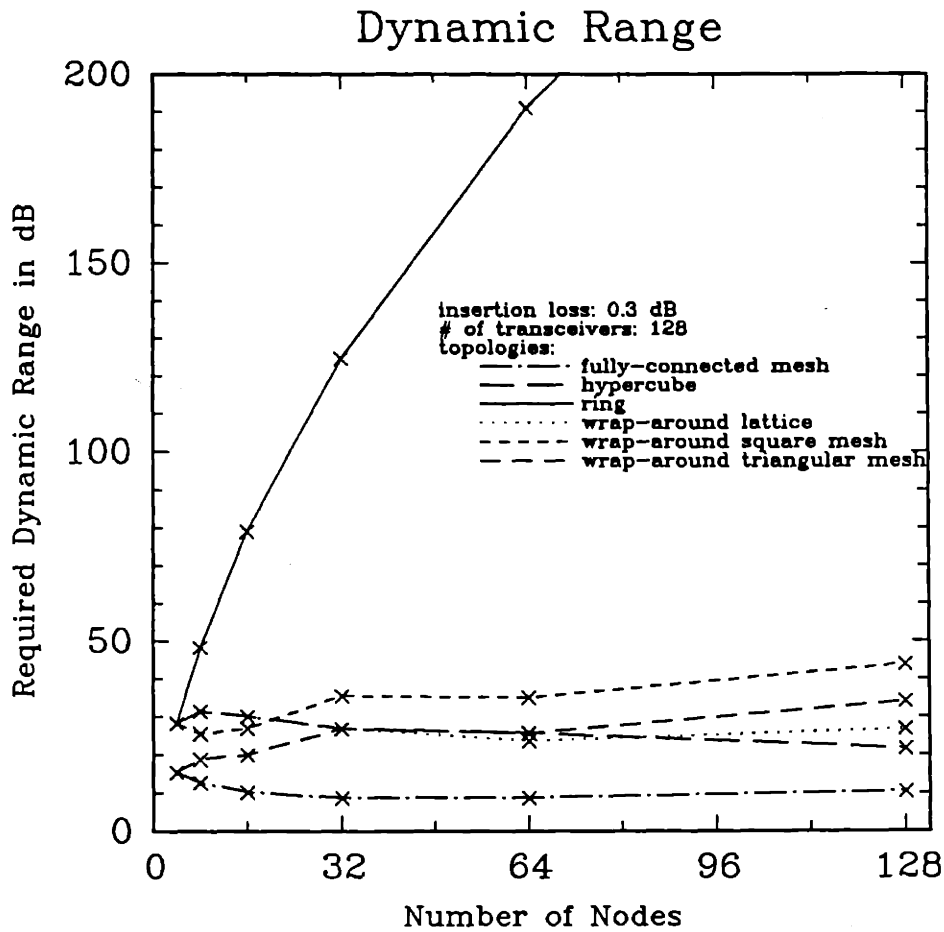

Figure 5.15: Dynamic Range vs. Number of Nodes

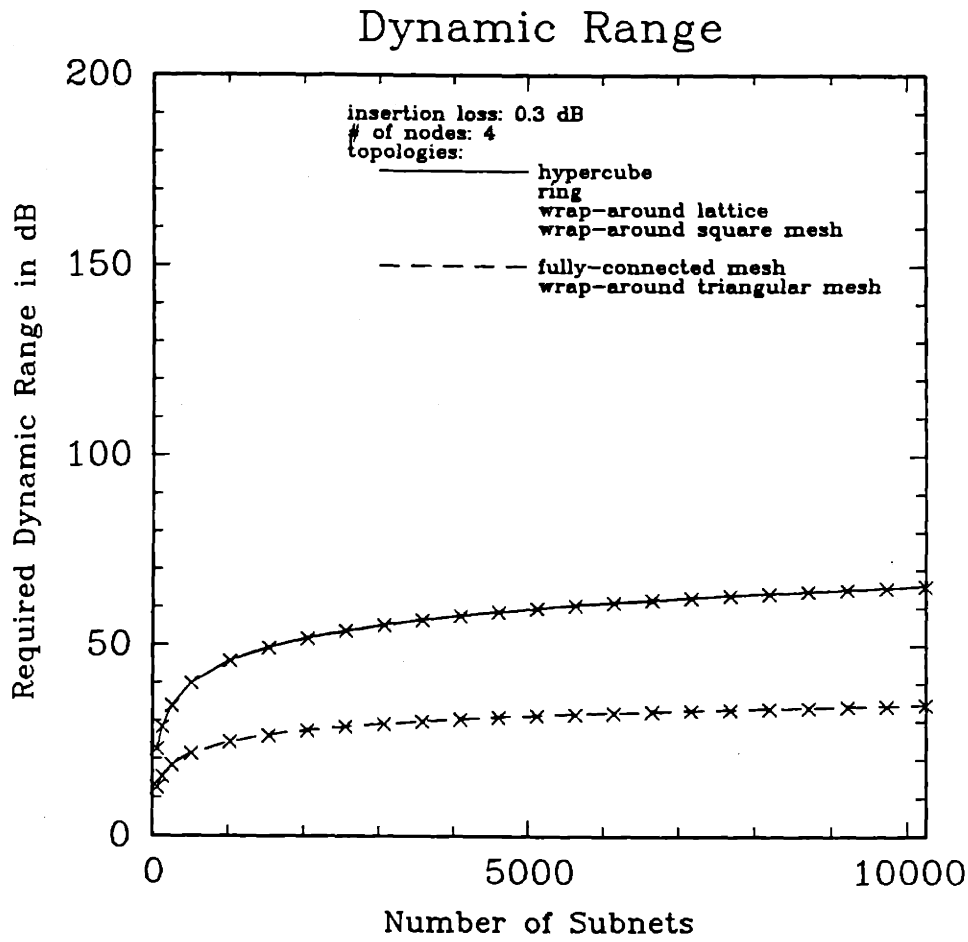

Figure 5.16: Dynamic Range vs. Number of Subnets, for Topologies with 4 Nodes

mean normalized power delivered. One would expect that a topology that minimizes the mean power, while maximizing (in most cases) the minimum power, would minimize the required dynamic range.

The ring requires receivers with the largest dynamic range, since the difference in power delivered between subnets on the same node, and subnets halfway around the ring from each other, is so great. Recall that, among the topologies examined, the ring minimizes the minimum power (this chapter), and maximizes the mean power (Chapter 4).

Figures 5.16–5.19 show how the required dynamic range changes as the number of subnets increases, for various topologies with 0.3 dB insertion loss. Each figure assumes a different number of nodes. The dynamic range increases with the number

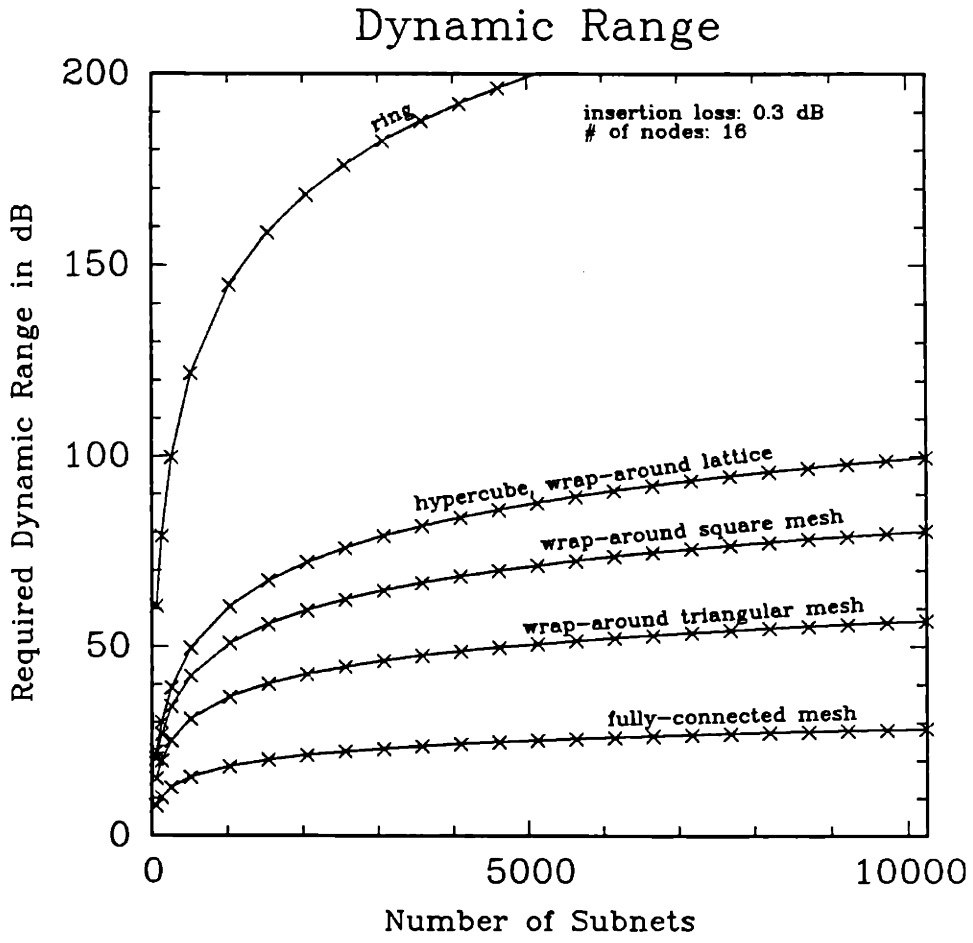

Figure 5.17: Dynamic Range vs. Number of Subnets, for Topologies with 16 Nodes

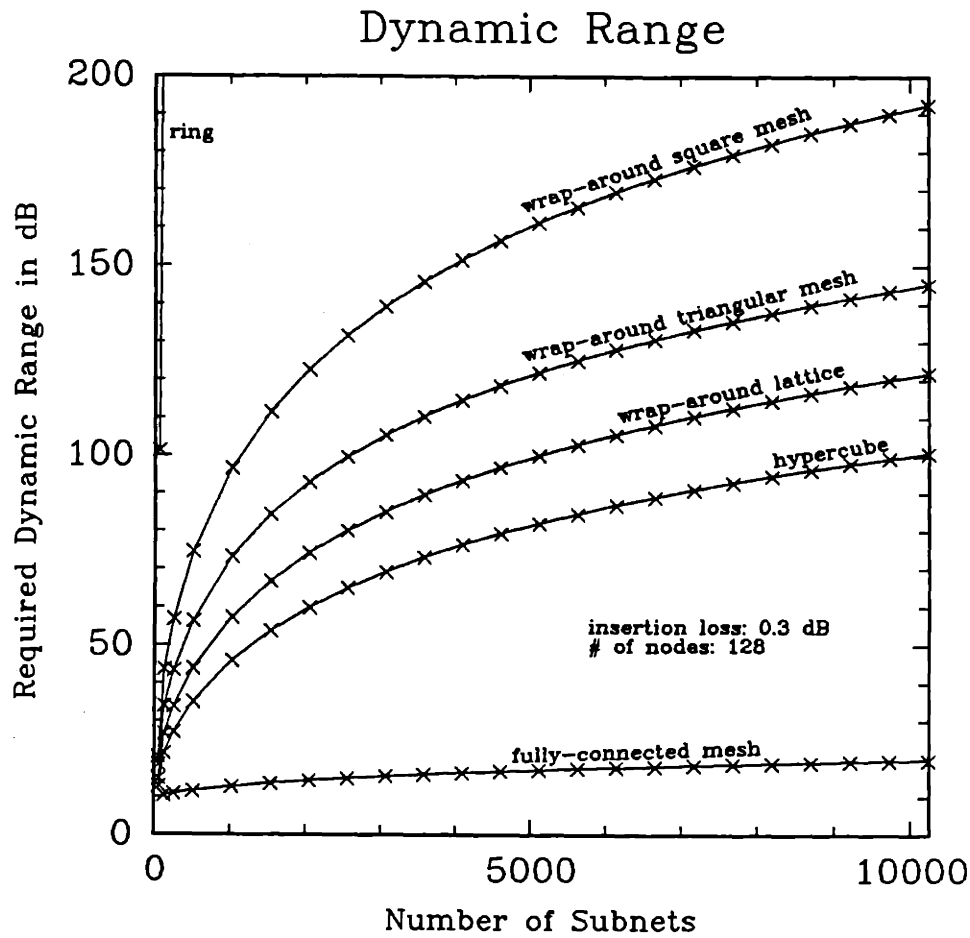

Figure 5.18: Dynamic Range vs. Number of Subnets, for Topologies with 128 Nodes

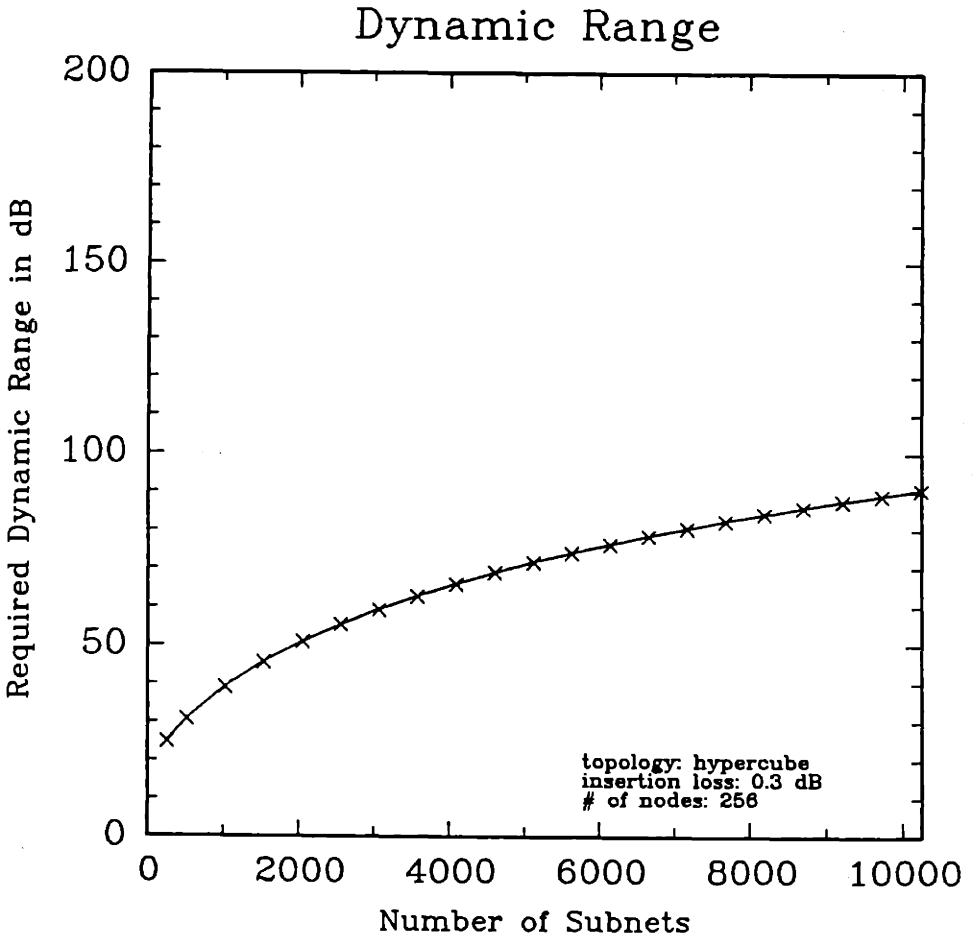

Figure 5.19: Dynamic Range vs. Number of Subnets, for 256-Node Hypercube

of subnets. The maximum power is delivered between subnets on the same node, so that increasing the splitting loss by increasing the number of subnets does not affect the strongest receptions very much. On the other hand, the minimum power is delivered between subnets as far away from each other as they can be, so that the accumulated effect of increased splitting loss over longer paths affects the minimum power more than the maximum power. Therefore, the required dynamic range grows with the number of subnets.

If, in a network supporting 128 subnets with 0.3 dB insertion loss, a dynamic range of less than 40 dB is desired, then Figure 5.15 indicates that, of the topologies examined, anything except a ring with more than 4 nodes, or a 128-node wrap-around square mesh, would work. Figures 5.16–5.19 show that, while maintaining the dynamic range below 40 dB, the fully-connected mesh can support over 10,000 subnets, as can the 4-node wrap-around triangular mesh. Any of the other four topologies can support 512 subnets within a 40 dB dynamic range, for 4 nodes. The 128-node and 256-node hypercubes can also support 512 subnets within a 40 dB dynamic range.

Figure 5.20 plots the dynamic range vs. the insertion loss for the topologies discussed in this section, with 128 subnets and the optimal number of nodes for supporting 128 subnets from Figures 3.2–3.5. An increase in insertion loss produces a greater increase in dynamic range in topologies with longer paths, such as the 128-node hypercube, than in topologies with shorter paths, such as the fully-connected mesh. Increasing the insertion loss will always increase the dynamic range, because loss along the long paths between transceivers delivering the minimum power to each other increases more than loss in the coupler shared by transceivers delivering the maximum power to each other. This effect is stronger in topologies with longer paths.

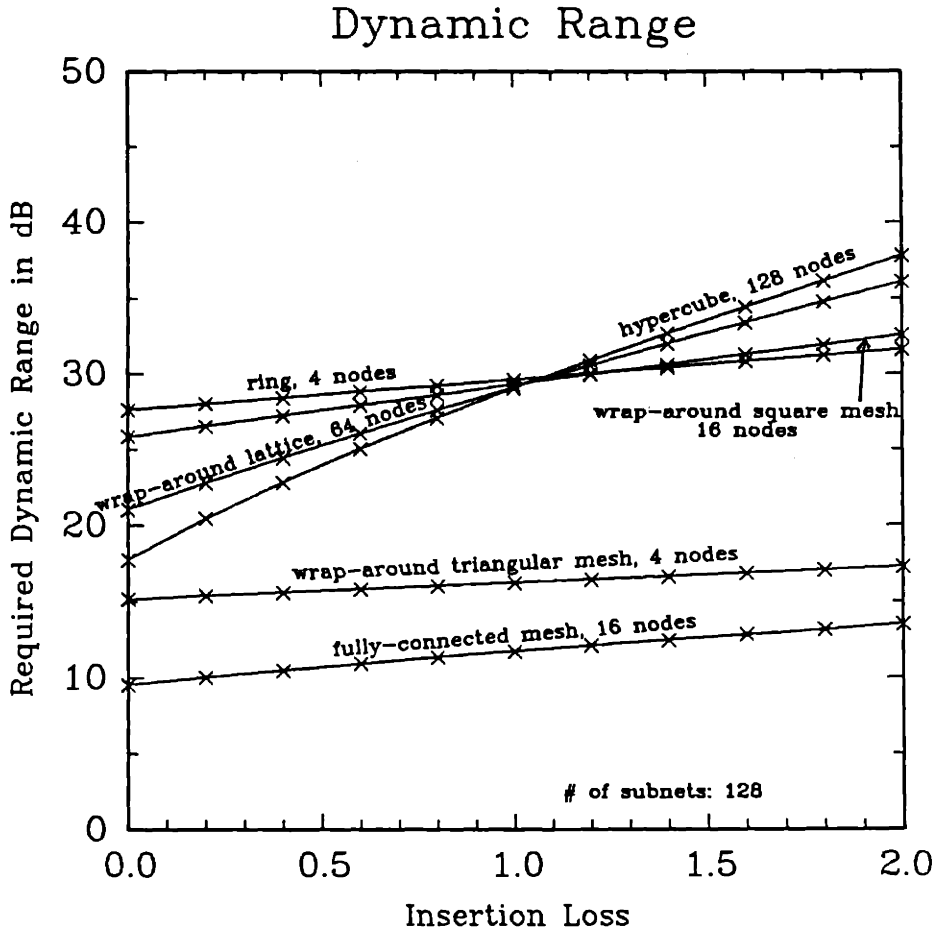

Figure 5.20: Dynamic Range vs. Insertion Loss

Table 5.3: Topologies Supporting 512 Transceivers Within a 50 dB Loss Budget

Topology	# Nodes	# Subnets	# Transceivers per Subnet
Fully-Connected Mesh	4,16,128	512	1
Fully-Connected Mesh	4,16,128	256	2
Fully-Connected Mesh	4,16,128	128	4
Hypercube	128	512	1
Hypercube	128	256	2
Hypercube	128	128	4
Hypercube	256	512	1
Hypercube	256	256	2
Wrap-Around Triangular Mesh	16	512	1
Wrap-Around Triangular Mesh	16	256	2
Wrap-Around Triangular Mesh	16	128	4

5.6 A Numerical Example

Consider the following scenario. A fiber optic local communication network is required to support 512 transceivers. The loss budget must be within 50 dB, and the dynamic range required of the receivers must be within 30 dB. Maximizing the number of nodes will help to keep the nodes close to the subnets, and minimizing the number of required receptions will keep the receivers as simple as possible. Smaller couplers are preferable to larger ones, and there is no constraint on the amount of fiber used. This scenario assumes all couplers have 0.3 dB insertion loss.

The topologies listed in Table 5.3 keep the loss budget within 50 dB. (See Figures 5.4–5.9.)

Keeping the dynamic range below 30 dB precludes using 512 subnets with either the hypercube or the wrap-around triangular mesh. Since the power margins for the

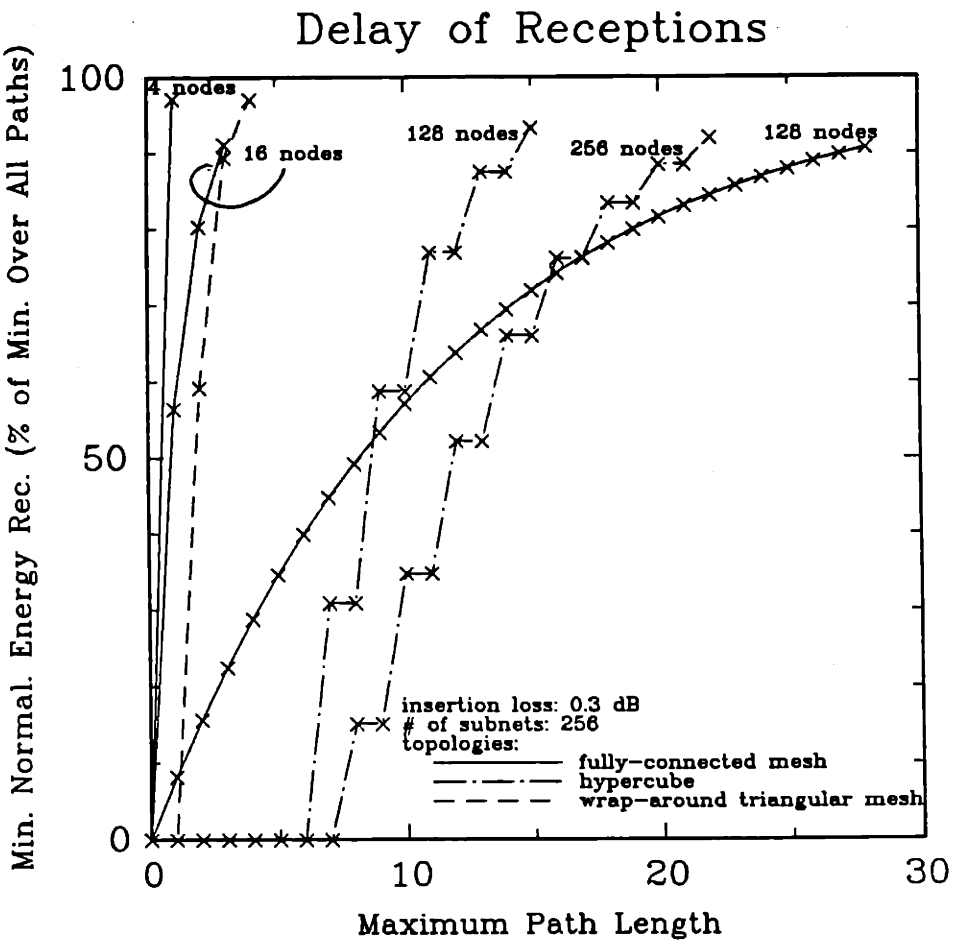

Figure 5.21: Delay of Receptions for Some Topologies Supporting 256 Subnets

remaining topologies allow 3 dB more loss, receivers will process enough receptions to collect at least fifty percent of the possible energy. For simplicity, assume that all receptions over paths with the same number of links arrive together to comprise one reception. Figures 5.21 and 5.22 show the delay of receptions in the remaining topologies, for 256 and 512 subnets. The results for 128 subnets are in Section 5.4. Table 5.4 shows the number of receptions, and the time span in number of links between the first and last receptions, for each topology.

Clearly, the fewest receptions and shortest time spans occur for the 4-node fully-connected mesh, the 16-node fully-connected mesh with 256 or 512 subnets, and the 16-node wrap-around triangular mesh with 256 subnets. On the other hand, maximizing the number of nodes would suggest using the hypercube. Since the 128-

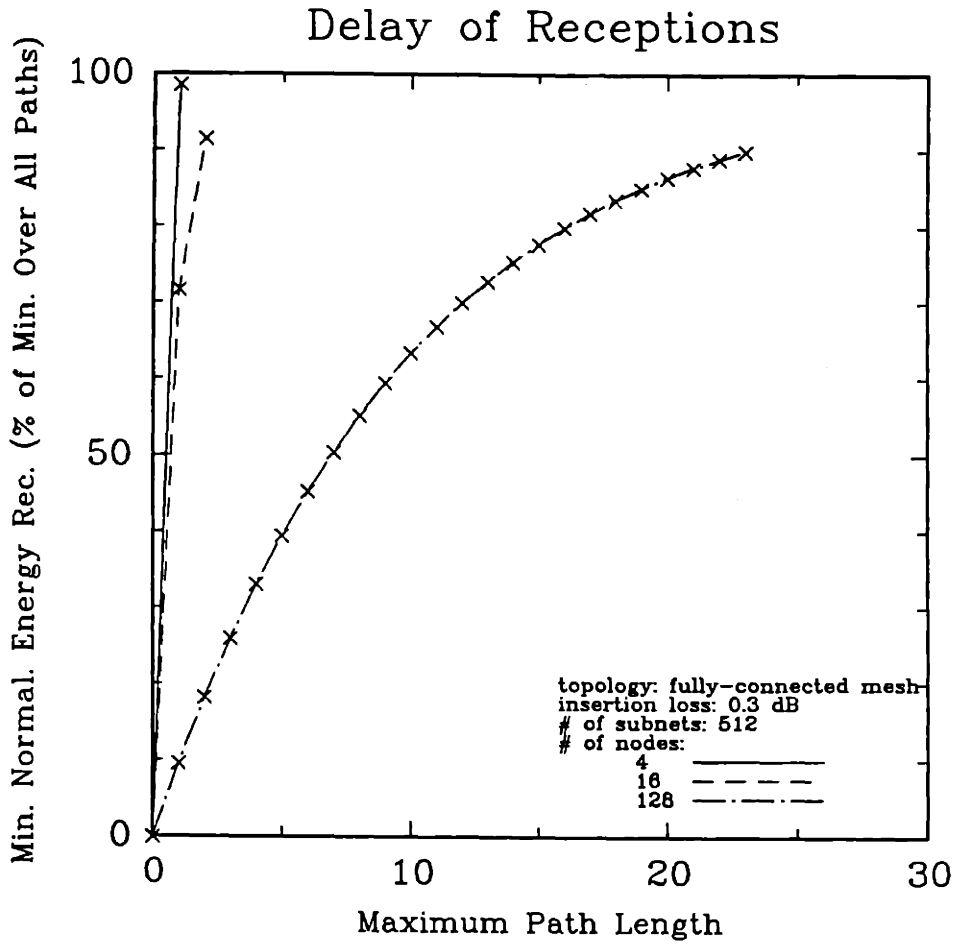

Figure 5.22: Delay of Receptions for the Fully-Connected Mesh Supporting 512 Subnets

Table 5.4: Required Number of Receptions and Time Span Between First and Last Receptions, for Topologies Supporting 512 Transceivers Within a 50 dB Loss Budget and a 30 dB Dynamic Range

Topology	# Nodes	# Subnets	# Receptions	Time Span (# Links)
Fully-Connected Mesh	4	512,256,128	1	0
Fully-Connected Mesh	16	512,256	1	0
Fully-Connected Mesh	16	128	2	1
Fully-Connected Mesh	128	512	7	6
Fully-Connected Mesh	128	256	9	8
Fully-Connected Mesh	128	128	10	9
Hypercube	128	256	2	2
Hypercube	128	128	3	4
Hypercube	256	256	3	4
Wrap-Around Triangular Mesh	16	256	1	0
Wrap-Around Triangular Mesh	16	128	2	1

Table 5.5: Comparison of Coupler Sizes for Several Topologies

Topology	# Nodes	# Subnets	Coupler Size
Fully-Connected Mesh	16	512	47×47
Fully-Connected Mesh	16	256	31×31
Fully-Connected Mesh	16	128	23×23
Hypercube	128	256	9×9
Wrap-Around Triangular Mesh	16	256	22×22
Wrap-Around Triangular Mesh	16	128	14×14

node hypercube with 256 subnets only requires one more reception than most of the 16-node topologies, the next step, presented in Table 5.5, is to compare it to the 16-node topologies based on coupler size. The 4-node topologies are dismissed, based on the requirement of maximizing the number of nodes.

Although the 128-node hypercube will not result in the simplest receiver, it does minimize the coupler size and maximize the number of nodes. Recall that maximizing the number of nodes increases the reliability of the subnet links by allowing the nodes to be placed close to the subnets, making the vulnerable links short. Presumably, choosing among robust topologies indicates a concern for reliability. Assuming that reliability is a higher priority than simplifying the receiver, the 128-node hypercube with 256 subnets is clearly an appropriate compromise for this application.

Chapter 6

Conclusions

6.1 Current State of the Research

Considering only the criterion of maximizing the minimum normalized power delivered over all paths, the fully-connected mesh topology performs best, as long as the number of nodes is chosen appropriately. The analysis of Chapter 4 suggests this, and the numerical results in Chapter 5 demonstrate this for particular cases. Other highly connected topologies should also do well, assuming that all nodes have nearly the same degree of connectivity. The reason for assuming that nodes have nearly the same degree of connectivity, is that in a highly irregular topology, in which the nodes which are furthest apart also have the lowest degree of connectivity, increasing connectivity between nodes that already have a high degree of connectivity may not increase the minimum normalized power delivered, but instead might decrease it. Under the assumption that nodes have nearly the same degree of connectivity, higher connectivity helps to increase the minimum normalized power delivered, because the more connected the topology, the more evenly power is spread out among the subnets.

Due to this even spreading of power, highly connected topologies also minimize the dynamic range of the power levels incident upon a receiver from various transmitters. Therefore, using a highly connected topology helps to accommodate the limitations of sensitivity and dynamic range in today's receivers.

Considering other criteria which are important in practical implementations reveals some unfortunate aspects of very highly connected topologies. For one thing, collecting enough energy for detection in a highly connected topology requires processing many weak receptions. This makes intersymbol interference difficult to deal with, especially at high bit rates. Two ways to alleviate this problem are to use fewer nodes, or less connectivity. Using fewer nodes could cause two more problems: 1) smaller power margin if the greater number of nodes had been optimal for the number of subnets and the insertion loss 2) less reliability for the links to the subnets, because using fewer nodes necessitates making these vulnerable links longer. In most cases, using less connectivity will decrease the minimum normalized energy received. This suggests a tradeoff between power margin and receiver complexity, assuming that receiver complexity increases with the number of required receptions.

Another unfortunate aspect of highly connected topologies is that they require larger couplers, because they have more neighboring nodes per node. How bad this is depends on the state of technology. Currently, larger couplers have more loss than smaller couplers, so that smaller couplers should allow better performance. On the other hand, more connected topologies have shorter paths, and are therefore less sensitive to increases in insertion loss. Thus, there is a technology dependent tradeoff between even distribution of power, effected by high connectivity, and low insertion loss, gained by using smaller couplers in a less connected topology. The optimal solution, depending upon the available couplers, is to use large couplers allowing more connectivity, if the increase in insertion loss is offset by the increased power margin due to distributing power more evenly in the more connected topology.

Section 5.6 contains an example of weighing these tradeoffs against the importance of the various design criteria for a particular application. In that example, the 128-node hypercube was the topology of choice, because it maximized the number of nodes, minimized the coupler size, and came close to the minimum number of receptions. Two things were compromised: the power margin was lower than for a 16-node fully-connected mesh or a 256-node hypercube, and the number of nodes was smaller than

for a 256-node hypercube. In general, emphasizing different criteria more heavily results in a different tradeoff being made. The best choice is application dependent, when several performance criteria are considered.

6.2 Future Research Directions

There are several ways to continue research on this type of network. First of all, the classes of topologies for which there are analytical results could be broadened. Secondly, the mathematical model could be expanded to allow for couplers that do not divide power evenly. Such a change to the model could be used for two purposes. It would enable taking account of realistic, available components, for which the power splitting is usually uneven. In addition, it would enable optimization over another design variable: splitting in the couplers. Although the unevenness in the power splitting of couplers changes, depending upon which input is used, splitting ratios could be fixed independently of the input used by allowing multiple fibers to run between nodes.

Another direction to take would be to determine the actual degree of robustness of the various topologies. This would involve determining how many links could be damaged before the received energy falls below the receiver sensitivity. I conjecture that more highly connected topologies will prove to be more robust. Highly connected topologies have more splitting loss in the nodes than less connected topologies. Therefore, if a link is damaged, causing a coupler to lose power irretrievably from the output connected to that link, a smaller percentage of the power will be lost in a more connected topology.

Performance measures other than the sum of the strengths of the receptions can be considered. For instance, in some applications, the sum of the squares of the strengths of the receptions is more important.

Another interesting study would be the use of wavelength sensitive devices to improve the performance of these networks. For example, a filter placed near a subnet

might serve to pass wavelengths destined for that subnet, and reflect other wavelengths back into the network. Using wavelength sensitive couplers in the nodes could accomplish passive localization and routing. This would alleviate power division somewhat, in that it would not be necessary to broadcast signals. Transmitters and receivers would tune to the correct frequency to communicate.

Finally, one could study the use of amplifiers in these networks. Of course, the network would no longer be passive. Although the amplifiers would boost the minimum power, they could create other problems. One danger would be creating noise and distortion in the signal. Another would be exacerbating the intersymbol interference by boosting echoes that would better be left weak and treated as noise.

The design and use of passive, fiber optic local communication networks is an active research area, in which there are still more questions than answers. Robust topologies is but one of many approaches, and only time and the progress of technology will tell which approach is best.

Appendix A

Proof of Lemma 1

If $f(\cdot)$ is a polynomial function, and S is a square, $n \times n$ matrix with eigenvalues $\{\nu_i | 1 \leq i \leq n\}$, then the eigenvalues of $A = f(S)$ are $\{\lambda_i = f(\nu_i) | 1 \leq i \leq n\}$.

PROOF:

$f(S)$ can be expressed

$$f(S) = \sum_{j=0}^{l} c_j S^j \tag{A.1}$$

for arbitrary l, where the c_j's are scalars.

I now prove two more lemmas to help with the proof of Lemma 1.

Lemma 9 *If S has eigenvalues $\{\nu_i | 1 \leq i \leq n\}$, then $c_j S^j$ has the same eigenvectors as S, with eigenvalues $\{c_j \nu_i^j | 1 \leq i \leq n\}$.*

PROOF OF LEMMA 9:

Let $\underline{x}_i$ be an eigenvector of S with eigenvalue ν_i.

$$c_j S^j \underline{x}_i = c_j \nu_i S^{j-1} \underline{x}_i = c_j \nu_i^2 S^{j-2} \underline{x}_i = \cdots = c_j \nu_i^j \underline{x}_i \tag{A.2}$$

Therefore, $\underline{x}_i$ is an eigenvector of $c_j S^j$ with eigenvalue $c_j \nu_i^j$.

Lemma 10 *Let A and B be two square, $n \times n$ matrices with the same eigenvectors $\{\underline{x}_i | 1 \leq i \leq n\}$. The eigenvalues of the matrices are such that*

$$A\underline{x}_i = \alpha_i \underline{x}_i, \quad 1 \leq i \leq n \tag{A.3}$$

$$B\underline{x}_i = \beta_i \underline{x}_i, \quad 1 \leq i \leq n \tag{A.4}$$

$C = A + B$ also has eigenvectors $\{\underline{x}_i | 1 \leq i \leq n\}$, with eigenvalues $\{\alpha_i + \beta_i | 1 \leq i \leq n\}$.

PROOF OF LEMMA 10:

$$C\underline{x}_i = (A+B)\underline{x}_i = A\underline{x}_i + B\underline{x}_i = \alpha_i\underline{x}_i + \beta_i\underline{x}_i = (\alpha_i + \beta_i)\underline{x}_i, \quad 1 \leq i \leq n \tag{A.5}$$

Lemmas 9 and 10, along with Equation A.1 expressing $f(S)$ in the form of a summation, prove Lemma 1.

Appendix B

Minimum Power for Two Topologies When S is Circulant

B.1 Fully-Connected Mesh

$$p_{min} = s \min_i \left[\frac{1}{n} \sum_{j=1}^{n} \frac{\overline{w}^{(i-1)(j-1)}}{1 - \sum_{k=1}^{n} s_k w^{(j-1)(k-1)}} \right] \tag{B.1}$$

For a fully-connected mesh,

$$s_k = \begin{cases} 0 & k = 1 \\ s & k \neq 1 \end{cases} \tag{B.2}$$

$$p_{min} = s \min_i \left[\frac{1}{n} \sum_{j=1}^{n} \frac{\overline{w}^{(i-1)(j-1)}}{1 - s \sum_{k=2}^{n} w^{(j-1)(k-1)}} \right] \tag{B.3}$$

Lemma 11 *Let* $w = \exp\left[\sqrt{-1}\frac{2\pi}{n}\right]$.

$$\sum_{r=0}^{n-1} w^{r(j-k)} = \begin{cases} 0 & j \neq k \\ n & j = k \end{cases} \tag{B.4}$$

[Dav79]

By Lemma 11,

$$\sum_{k=2}^{n} w^{(k-1)(j-1)} = \sum_{k=1}^{n} w^{(k-1)(j-1)} - 1 = \begin{cases} n-1 & j = 1 \\ -1 & j \neq 1 \end{cases} \tag{B.5}$$

Therefore,

$$p_{min} = s \min_i \left[\frac{1}{n} \left(\frac{1}{1-s(n-1)} + \sum_{j=2}^{n} \frac{\overline{w}^{(i-1)(j-1)}}{1+s} \right) \right] \tag{B.6}$$

Reference to Equation B.5 reveals that the expression in square brackets in Equation B.6 is minimized for $i \neq 1$. Therefore,

$$\begin{aligned} p_{min} &= \frac{s}{n} \left[\frac{1}{1-s(n-1)} - \frac{1}{1+s} \right] = \frac{s}{n} \left\{ \frac{1+s-1+s(n-1)}{[1-(n-1)s](1+s)} \right\} \\ p_{min} &= \frac{s^2}{[1-(n-1)s](1+s)} \end{aligned} \tag{B.7}$$

B.2 Ring

$$p_{min} = s \min_i \left[\frac{1}{n} \sum_{j=1}^{n} \frac{\overline{w}^{(i-1)(j-1)}}{1 - \sum_{k=1}^{n} s_k w^{(j-1)(k-1)}} \right]$$

For a ring,

$$s_k = \begin{cases} s & k = 2, n \\ 0 & \text{else} \end{cases} \tag{B.8}$$

$$p_{min} = s \min_i \left[\frac{1}{n} \sum_{j=1}^{n} \frac{\overline{w}^{(i-1)(j-1)}}{1 - s\left(w^{j-1} + w^{(n-1)(j-1)}\right)} \right] \tag{B.9}$$

But

$$w^{n-1} = \overline{w} \tag{B.10}$$

so that

$$p_{min} = s \min_i \left\{ \frac{1}{n} \sum_{j=1}^{n} \frac{\overline{w}^{(i-1)(j-1)}}{1 - 2s\cos\left[2\pi(j-1)/n\right]} \right\} \tag{B.11}$$

Intuitively, in the ring, the least power should be delivered to receivers at the node(s) furthest from the transmitting node. Recall that sa_i is the power delivered to a receiver on node i from a transmitter on node 1 ($a_i = a_{1i}$). To minimize sa_i over i, choose $i = n/2 + 1$ for n even, or $i = (n+1)/2$ for n odd. For n even:

$$\begin{aligned} p_{min} &= \frac{s}{n} \sum_{j=1}^{n} \frac{\overline{w}^{(j-1)n/2}}{1 - 2s\cos\left[2\pi(j-1)/n\right]} \\ p_{min} &= \frac{s}{n} \sum_{j=1}^{n} \frac{(-1)^{j-1}}{1 - 2s\cos\left[2\pi(j-1)/n\right]} \end{aligned} \tag{B.12}$$

For n odd:

$$
\begin{aligned}
p_{min} &= \frac{s}{n} \sum_{j=1}^{n} \frac{\overline{w}^{(j-1)(n-1)/2}}{1 - 2s\cos\left[2\pi(j-1)/n\right]} \\
p_{min} &= \frac{s}{n} \sum_{j=1}^{n} \frac{(-1)^{j-1} w^{(j-1)/2}}{1 - 2s\cos\left[2\pi(j-1)/n\right]}
\end{aligned}
\tag{B.13}
$$

Appendix C

of Transceivers Supported by a Fully-Connected Mesh

For the fully-connected mesh, the minimum normalized power delivered between all transmitter-receiver pairs is

$$p_{min} = \frac{s^2}{[1-(n-1)s]\,(1+s)} \tag{C.1}$$

Solving for s,

$$s^2 = p_{min}\left[-(n-1)s^2 - (n-2)s + 1\right] \tag{C.2}$$

$$0 = [1+(n-1)p_{min}]\,s^2 + (n-2)p_{min}s - p_{min} \tag{C.3}$$

$$s = \frac{-(n-2)p_{min} \pm \{(n-2)^2 p_{min}^2 + 4\,[1+(n-1)p_{min}]\,p_{min}\}^{1/2}}{2\,[1+(n-1)p_{min}]} \tag{C.4}$$

$$= \frac{-(n-2)p_{min} \pm (n^2 p_{min}^2 + 4p_{min})^{1/2}}{2+2(n-1)p_{min}} \tag{C.5}$$

$$= \frac{-(n-2) \pm (n^2 + 4/p_{min})^{1/2}}{2(n-1)+2/p_{min}} \tag{C.6}$$

Since $s > 0$, take the positive root:

$$s = \frac{g}{m/n + n - 1} = \frac{-(n-2) + (n^2 + 4/p_{min})^{1/2}}{2(n-1) + 2/p_{min}} \tag{C.7}$$

$$g\left[2(n-1) + \frac{2}{p_{min}}\right] = \frac{m}{n}\left[-(n-2) + (n^2 + \frac{4}{p_{min}})^{1/2}\right] + (n-1)\left[-(n-2) + (n^2 + \frac{4}{p_{min}})^{1/2}\right] \tag{C.8}$$

$$\frac{m}{n}\left[(n^2 + \frac{4}{p_{min}})^{1/2} - (n-2)\right] = g\left[2(n-1) + \frac{2}{p_{min}}\right] - (n-1)\left[(n^2 + \frac{4}{p_{min}})^{1/2} - n + 2\right] \tag{C.9}$$

$$m = \frac{2gn\left(\frac{1}{p_{min}} + n - 1\right)}{\left(n^2 + \frac{4}{p_{min}}\right)^{\frac{1}{2}} - n + 2} - n(n-1) \tag{C.10}$$

Appendix D

Proof of Lemma 6

Let $\{a_i | 1 \leq i \leq n\}$ *be the elements across the first row of* $A = (I - S)^{-1}$, *where* S *is the circulant node to node power distribution matrix of a passive FOLCN.*

$$a_1 > a_j, \quad 2 \leq j \leq n \tag{D.1}$$

Furthermore, $a_2 = a_3 = \cdots = a_n$ *if and only if* $i_n = n - 1$.

PROOF:

$$A = (I - S)^{-1} \tag{D.2}$$

$$(I - S)A = I \tag{D.3}$$

$$\begin{pmatrix} 1 & -s_2 & -s_3 & \cdots & -s_n \\ -s_n & 1 & -s_2 & \cdots & -s_{n-1} \\ -s_{n-1} & -s_n & 1 & \cdots & -s_{n-2} \\ \vdots & \vdots & \vdots & & \vdots \\ -s_2 & -s_3 & -s_4 & \cdots & 1 \end{pmatrix} \begin{pmatrix} a_1 & a_2 & a_3 & \cdots & a_n \\ a_n & a_1 & a_2 & \cdots & a_{n-1} \\ a_{n-1} & a_n & a_1 & \cdots & a_{n-2} \\ \vdots & \vdots & \vdots & & \vdots \\ a_2 & a_3 & a_4 & \cdots & a_1 \end{pmatrix}$$

$$= \begin{pmatrix} 1 & 0 & 0 & \cdots & 0 \\ 0 & 1 & 0 & \cdots & 0 \\ 0 & 0 & 1 & \cdots & 0 \\ \vdots & \vdots & \vdots & & \vdots \\ 0 & 0 & 0 & \cdots & 1 \end{pmatrix} \tag{D.4}$$

Multiplying these matrices yields the following system of equations:

$$\begin{aligned} a_1 - s_2 a_n - s_3 a_{n-1} - \cdots - s_n a_2 &= 1 && \text{(D.5)} \\ a_2 - s_2 a_1 - s_3 a_n - \cdots - s_n a_3 &= 0 && \text{(D.6)} \\ a_3 - s_2 a_2 - s_3 a_1 - \cdots - s_n a_4 &= 0 && \text{(D.7)} \\ &\vdots \\ a_n - s_2 a_{n-1} - s_3 a_{n-2} - \cdots - s_n a_1 &= 0 && \text{(D.8)} \\ & && \text{(D.9)} \end{aligned}$$

These equations are more useful in the following form:

$$\begin{aligned} a_1 &= 1 + s_2 a_n + s_3 a_{n-1} + \cdots + s_n a_2 && \text{(D.10)} \\ a_2 &= s_2 a_1 + s_3 a_n + \cdots + s_n a_3 && \text{(D.11)} \\ a_3 &= s_2 a_2 + s_3 a_1 + \cdots + s_n a_4 && \text{(D.12)} \\ &\vdots \\ a_n &= s_2 a_{n-1} + s_3 a_{n-2} + \cdots + s_n a_1 && \text{(D.13)} \end{aligned}$$

Recall that $s_i = 0$ or s, $2 \leq i \leq n$, and that the total normalized power delivered to all receivers must be less than 1. The total power delivered to all receivers on node i is $\frac{m}{n} s a_i$. Therefore,

$$\frac{m}{n} s \sum_{i=1}^{n} a_i < 1 \qquad \text{(D.14)}$$

Equations D.11–D.13 indicate that

$$a_i < s \sum_{i=1}^{n} a_i \leq \frac{m}{n} s \sum_{i=1}^{n} a_i < 1, \quad 2 \leq i \leq n \qquad \text{(D.15)}$$

Furthermore, Equation D.10 indicates that $a_1 > 1$, since at least two of the s_i's, $s \leq i \leq n$, must be positive in a robust topology. Therefore,

$$a_i < a_1, \quad 2 \leq i \leq n \qquad \text{(D.16)}$$

Thus the first part of the lemma is proven.

To prove the second part, I first show that if $i_n = n-1$, then $a_2 = a_3 = \cdots = a_n$. When $i_n = n-1$, then

$$s_i = \begin{cases} 0 & i = 1 \\ s & 2 \leq i \leq n \end{cases} \tag{D.17}$$

Equations D.11–D.13 can thus be rewritten.

$$a_2 = s\sum_{i=1}^{n} a_i - sa_2 \tag{D.18}$$

$$a_3 = s\sum_{i=1}^{n} a_i - sa_3 \tag{D.19}$$

$$\vdots$$

$$a_n = s\sum_{i=1}^{n} a_i - sa_n \tag{D.20}$$

Therefore,

$$a_2 = a_3 = \cdots = a_n = \frac{s}{1+s}\sum_{i=1}^{n} a_i \tag{D.21}$$

Therefore, if $i_n = n-1$, then $a_2 = a_3 = \cdots = a_n$.

Now if $a_2 = a_3 = \cdots = a_n$ implies that $i_n = n-1$, then the lemma will be proven. Let

$$a_i = \begin{cases} a_1 & i = 1 \\ a & 2 \leq i \leq n \end{cases} \tag{D.22}$$

Each of equations D.11–D.13 has i_n positive terms on the right hand side. At most one positive term has value sa_1; the other positive terms have value sa. If $k = n-1-i_n$ elements of $\{s_i | 2 \leq i \leq n\}$ have value 0, then k elements of $\{a_i | 2 \leq i \leq n\}$ have value $i_n sa$, and the rest have value $sa_1 + (i_n - 1)sa > i_n sa$. This violates the assumption that $a_2 = a_3 = \cdots = a_n$, unless $k = 0$. When $k = 0$, $i_n = n-1$, so that $a_2 = a_3 = \cdots = a_n$ implies $i_n = n-1$. Therefore, $a_2 = a_3 = \cdots = a_n$ if and only if $i_n = n-1$, so that the entire lemma is proven.

Appendix E

Bound on Chernoff Parameter When S is Circulant

$F_a(B_a)$ is the probability that a is less than or equal to B_a. a is a random variable taking on each of the values $\{a_i | 1 \leq i \leq n\}$ with probability $1/n$. $\{a_i | 1 \leq i \leq n\}$ are the elements across the first row of $A = (I - S)^{-1}$, where S is the circulant node to node power distribution matrix of a passive FOLCN. $\hat{t}$ is the value of t such that if $t < \hat{t}$, then

$$\begin{aligned} F_a(B_a) &< \frac{1}{n}, \text{ if } B_a < a_i, \ \forall i \\ \frac{1}{n}\sum_{i=1}^{n} e^{t(a_i - B_a)} &< \frac{1}{n} \quad \text{from Equation 4.49} \\ \sum_{i=1}^{n} e^{t(a_i - B_a)} &< 1 \end{aligned} \tag{E.1}$$

Equation E.1 holds if

$$\begin{aligned} e^{t(a_i - B_a)} &< \frac{1}{n}, \ \forall i \\ t(a_i - B_a) &< -\ln n, \ \forall i \\ t &< -\frac{\ln n}{a_i - B_a}, \ \forall i \\ t &< -\frac{\ln n}{\min_i a_i - B_a} \end{aligned} \tag{E.2}$$

Therefore,

$$\hat{t} = -\frac{\ln n}{\min_i a_i - B_a} \tag{E.3}$$

Appendix F

Proof of Lemma 7

The elements, $\{a_{(l-1)q+i} | 1 \leq l \leq p,\ 1 \leq i \leq q\}$, *and eigenvalues,* $\{\lambda_{(l-1)q+i} | 1 \leq l \leq p,\ 1 \leq i \leq q\}$, *of* A, *a level 2 circulant matrix of type* (p,q), *have the following relationships:*

$$a_{(l-1)q+i} = \frac{1}{pq} \sum_{k=1}^{p} \sum_{j=1}^{q} \lambda_{(k-1)q+j} \overline{w}_p^{(l-1)(k-1)} \overline{w}_q^{(i-1)(j-1)} \quad 1 \leq l \leq p, \quad 1 \leq i \leq q$$

$$\lambda_{(l-1)q+i} = \sum_{k=1}^{p} \sum_{j=1}^{q} a_{(k-1)q+j} w_p^{(l-1)(k-1)} w_q^{(i-1)(j-1)} \quad 1 \leq l \leq p, \quad 1 \leq i \leq q$$

Let Λ be the diagonal matrix of the eigenvalues of A. From Theorem 9,

$$A = (F_p \otimes F_q)^* \Lambda (F_p \otimes F_q) \tag{F.1}$$

$$a_{(l-1)q+i} = [\text{1st row of } (F_p \otimes F_q)^* \Lambda] \times [(l-1)q + i\text{-th column of } F_p \otimes F_q] \tag{F.2}$$

$$F_p^* = \frac{1}{\sqrt{p}} \begin{pmatrix} 1 & 1 & 1 & \cdots & 1 \\ 1 & w_p & w_p^2 & \cdots & w_p^{p-1} \\ 1 & w_p^2 & w_p^4 & \cdots & w_p^{2(p-1)} \\ \vdots & \vdots & \vdots & & \vdots \\ 1 & w_p^{p-1} & w_p^{2(p-1)} & \cdots & w_p^{(p-1)(p-1)} \end{pmatrix} \tag{F.3}$$

$$w_p = \exp\left[\sqrt{-1}\frac{2\pi}{p}\right] \tag{F.4}$$

F_q^* and w_q are obtained by inserting q for p in the last two equations.

Since the first row of F_p^* is all $(1/\sqrt{p})$'s, and the first row of F_q^* is all $(1/\sqrt{q})$'s, the first row of $(F_p \otimes F_q)^*$ is all $(1/\sqrt{pq})$'s. Therefore, the first row of $(F_p \otimes F_q)^* \Lambda$ is

$$\frac{1}{\sqrt{pq}} (\lambda_1 \ \lambda_2 \ \cdots \ \lambda_{pq}) \tag{F.5}$$

The $(l-1)q+i$-th column of $F_p \otimes F_q$ is the i-th column of F_q multiplied by each of the elements in the l-th column of F_p. Therefore, the $(l-1)q+i$-th column of $F_p \otimes F_q$ is:

$$\frac{1}{\sqrt{pq}} \times \Big(1 \ \overline{w}_q^{i-1} \ \cdots \ \overline{w}_q^{(q-1)(i-1)} \ \overline{w}_p^{l-1} \ \overline{w}_p^{l-1}\overline{w}_q^{i-1} \ \cdots \ \overline{w}_p^{l-1}\overline{w}_q^{(q-1)(i-1)} \ \cdots\cdots \ \overline{w}_p^{(p-1)(l-1)} \ \overline{w}_p^{(p-1)(l-1)}\overline{w}_q^{i-1} \ \cdots \ \overline{w}_p^{(p-1)(l-1)}\overline{w}_q^{(q-1)(i-1)}\Big)^T \tag{F.6}$$

$a_{(l-1)q+i}$ is the inner product of Expressions F.5 and F.6.

$$a_{(l-1)q+i} = \frac{1}{pq} \sum_{k=1}^{p} \sum_{j=1}^{q} \lambda_{(k-1)q+j} \overline{w}_p^{(l-1)(k-1)} \overline{w}_q^{(i-1)(j-1)} \quad 1 \le l \le p, \quad 1 \le i \le q \tag{F.7}$$

Instead of doing an even lengthier derivation to find $\lambda_{(l-1)q+i}$, I make use of the following lemma.

Lemma 12 *Let Ω_p be the diagonal matrix whose diagonal elements are $(1, w_p, w_p^2, \ldots, w_p^{p-1})$. Let A be a level 2 circulant of type (p,q), and let the blocks across the first row of A be $\{A_i | 1 \le i \le p\}$. Let Λ_k be the diagonal matrix of the eigenvalues of block A_k. The diagonal matrix of the eigenvalues of A is: [Dav79]*

$$\Lambda = \sum_{k=0}^{p-1} \Omega_p^k \otimes \Lambda_{k+1} \tag{F.8}$$

PROOF OF LEMMA 12: [Dav79], pp. 185–186

Denote a diagonal matrix, such as Λ, as $\mathrm{diag}(\lambda_1, \lambda_2, \ldots, \lambda_{pq})$. From Lemma 12,

$$\Lambda = \sum_{k=0}^{p-1} \left[\mathrm{diag}\left(1, w_p, w_p^2, \ldots, w_p^{p-1}\right)\right]^k \otimes \mathrm{diag}\left(\lambda_{k+1,1}, \lambda_{k+1,2}, \ldots, \lambda_{k+1,q}\right) \tag{F.9}$$

where $\lambda_{k+1,j}$ denotes the j-th eigenvalue of A_{k+1}.

$$\begin{aligned}\Lambda &= \sum_{k=0}^{p-1} \mathrm{diag}\left(1, w_p^k, w_p^{2k}, \ldots, w_p^{k(p-1)}\right) \\ &\qquad \otimes \mathrm{diag}\left(\lambda_{k+1,1}, \lambda_{k+1,2}, \ldots, \lambda_{k+1,q}\right) \qquad \text{(F.10)} \\ \lambda_{(l-1)q+i} &= \sum_{k=0}^{p-1} w_p^{(l-1)k} \lambda_{k+1,i} \quad 1 \le l \le p, \quad 1 \le i \le q \qquad \text{(F.11)}\end{aligned}$$

From Lemma 5,

$$\lambda_{k+1,i} = \sum_{j=1}^{q} a_{k+1,j} w_q^{(i-1)(j-1)} \quad 1 \le i \le q \qquad \text{(F.12)}$$

where $a_{k+1,j}$ is the j-th element on the first row of A_{k+1}. Therefore,

$$\begin{aligned}\lambda_{(l-1)q+i} &= \sum_{k=0}^{p-1}\sum_{j=1}^{q} a_{k+1,j} w_p^{(l-1)k} w_q^{(i-1)(j-1)} \quad 1 \le l \le p, \quad 1 \le i \le q \\ \lambda_{(l-1)q+i} &= \sum_{k=1}^{p}\sum_{j=1}^{q} a_{k,j} w_p^{(l-1)(k-1)} w_q^{(i-1)(j-1)} \quad 1 \le l \le p, \quad 1 \le i \le q \qquad \text{(F.13)}\end{aligned}$$

However, $a_{k,j} = a_{(k-1)q+j}$, the $[(k-1)q+j]$-th element of A.

$$\lambda_{(l-1)q+i} = \sum_{k=1}^{p}\sum_{j=1}^{q} a_{(k-1)q+j} w_p^{(l-1)(k-1)} w_q^{(i-1)(j-1)} \quad 1 \le l \le p, \quad 1 \le i \le q \qquad \text{(F.14)}$$

Appendix G

Minimum Power Delivered in a Hypercube Topology

The minimum power delivered between all transceiver pairs in a passive FOLCN with a node to node power distribution matrix, S, that is a level 2 circulant matrix of type (p, q), is

$$\begin{aligned} p_{min} &= s \min_{l,i} a_{(l-1)q+i} \\ p_{min} &= s \min_{l,i} \left[\frac{1}{pq} \sum_{k=1}^{p} \sum_{j=1}^{q} \frac{\overline{w}_p^{(l-1)(k-1)} \overline{w}_q^{(i-1)(j-1)}}{1 - \sum_{u=1}^{p} \sum_{v=1}^{q} s_{(u-1)q+v} w_p^{(k-1)(u-1)} w_q^{(j-1)(v-1)}} \right] \end{aligned} \quad \text{(G.1)}$$

s is given by Equation 4.1, and w_p and w_q are given in Theorem 11.

The node to node power distribution matrix of a hypercube topology, S, is a level 2 circulant of type $(2^{d-1}, 2)$. The number of nodes is $n = 2^d$. The lowest power level is delivered between transceivers on "opposite corners" of the hypercube. This corresponds to $a_n = a_{2^d}$, so that the right-hand side of Equation G.1 is minimized for $l = 2^{d-1}$, $i = 2$. Note that $w_2 = -1$.

$$p_{min} = \frac{s}{2^d} \sum_{k=1}^{2^{d-1}} \sum_{j=1}^{2} \frac{\overline{w}_{2^{d-1}}^{(2^{d-1}-1)(k-1)} (-1)^{j-1}}{1 - \sum_{u=1}^{2^{d-1}} \sum_{v=1}^{2} s_{(u-1)2+v} w_{2^{d-1}}^{(k-1)(u-1)} (-1)^{(j-1)(v-1)}} \quad \text{(G.2)}$$

The non-zero $s_{(u-1)2+v}$'s are s_2, s_3, s_5, s_9, ..., $s_{2^{d-1}+1}$. These terms correspond to

$u = 1$ while $v = 2$, and $v = 1$ while $u = 2, 3, 5, \ldots, 2^{d-2} + 1$. Thus

$$\begin{aligned}\sum_{u=1}^{2^{d-1}} \sum_{v=1}^{2} s_{(u-1)2+v} w_{2^{d-1}}^{(k-1)(u-1)} (-1)^{(j-1)(v-1)} &= s\left[(-1)^{j-1} + w_{2^{d-1}}^{k-1} + w_{2^{d-1}}^{(k-1)2} + w_{2^{d-1}}^{(k-1)4} \right. \\ &\qquad \left. + \cdots + w_{2^{d-1}}^{(k-1)2^{d-2}}\right] \\ &= s(-1)^{j-1} + s \sum_{x=0}^{d-2} w_{2^{d-1}}^{(k-1)2^x} \qquad \text{(G.3)}\end{aligned}$$

Therefore, for the d-dimensional hypercube, $n = 2^d$,

$$p_{min} = \frac{s}{2^d} \sum_{k=1}^{2^{d-1}} \sum_{j=1}^{2} \frac{\overline{w}_{2^{d-1}}^{(2^{d-1}-1)(k-1)} (-1)^{j-1}}{1 - s(-1)^{j-1} - s \sum_{x=0}^{d-2} w_{2^{d-1}}^{(k-1)2^x}} \qquad \text{(G.4)}$$

Appendix H

Delay of Receptions

The plots contained in this appendix show the minimum, normalized energy received, expressed as a percentage of the minimum, normalized energy received over all paths, vs. the maximum path length included in the calculation. All topologies have 128 subnets and 0.3 dB insertion loss. The various curves in each plot correspond to different numbers of nodes. Each curve stops after the first data point above ninety percent.

Suppose ninety percent of the minimum energy delivered over all paths allows a subnet to distribute to each receiver at least enough energy to support it. Collecting this amount of energy requires adding energy from some number of receptions, arriving over some time span. If the desired bit rate is chosen independently of this time span, then there might be intersymbol interference, requiring some equalization in the receiver, as mentioned in Section 1.2. A longer time span between the first and last required receptions, and a greater number of required receptions, result in a more complicated receiver.

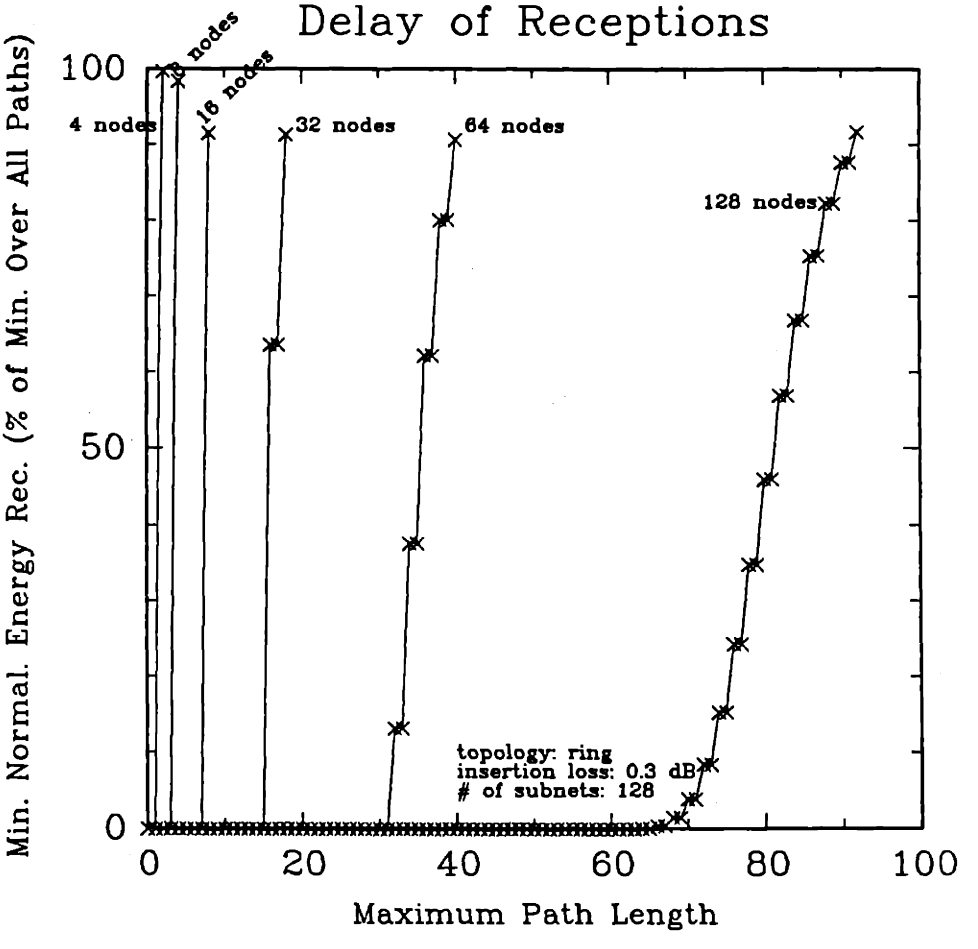

Figure H.1: Delay of Receptions in the Ring

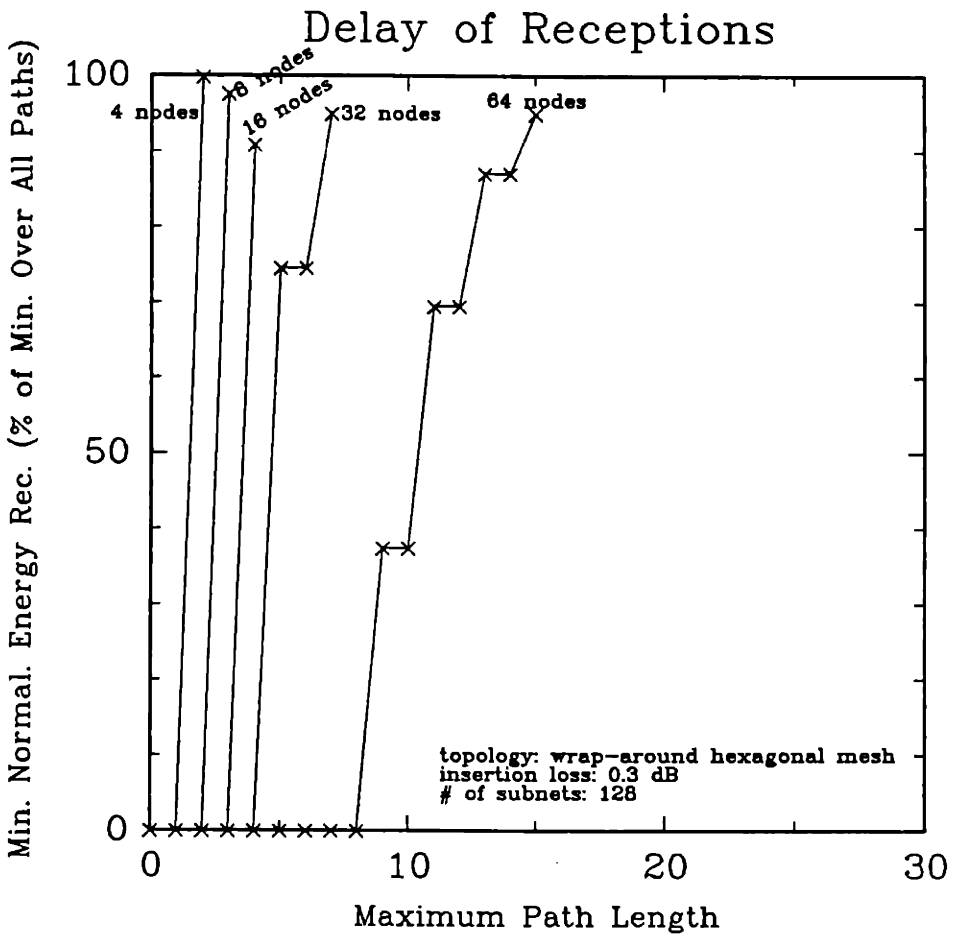

Figure H.2: Delay of Receptions in the Wrap-Around Hexagonal Mesh

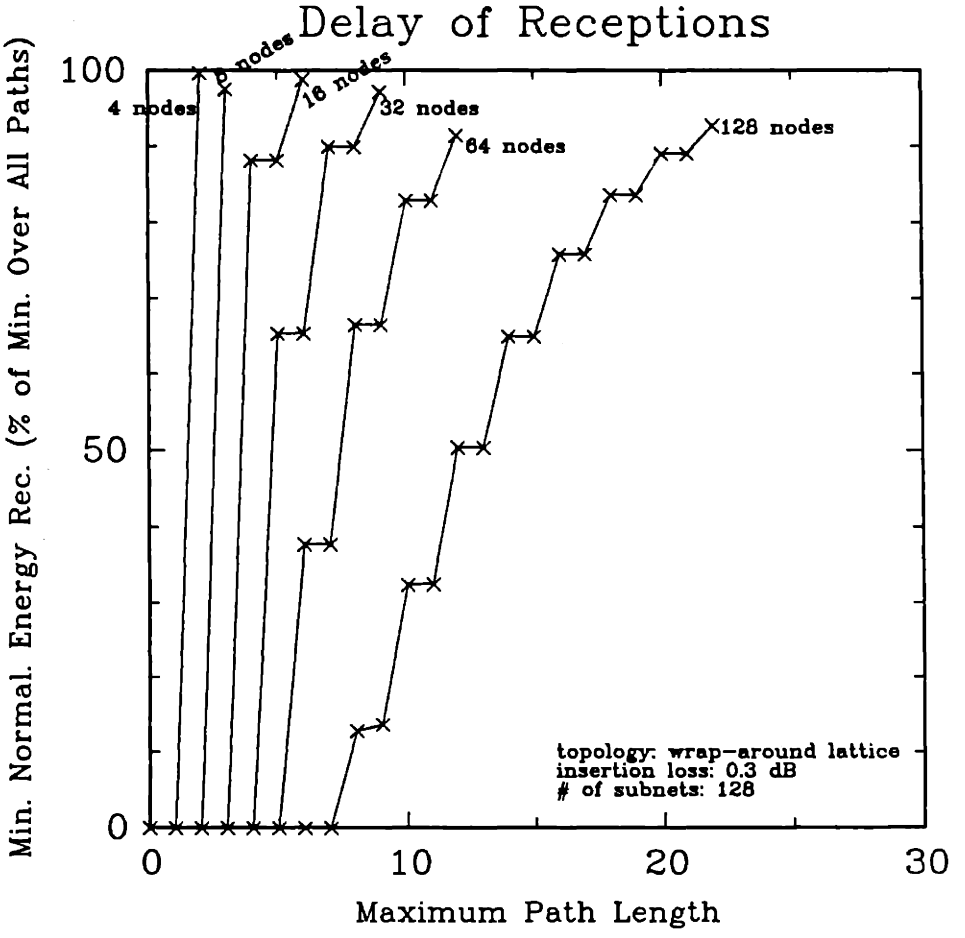

Figure H.3: Delay of Receptions in the Wrap-Around Lattice

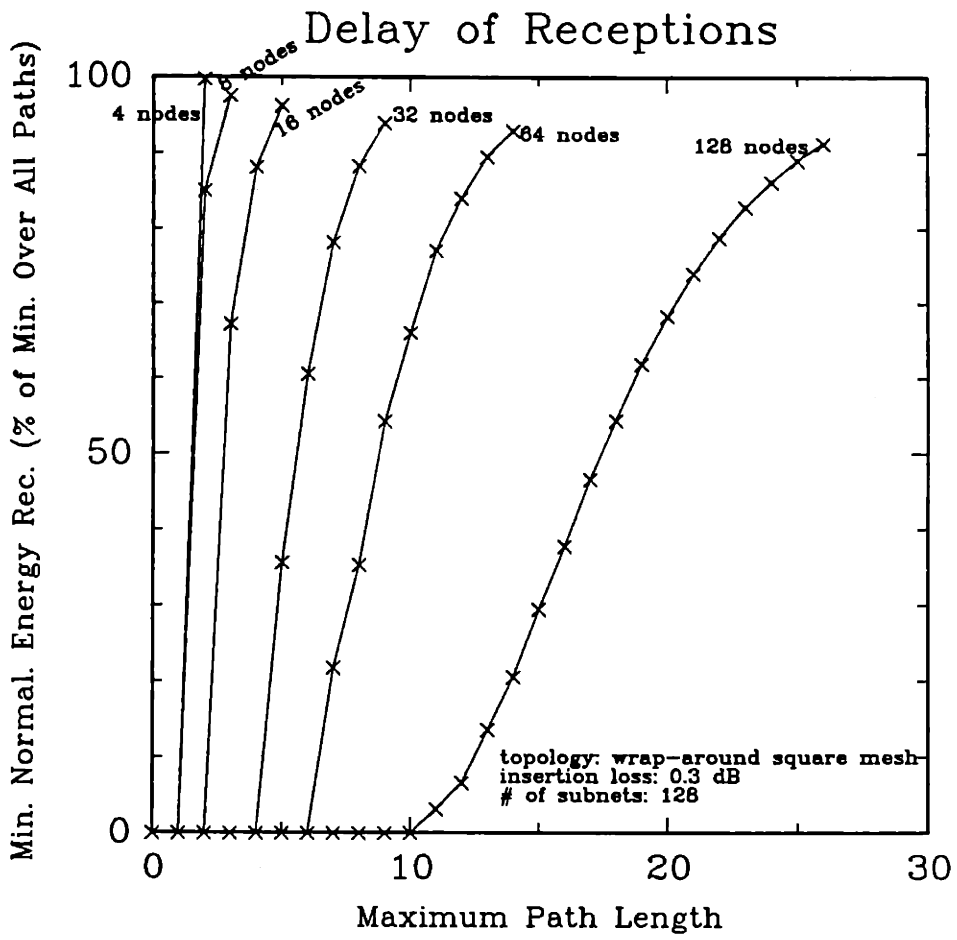

Figure H.4: Delay of Receptions in the Wrap-Around Square Mesh

Bibliography

Fiber Optics and Communications

[Abe86] Jerome D. Abernathy, "Power Division in Optical Local Area Networks," January 5, 1986, unpublished

[Alt88] Louise F. Alterman, "Performance of Fiber Optic Communication Networks with Multiple Paths," M.S. Thesis, Massachusetts Institute of Technology, Cambridge, November 1988

[Bak87] Donald G. Baker, *Monomode Fiber-Optic Design with Local-area and Long-Haul Network Applications*, Van Nostrand Reinhold Company, New York, 1987

[Dav87] A. W. Davis, M. J. Pettitt, J. P. King, S. Wright, "Phase Diversity Techniques for Coherent Optical Receivers," *Journal of Lightwave Technology*, Vol. LT-5, No. 4, pp. 561–572, April 1987

[Dix87] Roy C. Dixon, "Lore of the Token Ring," *IEEE Network Magazine*, Vol. 1, No. 1, pp. 11–18, January 1987

[Gal68] Robert G. Gallager, *Information Theory and Reliable Communication*, John Wiley & Sons, Inc., New York, 1968

[Ham88] Walid M. Hamdy, "Performance Analysis of Retrial Access Schemes for Optical Communication Networks with Slow and Fast tuning," M.S. Thesis, Massachusetts Institute of Technology, Cambridge, May 1988

[Hum89] Pierre A. Humblet, Massachusetts Institute of Technology, private communication, 1989

[Kal86] B. Michael Kale, "Manufacturability of 3×3 Single-Mode Fiber Optical Couplers," *SPIE, Vol. 722, Components for Fiber Optic Applications*, pp. 26–35, 1986

[Ken86] Robert S. Kennedy, Massachusetts Institute of Technology, private communication, 1986

[Lie86] Soung C. Liew, "Topologies and Power Division Characteristics of Fiber Optic Networks," M.S. Thesis, Massachusetts Institute of Technology, Cambridge, February 1986

[Moo86] Douglas R. Moore, "Wavelength Dependent Coupling in Single-Mode Fused Biconical Taper Couplers," *SPIE, Vol. 722, Components for Fiber Optic Applications*, pp. 11–18, 1986

[Mou87] Steven Moustakas, "The Standardization of IEEE 802.3 Compatible Fiber Optic CSMA/CD Local Area Networks: Physical Topologies," *IEEE Communications Magazine*, Vol. 25, No. 2, pp. 22–29, February 1987

[Per83] Stewart D. Personick, "Review of Fundamentals of Optical Fiber Systems," *IEEE Journal on Selected Areas in Communications*, Vol. SAC-1, No. 3, pp. 373–380, April 1983

[Per85] Stewart D. Personick, *Fiber Optics: Technology and Applications,* ©1985 Plenum Press, New York

[Pri58] R. Price, and P. E. Green, Jr., "A Communication Technique for Multipath Channels," *Proceedings of the IRE*, Vol. 46, No. 3, pp. 555–570, March 1958

[Pro83] John G. Proakis, *Digital Communications,*" ©1983 McGraw-Hill, Inc., United States

[Ree86] Jeffrey W. Reedy, "The TDM Ring—A Fiber Optic Transport System for Campus or Metropolitan Networks," *IEEE Journal on Selected Areas in Communications*, Vol. SAC-4, No. 9, pp. 1474–83, December 1986

[Ros87] Floyd E. Ross, "Rings are 'Round for Good," *IEEE Network Magazine*, Vol. 1, No. 1, pp. 31–38, January 1987

[Tam84] Toshifumi Tamura, Masuru Nakamura, Shigeru Ohshima, Takao Ito, and Takeshi Ozeki, "Optical Cascade Star Network — A New Configuration for a Passive Distribution System with Optical Collision Detection Capability," *Journal of Lightwave Technology*, Vol. LT-2, No. 1, pp. 61–66, February 1984

[Wag85] Stuart S. Wagner, "Multiplexing Methods for Fiber Optic Local Communication Networks," Ph. D. dissertation, Massachusetts Institute of Technology, Cambridge, June 1985

[Wag87] Stuart S. Wagner, "Optical Amplifier Applications in Fiber Optic Local Networks," *IEEE Transactions on Communications*, Vol. COM-35, No. 4, pp. 419–26, April 1987

[WCK87] R. E. Wagner, N. K. Cheung, and P. Kaiser, "Coherent Lightwave Systems for Interoffice and Loop-Feeder Applications," *Journal of Lightwave Technology*, Vol. LT-5, No. 4, pp. 429–438, April 1987

[Yos85] Tetsuo Yoshizawa, "Plastic Connectors," *Japan Annual Reviews in Electronics, Computers, and Telecommunications, Vol. 17, Optical Devices and Fibers (1985/1986)*, Y. Suematsu (ed.), Ohmsha, LTD., pp. 151–158, 1985

Mathematics

[Dav79] Philip J. Davis, *Circulant Matrices*, John Wiley & Sons, New York, 1979

[Fie86] Miroslav Fiedler, *Special Matrices and Their Applications in Numerical Mathematics*, Martinus Nijhoff Publishers, Dordrecht/Boston Lancaster, 1986

[Gan59] F. R. Gantmacher, *Applications of the Theory of Matrices*, Interscience Publishers, Inc., New York, 1959

[Gan60] F. R. Gantmacher, *The Theory of Matrices, Vol. 1*, Chelsea Publishing Company, New York, 1960

[Her75] I. N. Herstein, *Topics in Algebra, 2nd ed.*, John Wiley & Sons, New York, 1975

[Min88] Henryk Minc, *Nonnegative Matrices*, John Wiley & Sons, New York, 1988

[Par60] Emanuel Parzen, *Modern Probability Theory and Its Applications*, John Wiley & Sons, Inc., New York, 1960

[Sen81] E. Seneta, *Non-negative Matrices and Markov Chains*, Springer-Verlag New York Inc., 1981